

## ABSTRACT

Title of Document: GENETIC DETERMINANT OF  
SILICIBACTER SP. TM1040 MOTILITY

Rooge Suvanasuthi  
Master of Science, 2008

Directed By: M. Robert Belas, Professor  
University of Maryland Biotechnology Institutes,  
Center of Marine Biotechnology

*Silicibacter sp.* TM1040 is a member of the Roseobacter clade. Roseobacters play an important role in sulfur cycling in the ocean by degrading dimethylsulfoniopropionate (DMSP). Roseobacters are found in communities associated with most marine habits, especially with marine algae. Therefore, the ability to sense, move towards and maintain the interaction is an important physiological trait for the symbiosis between roseobacters and dinoflagellate. Previous work from our laboratory demonstrated that TM1040 is chemotaxis towards DMSP and DMSP catabolites, and motility of TM1040 is important for growth of *P. piscicida*. In contrast to enteric bacteria, little is known about the genes regulating motility in roseobacter species. This study, revealed similarities between the genes associated with motility in TM1040 and those from other  $\alpha$ -proteobacteria species, but most importantly, it identified three new regulators that maybe involved in regulating the motility of TM1040.

GENETIC DETERMINANTS OF *SILICIBACTER* SP. TM1040 MOTILITY

By

Rooge Suvanasuthi

Thesis submitted to the Faculty of the Graduate School of the  
University of Maryland, College Park, in partial fulfillment  
of the requirements for the degree of  
Master of Science  
2008

Advisory Committee:

Dr. M. Robert Belas, Professor, Chair

Dr. Frank T. Robb, Professor

Dr. Harold J. Schreier, Associate professor

© Copyright by  
Rooge Suvanasuthi  
2008

## Dedication

To my parents whom always was there for me at all times.

## Acknowledgements

I would like to thank M. Robert Belas, Professor for the time he spent in teaching me how to think and work like a scientist, and also for the opportunity to obtain my master degree in science. I am also grateful to my parents, Pirojana and Pimpa Suvanasuthi for all their support. I would also like to thank Drs. Frank T. Robb, Harold J. Schreier, Todd Miller, and Pongpan, Laksanalamai, Anchalee Laksanalamai, and the current and former members of the Belas laboratory for their help and comments. This research was supported by grant MCB0446001 from the National Science Foundation.

# Table of Contents

Dedication .....	ii
Acknowledgements .....	iii
Table of Contents .....	iv
List of Tables .....	vi
List of Figures .....	vii
Chapter 1: Background .....	1
1.1 Physiology and symbiosis of the Roseobacter clade .....	1
1.1.1 Physiology of the Roseobacter clade .....	1
1.1.2 Interaction of roseobacters and dinoflagellates.....	2
1.2 Mechanisms of bacteria motility.....	6
1.2.1 Bacteria Chemotaxis .....	6
1.2.2 Bacteria Flagellar biosynthesis .....	10
Chapter 2: Genetic determinants of <i>Silicibacter sp.</i> TM1040 motility.....	15
2.1 Summary .....	15
2.2 Material and Methods .....	16
2.2.1. Bacterial strains and growth conditions.....	16
2.2.2. Genomic analysis .....	16
2.2.3. Transposon mutagenesis .....	19
2.2.4. Motility analysis.....	19
2.2.5. Measurement of the percentage of motile cells and cells in rosettes, in a population. ....	20
2.2.6. Flagellar staining.....	21
2.2.7. Detection of flagellin protein.....	21
2.2.8. Measurement of antibiotic production .....	22
2.2.9. Congo red (CR) binding.....	22
2.2.10. Biofilm formation .....	23
2.2.12. Cell elongation .....	24
2.2.13 Construction of pRSI506 for complementation of <i>flaC</i> mutant.....	24
2.2.14 Construction of pRSI507 for site specific mutagenesis of <i>flaC</i> .....	25
2.2.15 Measurement of cell elongation of site specific mutagenesis of <i>flaC</i> (RSI02).....	32
2.3.1. Organization of the flagellar loci .....	33
2.3.2. Identification of flagellar genes by transposon mutagenesis .....	41
2.3.3. Identification of three novel regulators .....	42
2.3.4. Flagella are synthesized by some Mot <sup>-</sup> mutants .....	50
2.3.5. Mutation in <i>flaC</i> bias the cell towards the motile phase.....	53
2.3.6. Motility defects also alter the cell surface .....	57
2.3.8. Mutation in <i>flaC</i> is not defective in chemotaxis .....	62
2.3.9. Mutation in <i>flaC</i> has filamentous cells .....	62
2.3.10. Complementation of <i>flaC</i> mutant (HG1016) and over expression of FlaC .....	68
2.3.11. <i>flaC</i> mutation via site specific recombination .....	76

2.3.11. The second transposon in the <i>flaC</i> mutant.....	79
2.3.12. Distribution of the flagellar genes among the <i>Roseobacter</i> clade .....	84
2.4 Conclusion .....	87
Chapter 3: Discussion .....	89
Appendix A: Media and Solutions.....	96
Appendix B: Protocols.....	106
Reference .....	122

## List of Tables

### Chapter 2.

**Table 1.** Bacterial strains used in this study

**Table 2.** Phenotype of Mot<sup>-</sup> mutants

**Table 3.** Comparison of the diameter of partial motile colonies to TM1040, in 2216 semi-solid motility agar plates

**Table 4.** Comparison of % motile cells and % cells forming rosettes of TM1040 and *flaC*

**Table 5.** Comparison of cell elongation in various concentration of peptone

**Table 6.** Comparison of cell elongation during growth at 25°C and 30°C

**Table 7.** Pigment production of *flaC* complementation and FlaC overexpression strains

**Table 8.** Antibiotic production of *flaC* complementation and FlaC overexpression strains

**Table 9.** Motility in 2216 semi-solid agar of *flaC* complementation and FlaC over expression strains, at 30°C

**Table 10.** Observation of population of motile cells in *flaC* complementation and FlaC over expression strains

**Table 11.** Cell elongation of *flaC* complementation

**Table 12.** Comparison of TM1040 flagellar genes with other *Roseobacter* clade genomes<sup>a</sup>

# List of Figures

## Chapter 1.

**Figure 1** Degradation pathway of DMSP

**Figure 2** Scanning Electro Microscope of TM1040

**Figure 3** Chemotaxis pathway of *E. coli* and *S. Typhimurium*

**Figure 4** Flagellar Structure base on *E. coli*

**Figure 5** Flagellar regulation in *E. coli*, *S. meliloti*, *R. sphaeroides*, and *C. crescentus*

## Chapter 2

**Figure 6** Plasmid map of pRSI505

**Figure 7** Plasmid map of pRSI506

**Figure 8** Confirming presence of pRSI506 in HG1016 and RSI01

**Figure 9** Plasmid map of pRSI507

**Figure 10** Confirming the presence of pRSI507 in TM1040

**Figure 11** Flagellar loci on the TM1040 genome

**Figure 12** Flagellar loci of *R. sphaeroides* (fla2 flagellar loci) and *S. meliloti*

**Figure 13** Other flagellar loci on the genome of TM1040

**Figure 14** Motility in semi-solid agar

**Figure 15** Domains of the three new regulatory proteins

**Figure 16** Genetic loci of *flaB*, *flaC*, and *flaD*

**Figure 17** SDS-PAGE detection of flagellin

**Figure 18** Electron microscopy of TM1040, *motB1*, *flaC*, and *fliC3* mutants

**Figure 19** Flagellins of TM1040

**Figure 20** Alignment of upstream region of *fliC 3* and *fliC1*

- Figure 21** Motility of TM1040 and *flaC* mutant (HG1016) in semi-solid agar plate
- Figure 22** Defects in *flaC* result defect in pigment production and antibiotic production
- Figure 23** Biofilm formation
- Figure 24** Detection of outer cell surface changes
- Figure 25** Chemotaxis plate assay
- Figure 26** Filamentous cells of the *flaC* mutant
- Figure 27** Comparison of cell elongation of RSI02 to TM1040 and HG1016
- Figure 28** Motility of RSI02 on 2216 semi solid agar compared to TM1040 and HG1016
- Figure 29** PCR of *flaC*::EZ-Tn5 fragment and restriction analysis HG1016 rescue clone plasmid
- Figure 30**  $\beta$ -glucuronidase operon
- Figure 31** Mutation in kanamycin resistant gene in EZ-Tn5 transposon
- Figure 32** Predicted diagram of TM1040 hierarchy including FlaBCD

# Chapter 1: Background

## 1.1 Physiology and symbiosis of the Roseobacter clade

### 1.1.1 Physiology of the Roseobacter clade

The Roseobacter clade is a taxonomic group in the  $\alpha$ 3-Proteobacteria branch. The members of this clade share >89% identity at the 16S rRNA level, and the clade is comprised of 17 genera that are represented by 36 species and hundreds of uncharacterized isolates and clone sequence (22). Roseobacters are responsible for dimethylsulfoniopropionate (DMSP) catabolism (34), the major source of organic sulfur in the ocean (71). Dinoflagellates and other phytoplankton are primary producers of DMSP in the ocean (43, 117). The abundance and activity of *Roseobacter* species is significantly correlated with DMSP-producing dinoflagellates and other phytoplankton, establishing a physiological and ecological linkage between dinoflagellates and roseobacters (35, 121). There are two major pathways of DMSP degradation: (i) the lyase or cleavage pathway that produces dimethyl sulfide (DMS) (34, 50, 118), a volatile gas that is released into the atmosphere and oxidized into sulfur aerosols leading to cloudiness, and (ii) the demethylation/dethiolation pathway in which sulfur in the DMSP is maintained in the bacteria or ocean (Fig. 1) (40, 44, 106, 122). Therefore, the DMSP degradation is a key step in controlling the marine sulfur cycle (22, 33, 44).

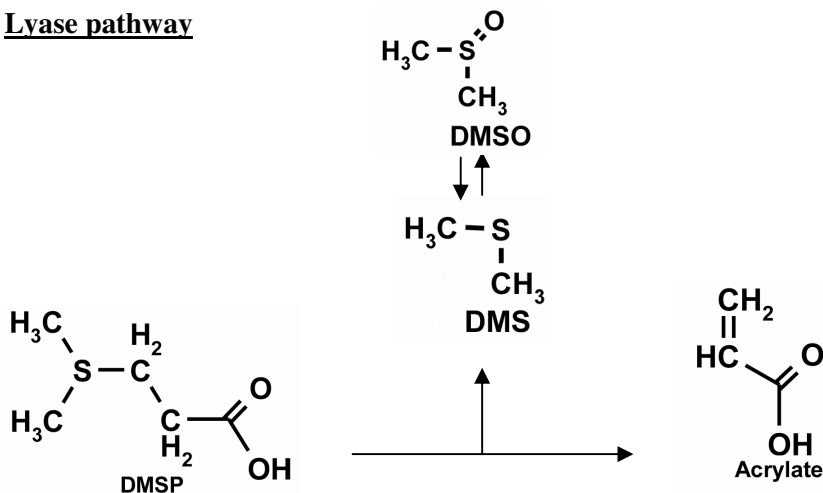
Roseobacters are exclusively marine or hypersaline and have diverse physiological traits (such as sulfur metabolism, secondary metabolites, rosette formation, toga-like morphologies, poly- $\beta$ -hydroxybutyrate granules) that are unique adaptations for their diverse habits (22). In contrast to many other marine bacteria taxa, Roseobacters isolates can be readily grown in laboratory cultures (22). Motility in most of these species is achieved by means of one or more, flagella (33, 48, 66, 84, 87). DNA sequences from roseobacters can be

found in populations associated with coastal biofilms, sponges, sea grasses, diseased corals, cephalopods, hypersaline microbial mats, and polar sea ice. Moreover, roseobacters are most abundant in bacteria populations associated with marine algae (22).

### 1.1.2 Interaction of roseobacters and dinoflagellates

Several studies on roseobacter species have reported on the interaction of roseobacters and their dinoflagellate hosts. For example, Silva *et al.* (1985) demonstrated that *Gymnodinium splendens* and *Glenodinium foliaceum* contain intranuclear bacteria, using light and electron microscopy (89, 90). *Pfiesteria piscicida*, a heterotrophic dinoflagellate that uses a feeding tube called peduncle to feed on phytoplanktons. This type of feeding is also called myzocytosis (55, 107). *P. piscicida* has also been demonstrated to absorb nitrogen compounds such as ammonia, nitrate, urea and glutamate (53). In addition, *P. piscicida* can also harbor intact chloroplasts after feeding on algae prey in its food vacuole (54), but it is still unclear on how much photosynthesis would contribute to the growth because these dinoflagellates cannot be grown autotrophically (23, 24). In 1997, *P. piscicida* was implicated in the deaths of fish in Chesapeake bay (41). *P. piscicida* can be maintained in laboratory culture with its associated bacterial community of which 50% of the isolates are members of the roseobacter clade (2). In an axenic culture of *P. piscicida*, the growth rate of the dinoflagellate decreases, indicating the requirement of its bacteria community (2). This interaction may be facilitated through the physiology stage of the members of the bacteria community. Previous studies by Bruhn *et al.* (21), have shown that 57% of *Roseobacter* strains examined have a biphasic life: the motile stage, found in early-to-mid-exponential stages of growth, characterized by small flagellated, highly motile and chemotactic cells, while the sessile stage occurs in late stationary phase of growth and loss of motility and flagella, and formation of a biofilm and aggregates of cells called rosettes (21).

### Lyase pathway



### Demethylation/dethiolation pathway

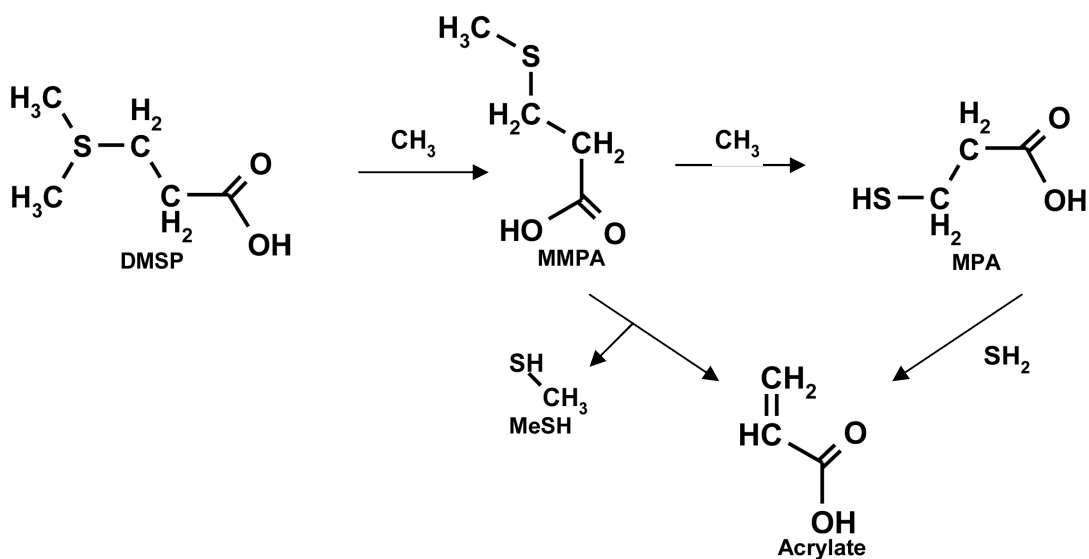


**FIG1.** Degradation pathway of DMSP. Degradation of DMSP may occur by lyase pathway, producing DMS and Acrylate. In some cases, DMS can also be oxidized to DMSO. The other degradation pathway of DMSP is demethylation/dethiolation pathway, producing MMPA. The MMPA may further be demethylate producing MPA followed by removal of hydrogen sulfide or dethiolation producing acrylate and MeSH.

In addition to biofilm development, the sessile life stage is also characterized by the production of a yellow-brown extracellular pigment and an antibiotic compound, tropodithietic acid (32). The interactions between *P. piscicida* and the bacteria was shown by using fluorescent in situ hybridization (FISH) and confocal laser scanning microscopy (CFLSM) indicating the location of the bacteria on the cell surface and within the *P. piscicida* cell (2). Dimethylsulfoniopropionate (DMSP) that is produced by *Pfiesteria*, DMSP metabolites, and heat labile molecule in *Pfiesteria* homogenate, are also chemotactic attractants of TM1040 (66). Roseobacter isolates from the *Pfiesteria* culture can also enhance the predation rate of *P. piscicida* on its prey, *Rhodomonas*, which increases growth (3).

The marine bacterium *Silicibacter* sp. TM1040 (hereafter TM1040) was originally isolated from a laboratory microcosm culture consisting of dinoflagellates, prey algae, plus naturally-occurring bacteria (2, 64). TM1040 is a member of the *Roseobacter* clade in the  $\alpha$ -3 subclass of the class Proteobacteria, and is motile via at least three polar flagella (Fig. 2) (66). In addition, TM1040 degrades DMSP using the demethylation pathway (64).

TM1040 is actively chemotactic towards DMSP produced by *P. piscicida*, bacterial breakdown products of DMSP, ex. 3-methylmercaptopropionate (MMPA), and amino acids (66). In earlier work, we have demonstrated a symbiosis between TM1040 and *P. piscicida*. This symbiosis exists such that dinoflagellates obligately require TM1040 or physiologically equivalent bacteria for growth . through a combination of physical attachment of the bacteria to the dinoflagellate cell surface which the presence of bacteria enhances growth of the dinoflagellate (65). Motility TM1040 is also require by the *P. piscicida* in order to achieve normal growth rate (65). Previous work from our laboratory also demonstrates that TM1040 has a biphasic life cycle, motile and sessile stage, that is hypothesis to facilitate in the association with *P. piscicida* (21).

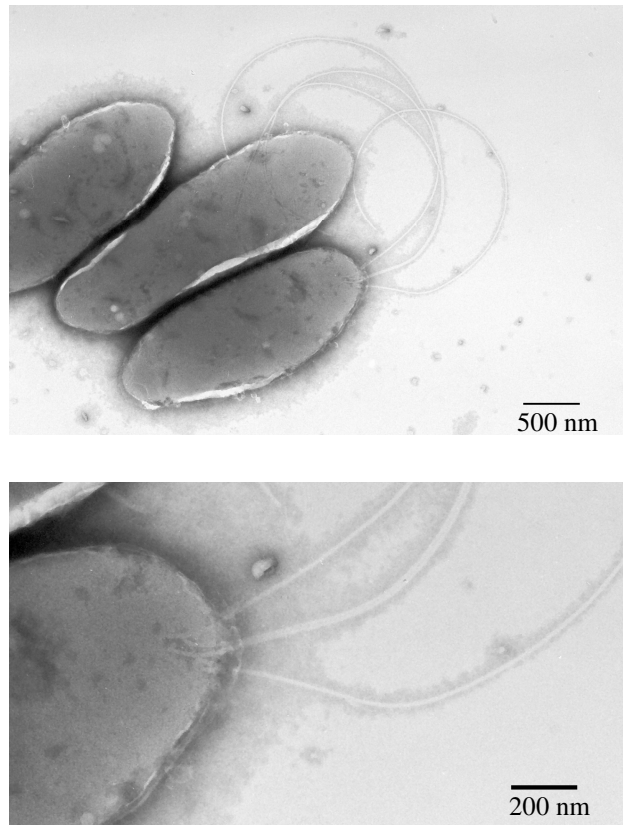


**Fig. 2** Scanning Electro Microscope of TM1040. The image shows the three polar flagella of TM1040. (A) Scale bar represents 500 nm and (B) Close up image of the polar flagella, scale bar representing 200 nm (image provided by Dr. Shin-ichi Aizawa, CREST Soft Nano-Machine Project, Innovation Plaza Hiroshima, 3-10-23 Kagamiyama, Higashi-Hiroshima 739-0046, Japan).

## 1.2 Mechanisms of bacteria motility

### 1.2.1 Bacteria Chemotaxis

Bacteria swim towards attractant molecules by responding to the increasing chemical gradient, which causes a reversal of the rotation of the flagella in a behavior called chemotaxis. The change of direction of flagella rotation in enteric bacteria, such as *Escherichia coli* and *Salmonella Typhimurium*, causes two types of swimming behaviors, smooth swimming and tumbling (69). In smooth swimming the flagella rotate counter-clockwise (CCW), defined by looking at the end of the flagellum, causing the filament to form a bundle. This causes the cell to move forward. When rotating in a clockwise direction, the flagellar bundle will disperse, causing the cells to tumble and change direction (69). In the absence of an attractant the frequency of tumble is increased, to change direction of the cell, and in contrast, in the presence of an attractant gradient, the duration of smooth swimming is extended (by tumbling suppression) and directs the cell up the attractant gradient (69).

The bacteria cell senses attractant and repellent signals through membrane receptor, chemotaxis proteins, also called methyl-accepting chemotaxis proteins (MCPs) (46). The MCPs have a transmembrane domain that contain a ligand binding domain and a cytoplasmic domain which is the signal transducer domain or HAMP (Histidine kinases, Adenylyl cyclases, Methyl binding proteins, Phosphatases) domain (109). In *E. coli* and *S. Typhimurium*, the MCPs are localized at the membrane. Both species have five MCPs, which four receptors are common in both species: Tar, Tsr, Trg, and Aer that senses serine, aspartate, ribose and galactose, and oxygen, respectively (14, 46, 97). The unique receptor in *E. coli* is Tap and in *S. typhimurium* is Tcp that senses dipeptides and citrate, respectively (61, 115). In an unoccupied MCP, CheW (adaptor protein) couples CheA (Histidine kinase) to the MCP receptor where CheA is simulated to autophosphorylate at a histidine residue (72). Phosphorylated CheA (CheA-P) donates its phosphate to both CheY (flagellar-motor-

binding protein) and CheB (methyltransferase) proteins at their aspartate residue (19, 58, 72). Phosphorylated CheY (CheY-P) then binds to FliM, a protein component of the C-ring of the flagellum, and alters the direction of the flagellum rotation from CCW to CW causing the cell to tumble (105, 111) (Fig. 3). When the MCP is occupied by the ligand, the autophosphorylation activity of CheA is reduced and leads to reduced tumbling and increased smooth swimming (101).

In order for the bacteria to respond to temporal changes or spatial concentration gradients of chemoeffectors rather than a uniform concentration, adaption must be achieved (76). The process of adaption is achieved by methylation and demethylation of MCPs by the methyltransferase CheR and methyltransferase CheB, respectively (52, 104). Unoccupied MCPs are methylated by CheR, leading to autophosphorylation of CheA (11, 99). CheA-P can phosphorylate CheB (CheB-P) and increases the demethylation of MCPs, functioning as a feedback mechanism for demethylation of the receptors (10, 98). Another feedback mechanism is mediated by CheZ that dephosphorylates CheY and result in decreased frequency of CW rotation of the flagellum (47).

In contrast to the well-studied chemotaxis and motility mechanisms of the enteric bacteria, much less is known about these mechanisms in non-enteric bacteria. Many non-enteric bacteria, like marine bacteria, live in chemically diverse environments that do not resemble the mammalian intestine. Therefore, it is not unexpected that the chemotaxis and motility behavior of these bacteria may be different from enteric bacteria mechanisms (8, 67).

Non-enteric bacteria such as *Rhodobacter sphaeroides* and *Sinorhizobium meliloti* do not swim via a smooth swim-tumble motility like *E. coli*, but instead have a swim-stop behavior (8). The flagella of both species have a unidirectional motor that rotates only in a CW direction. Unlike *E.coli*, the cell changes its orientation by altering the flagellar motor speed in response to environmental signals (8, 36, 120). Upon sensing a reduction of attractant, *R. sphaeroides* responds by stopping its swimming. During this period the filament

winds up to form a coil against the cell, which reduces rotation and facilitates the re-orientation of the cell (7, 8, 77). In *S. meliloti*, asynchronous slow speed rotation of an individual flagellum causes the cell to change its path, but at high speed rotation the flagella comes together forming a bundle that propels the cell forward (8, 79). Another difference between *E. coli* and non-enteric bacteria, such as *R. sphaeroides*, is the chemotaxis mechanism. In *E. coli*, the MCPs are typically membrane-bound but, in contrast, some MCPs in *R. sphaeroides* are also localized in the cytoplasm (37). It is predicted that these cytoplasmic MCPs are used to monitor the metabolic state of the cells through an unknown mechanism (110). In support of this idea, a broad range of structurally unrelated metabolites were shown to inhibit the chemotaxis of *R. sphaeroides* suggesting that metabolic intermediates are involved in the sensory signaling system. This finding also couples the metabolic pathways to the chemotaxis systems (82). In contrast to *E. coli*, multiple copies of receptors and chemotaxis proteins are also present in *R. sphaeroides* and *S. meliloti* (8). Multiple copies of the sensory proteins could enhance chemotaxis by clustering of the receptors and signal transducer proteins to increase signal sensitivity (56). These adaptations in the chemotaxis mechanism are to facilitate survival in environments that are different from the enteric bacteria (8).

The genome of *Silicibacter sp.* TM1040 contains 20 MCPs of which fourteen are likely to be located in the cytoplasm (70), suggesting that TM1040 is capable of sensing a wide variety of environmental signals. TM1040 is highly chemotactic towards heat-labile compounds in a dinoflagellate homogenate, DMSP and its metabolite products (acrylate, MMPA, and MPA), and amino acids, especially methionine (66). This suggests that TM1040 has adapted its chemotaxis mechanisms to sense the dinoflagellate in order to respond and swim towards the dinoflagellate in oligotrophic environment like the ocean.

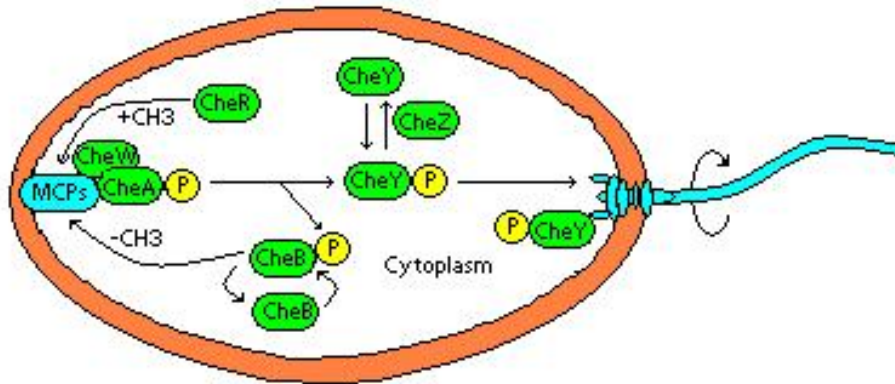


**FIG. 3** Chemotaxis pathway of *E. coli* and *S. Typhimurium*. Unoccupied MCP, CheW couples CheA with MCP receptors and stimulate autophosphorylation of CheA (72). The phosphorylated CheA (CheA-P) proteins then transfer the phosphate to both CheY and CheB proteins (19, 58, 72). Phosphorylated CheY (CheY-P) binds to the C-ring of the flagellum and alters the direction of the flagellum rotation from CCW to CW causing the cell to tumble (105, 111). During adaptation process, unoccupied MCPs are methylated by CheR, leading to autophosphorylation of CheA (11, 99). CheA-P proteins can phosphorylate CheB (CheB-P) and increases the demethylation of MCPs, functioning as a feedback mechanism for demethylation of the receptors (10, 98). Another feedback mechanism is mediated by CheZ that dephosphorylates CheY and result in the decreased frequency of CW rotation of the flagellum (tumbling) (47).

### 1.2.2 Bacteria Flagellar biosynthesis

The critical structure that allows the bacterial cell to swim is the flagellum. The number per cell and position of flagella vary among the species, ranging from one polar flagellum (monotrichous) to multiple flagella around the cells (peritrichous). The bacterial flagellum is composed of 4 ring structure (C-ring, MS-ring, P-ring, and L-ring), a motor-stator, hollow rod, hook, and filament (Fig. 4). It is assembled, in order, starting from the inner membrane cytoplasmic surface and extends through the membrane and out to the exterior of the cell. The assembly process begins with the formation of the MS-ring in the inner membrane by FliF, which interacts with and is followed in assembly by the C-ring (FliM, FliN, and FliG) that forms a cup-like structure in the cytoplasm. A type-III secretion system (TTSS) export apparatus is next formed in the middle of the C-ring by FlhA, FlhB, FliO, FliP, FliQ and FliR allowing the export of other flagellum specific components through the TTSS (59). The rod (FlgB, FlgC, FlgF, FlgG, and FlgJ) is assembled traversing the periplasmic space along with the formation of P-ring (FlgI), and L-ring (FlgH) in the periplasmic space and outer membrane, respectively (59). The hook (FlgE) and hook junction proteins (FlgK and FlgL) are then formed at the exterior of the outer membrane after transition through the hollow rod. Similarly and following hook assembly, flagellins (FliC) are exported to form the filament extending from the hook junction proteins (59), and terminating in the capping protein, FliD (59). At this point multiple copies of the motor proteins assemble around the basal-body (MS-ring, rod, P-ring, and L-ring) in the inner membrane and participate in torque generation to rotate the flagellum (20, 119). Torque is provided by proton motive force and protons in enterics and other terrestrial bacteria, and by sodium in the case of many marine bacteria (60).

Flagellum assembly is coordinated with the regulation of the flagellar genes. In enteric bacteria the flagella regulon is categorized into three hierarchical transcriptional

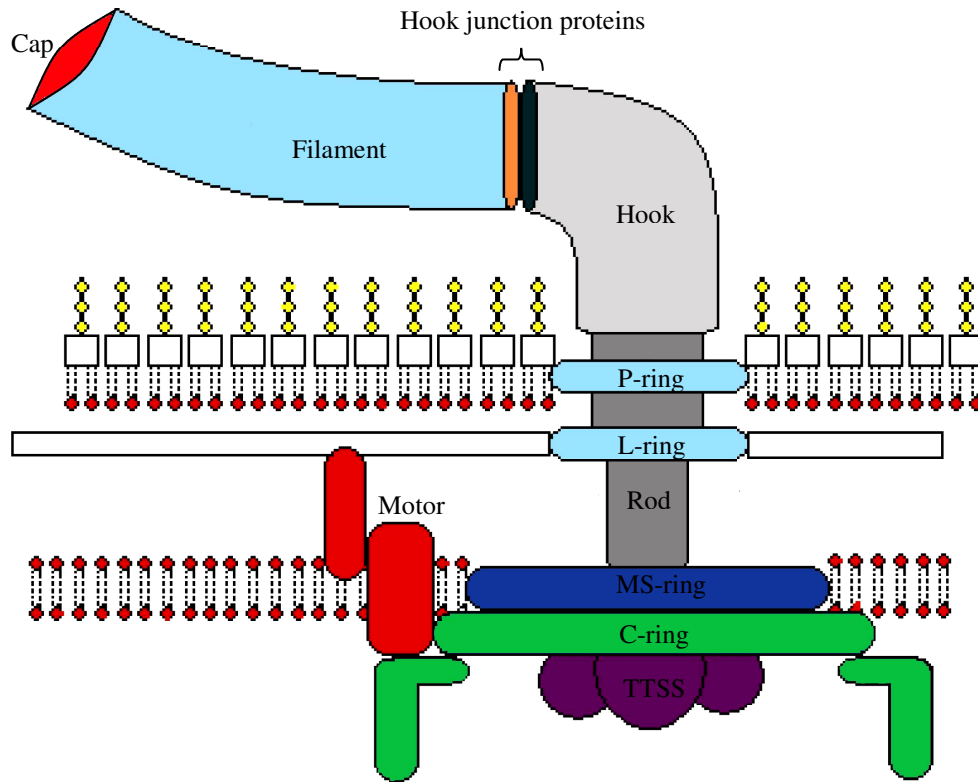


**FIG. 4** Flagellar Structure base on *E. coli*. The flagellum is composed of the MS-ring (FliF), C-ring (FliG, FliM, FliN), Type Three Secretion System (TTSS) or export apparatus (FlhA, FlhB, FliO, FliP, FliQ and FliR), Rod (FlgB, FlgC, FlgF, FlgG, and FlgJ), P-ring (FlgI), L-ring (FlgH), Hook (FlgE), Hook junction proteins (FlgK and FlgL), Filament (FliC) and Filament cap proteins (FliD).

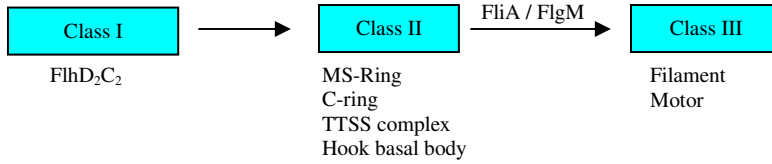
classes (class I, class II, and class III) each of which is regulated by the expression of the previous class. Class I genes consists of the master regulator *flhDC* that encodes the transcription activator FlhD<sub>2</sub>C<sub>2</sub> and upregulates the transcription of class II genes (26). Many regulators of *flhDC* have been discovered. For example, during high osmolarity, the OmpR negatively regulates the *flhDC* operon (88). In contrast, CAP-cAMP upregulates flagellum synthesis (1, 91). Histone-like-nucleoid-structuring (H-NS) proteins have both positive and negative regulation effect on *flhDC* expression (94, 95). Quorum sensing also play a role in the regulation of *flhDC* expression via QseCB (96).

Class II genes encode proteins that form the C-ring, export apparatus, basal-body, hook, and hook junction proteins. The class II genes also include *fliA* ( $\sigma^{28}$  subunit) and *flgM* that encodes an anti-sigma factor inhibiting FliA function. FlgM binds to FliA and prevents premature expression of class III genes but after completion of the basal body and hook complex, FlgM is exported out of the cell, leaving FliA free to upregulate the class III genes (FliC, flagellin, and motAB, the motor proteins) (Fig. 5) (59).

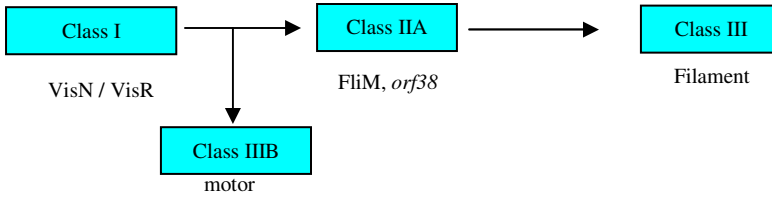
Not all groups of bacteria follow this model of flagellar regulation. For example, in  $\alpha$ -proteobacteria, *S. meliloti* utilizes LuxR-type transcription activators, VisN and VisR, as the class I master regulators (93). The motor proteins (MotA, MotB, and MotC) are included into class IIB because the expression of the flagellin (class III) requires expression of class IIA genes (*fliM* and *orf38*) but not the motor proteins (Fig. 5) (93). Flagellar regulation in *R. sphaeroides* is regulated in a four-tiered hierarchical cascade. The master regulator (FleQ) is an enhancer-binding protein that, together with  $\sigma^{54}$ , upregulates transcription of class II genes (81). The class II genes also include another enhancer-binding protein (FleT) that interacts with FleQ and improves binding to DNA (81). Together, FleQ/FleT and  $\sigma^{54}$ , upregulate class III genes that also encode FliA ( $\sigma^{28}$ ) and the anti-sigma factor, FlgM (81). After completion of the hook-basal body complex, FlgM is exported out of the cell and FliA is free to upregulate the flagellin gene (FliC, class IV) (Fig. 5) (81).

Similarly, another well studied  $\alpha$ -proteobacterium, *Caulobacter crescentus*, uses a two component signal transduction system CckA (histidine kinase) and CtrA (response regulator) as the class I master regulatory circuit (39, 85). In contrast to *flhDC* in *E. coli* that regulates flagellar and fimbriae synthesis, CtrA is also a global regulator that regulates genes involved in polar morphogenesis, DNA replication initiation, DNA methylation, cell division, and cell wall metabolism (49). The class II genes encode for two additional regulators, FlbD and FliX, that couple the transcription of early class II basal body complex genes to the expression of class III and class IV genes (73, 113). The flagellin (class IV) in *C. crescentus* is also regulated at the post-transcriptional level by FlbT and FlaF that function opposing one another in regulating the expression of flagellin (57). FlbT negatively regulates flagellin by inhibiting translation and destabilize the mRNA while FlaF positively regulates filament synthesis by mediating flagellin secretion or assembly (Fig. 5) (6, 57). As mentioned above, regulation of flagella biosynthesis in  $\alpha$ -proteobacteria is different from the well studied enteric bacteria and also varies among the members of the  $\alpha$ -proteobacteria. It is tempting to propose that in the Roseobacter clade also have their unique way of regulating flagella biosynthesis. Little is known about regulation in flagella synthesis in roseobacters. Recent works from our laboratory has shown that TM1040 has homologs to both known and unknown flagella structural and regulatory genes (65, 70). To expand the knowledge of flagella biosynthesis in the roseobacter clade, this study has used genomic and genetic approaches to confirm the flagella gene homologs relation to flagella biosynthesis and to identify novel regulatory genes.

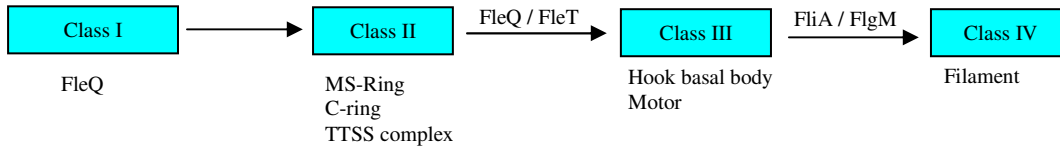
*E. coli*



*S. meliloti*



*R. sphaeroides*



*C. crescentus*

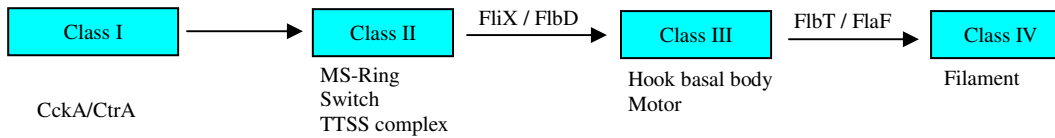


**Fig. 5** Flagellar regulation in *E. coli*, *S. meliloti*, *R. sphaeroides*, and *C. crescentus*.

## Chapter 2: Genetic determinants of *Silicibacter sp.* TM1040

### motility

#### 2.1 Summary

The alphaproteobacterium *Silicibacter sp.* TM1040, a member of the marine *Roseobacter* clade, that form a symbiosis with the dinoflagellate *Pfiesteria piscicida*. The initial phase of the symbiosis requires the bacteria to chemotactically sense and respond by swimming toward the planktonic host which is followed by biofilm formation on the surface of the dinoflagellate. In this study, we identified genes involved in regulation and biosynthesis of the *Silicibacter sp.* TM1040 flagellum. A genomic analysis uncovered over 40 Open Reading Frames (ORFs) with homology to known flagellar structural and regulatory genes, e.g., CckA, CtrA, FlaF and FlbT, proteins known to be crucial in the regulation of motility in other alphaproteobacteria. The genomic analysis also revealed two copies of MotA, MotB, and FlgF, and six copies of flagellin. The genomic results were supported by a genetic approach using random transposon mutagenesis to construct a bank of mutants with defects in motility. The genetic approach also suggests that among the multiple alleles of *motA*, *motB*, *flgF*, and *fliC* that only one of the copies (*motA1*, *motB1*, *flgF2*, and *fliC3*) may be required for motility. Among the regulatory genes identified by mutagenesis were *cckA* and *flaF*, as well as three new genes (*flaB*, *flaC*, and *flaD*) that encode novel proteins with sensory or regulatory domains. Bioinformatic and phenotypic analyses suggest that FlaC may function near the top of the regulatory hierarchy and acts to control the biphasic motile-to-sessile switch, FlaB may function as a phosphorelay protein acting at a lower point in the hierarchy, while the role of FlaD is likely to involve participation as a transcription activator of the motor genes. The significance of this finding is that these three novel regulators are

involved with flagella function and biosynthesis of TM1040 and is also hypothesized to be similar in other members of the roseobacter clade.

## 2.2 Material and Methods

### 2.2.1. Bacterial strains and growth conditions

The strains used in this study are listed in Table 2. Bacteria were routinely grown in 2216 Marine broth (Difco) with shaking or on 2216 agar medium (2216 Marine Broth with 15 g Bacto agar per 1 liter) at 30°C. *Escherichia coli* DH5α λpir was maintained in Luria-Bertani (LB) broth (Sambrook *et al.*, (1989)) or LB agar (LB broth plus 15g Bacto agar per liter) at 37°C. When required, kanamycin was added at a final concentration of 120 µg per ml for TM1040 and 40 µg per ml for *E. coli*.

### 2.2.2. Genomic analysis

The annotation of the genome TM1040 was recently published (70) and is available from GenBank (NC\_008044) or Roseobase ([www.roseobase.org](http://www.roseobase.org)). The annotation of a respective gene was confirmed using its deduced amino acid sequence in BLASTP searches (5) of the GenBank ([www.ncbi.nlm.nih.gov](http://www.ncbi.nlm.nih.gov)), Roseobase, and the Gordon and Betty Moore Foundation Marine Microbial Genome Sequencing Project (<https://research.venterininstitute.org/moore/>) database was used to search for homologs in other roseobacter genomes. Homologs with an E value cutoff of  $10^{-5}$  or less were considered

**Table 1.** Bacterial strains used in this study

Strains	Genotype <sup>a</sup>	Locus tag <sup>b</sup> of inserted gene	Predicted Function	Source or reference
TM1040	Wild type			(66)
DH5 $\alpha$ $\lambda$ pir	DH5 $\alpha$ lysogenized with $\lambda$ pir			(45)
HG1006	<i>flaB</i> ::EZ-Tn5, Km	TM1040_1206	Histidine kinase A (phosphoacceptor) domain	This study
HG1016	<i>flaC</i> ::EZ-Tn5, Km	TM1040_0051	Two component signal transduction response regulator	„
HG1030	<i>fliM</i> ::EZ-Tn5, Km	TM1040_1506	C-ring	„
HG1032	<i>flhA</i> ::EZ-Tn5, Km	TM1040_2953	Export apparatus	„
HG1033	<i>motB1</i> ::EZ-Tn5, Km	TM1040_2938	Motor complex	„
HG1036	<i>flgL</i> ::EZ-Tn5, Km	TM1040_2941	Hook junction protein	„
HG1039	<i>flhB</i> ::EZ-Tn5, Km	TM1040_2955	Export apparatus	„
HG1046	<i>flaD</i> ::EZ-Tn5, Km	TM1040_1731	Helix-turn-helix MarR domain	„
HG1049	<i>flaE</i> ::EZ-Tn5, Km	TM1040_0722	Glycosyl transferase	„
HG1063	<i>flgH</i> ::EZ-Tn5, Km	TM1040_2958	L-ring	„
HG1091	<i>fliR</i> ::EZ-Tn5, Km	TM1040_2954	Export apparatus	„
HG1098	<i>flgE</i> ::EZ-Tn5, Km	TM1040_2939	Hook	„
HG1099	<i>fliG</i> ::EZ-Tn5, Km	TM1040_1009	C-ring	„
HG1100	<i>flaI</i> ::EZ-Tn5, Km	TM1040_2975	Unknown function, cytoplasmic protien, 13.4 kDa, pI = 5.86	„
HG1101	<i>fliC3</i> ::EZ-Tn5, Km	TM1040_2974	flagellin	„
HG1118	<i>flaF</i> ::EZ-Tn5, Km	TM1040_2973	Regulator	„
HG1122	<i>flaG</i> ::EZ-Tn5, Km	TM1040_3778	mannose-6-phosphate isomerase	„
HG1135	<i>pflI</i> ::EZ-Tn5, Km	TM1040_2949	Motor associated	„
HG1139	<i>flgF2</i> ::EZ-Tn5, Km	TM1040_2971	Proximal Rod	„

HG1148	<i>fliF</i> ::EZ-Tn5, Km	TM1040_2947	MS-ring	„
HG1162	<i>flgG</i> ::EZ-Tn5, Km	TM1040_2960	Distal rod	„
HG1192	<i>fliL</i> ::EZ-Tn5, Km	TM1040_2948	Motor associated	„
HG1205	<i>flaA</i> ::EZ-Tn5, Km	TM1040_2952	Motor associated	„
HG1212	<i>motA1</i> ::EZ-Tn5, Km	TM1040_2951	Motor complex	„
HG1216	<i>flgK</i> ::EZ-Tn5, Km	TM1040_2940	Hook junction protein	„
HG1234	<i>flgI</i> ::EZ-Tn5, Km	TM1040_2942	P-ring	„
HG1241	<i>cckA</i> ::EZ-Tn5, Km	TM1040_1228	Regulator	„
HG1245	<i>fliK</i> ::EZ-Tn5, Km	TM1040_2977	Hook-length control	„
HG1246	<i>fliI</i> ::EZ-Tn5, Km	TM1040_2966	Export ATPase	„
RSI01	TM1040 Rif <sup>r</sup>			„
RSI02	<i>flaC</i> ::pRSI507			„

---

<sup>a</sup> Km, Kanamycin resistance; Rif<sup>r</sup>, Rifampicin resistance

<sup>b</sup> Locus tag based on the NCBI GenBank database.

significant. Maps of the flagellar loci were made by importing the nucleotide sequence of each flagellar gene into GenomBench version 2.0.0 (a component of Vector NTI Advance 10.0.01, Invitrogen, Carlsbad, California, USA).

### 2.2.3. Transposon mutagenesis

Electrocompetent cells of TM1040 were prepared as described in Appendix B (65). Random transposon mutagenesis using EZ-Tn5 <R6K $\gamma$ ori/KAN-2> (Epicentre, Madison, Wisconsin) was conducted as previously described by Miller *et al*, (2006) with minor changes. A 65- $\mu$ l sample of electrocompetent cells of TM1040 was mixed with 25 ng of the transposome. The mixture was electroporated in a 0.2 cm electroporation cuvette at 2.5 Kv per cm, 400 ohms and 25  $\mu$ F using a Bio-Rad Gene Pulser (Bio-Rad, Hercules, California). The cells were suspended in 1 ml of prewarmed HIASW (25 g Heart infusion medium [Difco] plus 15 g Instant Ocean sea salts [Aquarium Systems, Mentor, Ohio] per liter) and incubated at 30°C with shaking for 2 h. Following incubation, 100  $\mu$ l samples of the culture were spread on HIASW agar (HIASW with 1.5% Bacto agar) containing kanamycin, and incubated for 48 h at 30°C. Kanamycin-resistant colonies were transferred to a 7-by-7 array on 2216 agar containing kanamycin to facilitate future analysis. The sequence flanking the transposon was obtained by rescue-cloning as described in Appendix B (65).

### 2.2.4. Motility analysis

Mutants with defects in wild-type swimming (Mot<sup>-</sup>) were screened as described by Miller and Belas (2006) using semi-solid 2216 motility plates (2216 Marine broth supplemented with 0.3 g Bacto agar per liter) or marine motility plates [0.1 % peptone, 200 mM NaCl, 50 mM MgSO<sub>4</sub>, 10 mM KCl, 10 mM CaCl<sub>2</sub>.2H<sub>2</sub>O, 240  $\mu$ M K<sub>2</sub>HPO<sub>4</sub>, (70 mM Tris-HCl pH 7.5), 0.3 % agar per 100 ml] and incubate at 30°C for 3 days.

In addition, 3  $\mu$ l of overnight cultures of mutants, grown in 2216 Marine Broth at 30°C with shaking, were also examined for motility using phase contrast microscopy with a 20x objective lens on a Nikon Optiphot microscope. Mutants with one or more cells swimming were scored as motile.

#### 2.2.5. Measurement of the percentage of motile cells and cells in rosettes, in a population.

TM1040 and HG1016 were grown in 2216 Marine broth at 30°C with shaking for 14 h. Seven microliters of culture was examined by phase contrast microscopy (Olympus BX60, Center Valley, Pennsylvania) using 40x objective lens. Five random fields were recorded for 1 sec (20 frames/sec) using a Qicam Fast 1394 camera. Analysis was done with Volocity software (V4.1.0, Improvision, England) as follows (measurement parameters are described in Appendix B).

The culture was separated into three types of cells: (i) single motile cells, (ii) single non-motile cells, and (iii) cells in rosettes. The total number of cells in rosettes (a rosette was defined as cells aggregates  $> 5 \mu\text{m}^2$ ) was estimated by calculating the average number of cells in a rosette and multiplying this value by the total number of rosettes in the field. Single cells (both motile and nonmotile) were defined as bodies of  $\leq 5 \mu\text{m}^2$ . The percentage of motile cells was calculated using motion analysis of a 1 s video clip recorded from a field (five fields total). The number of motile cells obtained was then subtracted from the total count of single cells in that field to determine the amount of non-motile single cells. The experiment was run in quadruplicate. The mean, standard deviation, and statistical analysis (Unpaired T Test, 95% CI, P-value  $< 0.05$ ) of all four flask for percentage of motile cells, single cells, and cells forming rosettes were determined using Prism 4.0 statistic software (GraphPad).

### 2.2.6. Flagellar staining

Flagellar filaments were stained for light microscopy using the RYU flagellar stain (Remel, Lenexa, Kansas) according to the recommendations of the manufacturer. Overnight culture of TM1040 or mutant grown 2216 at 30°C with shaking was pipette onto a glass slide and covered with cover a cover slip. Ten microliters of RYU flagellar stain was added to the side of the cover slip, allowing the stain to flow between the cover slip and the side. After ten minutes of incubation at room temperature, the stained culture was observed with phase contrast microscope using 40x objective lens on a Nikon Optiphot microscope.

### 2.2.7. Detection of flagellin protein

Flagella were purified as described by Kanbe *et al.* (42), with the following changes. After overnight incubation, cells were removed from 2216 Marine broth by centrifugation (10,000 x g for 5 min at 4°C). Detach flagella were precipitated by adding polyethylene glycol (PEG 8000, Sigma) (8% PEG 8000, 0.4 mM NaCl) to a final concentration of 2%. After 60 m on ice, the bundles of flagella were precipitated by low speed centrifugation (17,400 x g for 15 min at 4°C). Flagella bundles were resuspend in 50 mM Tris-HCl pH 7.5, and the protein in each sample determined (BCA kit, Pierce, Rockford, IL).

Flagellin protein was separated by sodium dodecyl sulfate polyacrylamide gel electrophoresis (SDS-PAGE) by loading 3 µg of total protein (prior to mixing with 5x protein loading dye and boiling for 5 min) (see Appendix A for recipe) from the flagella preparation on a 15% polyacrylamide gel (see Appendix A for recipes) (31). Protein bands were visualized using a Typhoon 9410 (Amersham Biosciences, Piscataway, NJ) and a 555 nm emission filter and a 488 nm excitation filter after staining with Coomassie Fluor Orange Protein gel Stain (Molecular Probes, Invitrogen, Carlsbad, CA) following the manufacturer's recommendation.

The size of the flagellin bands were calculated using ImageQuant software (Amersham Biosciences, Piscataway, NJ) by inputting the size of the Broad Range Marker (Bio-Rad, Hercules, CA) (200, 116, 97, 66, 45, 31, 21, 14, and 6.5 kDa) into the program for generating a standard curve with the migration distance in the gel. At this point, ImageQuant automatically calculate the size of the selected bands (flagellin) in the sample lane compare to the standard curve. The intensity of the flagellin bands were calculated by giving an arbitrary value of 1 to the 34 kDa flagellin band of TM1040, since the exact amount of flagellin is not known, to normalize the intensity of flagellins bands in HG1016. All calculation were done in ImageQuant software.

#### 2.2.8. Measurement of antibiotic production

Antibiotic production was measured using the well diffusion assay with *Vibrio anguillarum* strain 90-11-287 described by Bruhn *et al.* (2007). Briefly, spent medium from a culture was added into a well that was created by using the end of a 200 µl pipette tip in a 1% agar plate containing *V. anguillarum* and incubated at room temperature for 24 h (see detailed protocol in Appendix B). After incubating room temperature, the diameter of the inhibition zone of each sample was measured.

#### 2.2.9. Congo red (CR) binding

CR binding was used to qualitatively assess changes in the cell surface of Mot<sup>-</sup> mutants. Two microliters of an overnight culture was spotted on 2216 agar containing 100 µg CR per ml (27) and the bacteria were incubated at 30°C overnight. The relative color of the mutant colony was compared to a colony of TM1040 inoculated on the same plate as a control. Digital photographs of the colonies were cropped and the color contrast of the entire

plate was increased to show the difference in Congo red binding using Adobe Photoshop CS2.

#### 2.2.10. Biofilm formation

Biofilm formation was assessed by crystal violet (CV) staining using the method of O'Toole and Kolter (74) with minor changes. Bacteria were incubated for 16 h at 30°C with vigorous shaking in 30 x 100 mm glass tubes containing 0.5 ml 2216 broth. Following incubation, the liquid culture was discarded and each tube rinsed with 35 ppt artificial seawater (ASW, 40 g of Instant Ocean in 1 liter of distilled water) to remove loosely attached cells. Cells attached to the tube wall as a biofilm were stained by adding 1 ml CV solution (Becton, Dickinson and company, Sparks, MD) for 30 min at room temperature, with a subsequent wash using ASW to remove unbound CV. CV was eluted from the stained bacteria with a 1:1 solution of dimethyl sulfoxide (DMSO) (Fisher Scientific, Hanover Park, IL) and 95% ethanol (Val Tech Diagnostics Inc., Brackenridge, PA). The amount of CV obtained was measured by spectroscopy at 560 nm using a Bio-Rad model 680 microplate reader.

#### 2.2.11. Chemotaxis assay

A single colony of TM1040 and HG1016 was inoculated in marine motility broth and incubated at 30°C for 3 days. The periphery of motile colonies from both cultures were inoculated onto the same plate of marine basal medium formula #2 (described in Appendix A) containing 10 mM of attractant (one attractant per plate, Methionine, Valine, Glycine, Alanine, Phenylalanine, Succinic acid, Fumarate, malic acid, and acetate). Duplicate plates

containing each attractant were inoculated. The plates were incubated at 30°C for 3 days and the diameter of the motile colonies was measured.

#### 2.2.12. Cell elongation

Cell elongation was observed from overnight cultures of TM1040, HG1016, and RSI02 grown in marine motility broth or 2216 broth at 30°C with shaking. Five to seven microliters of culture was spotted on a glass slide, covered with a cover slip, and observed with phase contrast microscope. The Nikon Optiphot microscope was used for the preliminary experiments where data was recorded as (+) or (-) for elongation and non-elongation, respectively. The Olympus BX60, Qicam Fast 1394 camera, and Volocity software were used for detailed measurement of cell elongation. Snap shots of at least five fields were taken and the cell length of 50 cells of each sample were measured in Volocity software, using the measure tool. The statistical analysis was done by using the Newman-Keuls multiple comparison test in GraphPad software.

#### 2.2.13 Construction of pRSI506 for complementation of *flaC* mutant

In order to complement the *flaC* mutant and over express FlaC, *flaC* was amplified from the genome using FlaC-F primer (CAGTCCCATCCTCAGATCCACTC) and FlaC-R primer (GACAGGGAGGATGCATATCGTGAC) that amplifies *flaC* with 235 bp upstream and 100 bp downstream which yields a PCR fragment of 1022 bp (Fig. 6A). The PCR fragment was ligated into the pCR2.1 (Invitrogen, Carlsbad, CA), electroporated into *E. coli* strain DH5 $\alpha$  and selected for kanamycin resistant colonies to obtain pRSI505 (Fig. 6B). The *flaC* fragment was digested from pRSI505 with EcoRI and ligated into pRK415 that was digested with the same enzyme. The ligation reaction was then electroporated into *E. coli* strain S17-1 $\lambda$ pir, screened with X-Gal (40  $\mu$ g/ml), and selected for tetracycline (15  $\mu$ g/ml)

resistance colonies to obtain pRSI506 (Fig. 7). The pRSI506 plasmid and pRK415 (control) was transferred into HG1016 (for complementation) and RSI01 (TM1040 rifampicin resistance) (for over expression of FlaC) by biparental mating. Colonies of HG1016 with pRSI506 or pRK415 were selected for kanamycin (120 µg/ml) and tetracycline (15 µg/ml) resistance on HIASW10 (heart infusion artificial sea water 10 ppt). The colonies of RSI01 containing pRSI506 or pRK415 were selected for rifampicin (100 µg/ml) and tetracycline (15 µg/ml) resistance on HIASW10. The presence of pRSI506 or pRK415 in HG1016 and RSI01 were confirmed by colony PCR (Fig. 8). The pRK415 in both HG1016 and RSI01 were determined by using M13 Forward (-20) primer (GTAAAACGACGGCCAG) and M13 Reverse primer (CAGGAAACAGCTATGAC) to amplify a 100 bp band from pRK415 (Fig. 8A and Fig. 8 B, lane 6-9). The *flaC*::EZ-Tn5 (3022 bp) in HG1016 and wild-type *flaC* (1022 bp) in RSI01 were also amplified to confirm that the host strains were correct (Fig. 8D, lane 8-11). The pRSI506 in HG1016 was confirmed by amplifying a 1022 bp band (representing *flaC* on the plasmid) and 3022bp (representing *flaC*::EZ-Tn5 on the chromosome) using *flaC*-F and *flaC*-R primers (Fig. 8C and Fig. 8D, lane 6 and 7). The pRSI506 in RSI01 was confirmed by using M13 Forward (-20) and M13 Reverse primers to amplify a 1055 bp band containing the *flaC* fragment from the plasmid (Fig. 8C and Fig. 8B, lane 10-11). In addition, inner-ctrA-F (CGCATTCTTCTGGTCGAGGATGAT) and inner-ctrA-R primers (AGCACATAGCCACGGCCCC) were used to amplify a 659 bp fragment from the *ctrA* gene on the chromosome of RSI01 to confirm that it was the correct host strain (Fig. 8 D, lane 14 and 15).

#### 2.2.14 Construction of pRSI507 for site specific mutagenesis of *flaC*

In order to try to reconstruct the mutation in *flaC*, the inner region of *flaC* contain 456 bp (from bp 109-564) was amplified from pRSI505 using *flaC*-inner-F primer

(AACTGCAGGATGGCCAAGGAGCGATG, underline bases are *Pst*I over hang with 2 bp for enzyme binding) and *flaC*-inner-R primer (TCCCCCGGGATTGTAGCCCCAGACCTCGT, underline bases are *Sma*I over hang with 3 bp for enzyme binding) (Fig. 9A). After digesting the PCR product with *Pst*I and *Sma*I, it was ligated with pK18mobsacB that was digested with the same enzymes. The plasmid was called pRSI507 (Fig. 9B). The pRSI507 was electroporated into TM1040 and select for kanamycin resistant (120 µg/ml) colonies on HIASW. The presence of pRSI507 was confirmed by colony PCR using a pair of primers that one primer binds to the kanamycin resistance gene on the pRSI507 (pK18mobsac-Kan-R primer) and the other primer binds on the chromosome (*flaC*-R primer) to amplify a 1982 bp band (Fig. 10A and B). An internal control that amplified an internal region of *ctrA* (659 bp) from the chromosome was also included (Fig. 10B). Nine clones out of 11 contained pRSI507 that recombined into *flaC* on the chromosome (Fig. 10B, lanes 4-8, 10-12, and 14). One of the nine clones chosen was called RSI02.

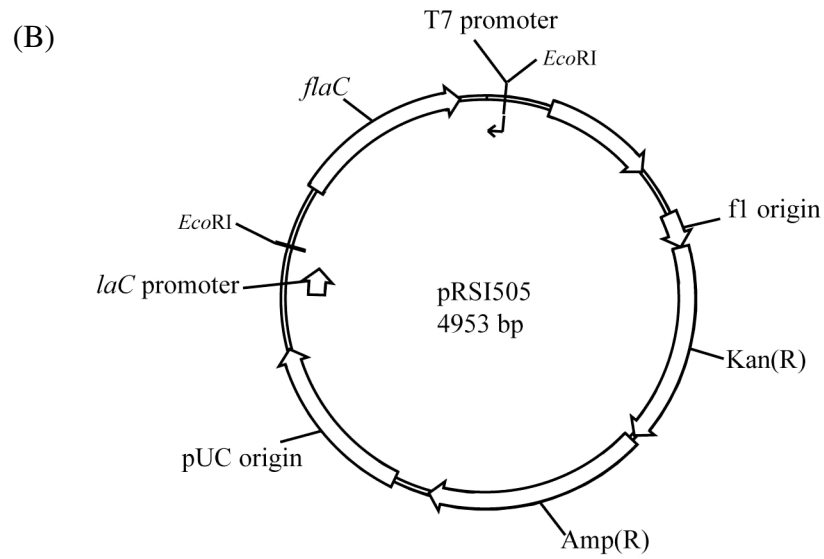
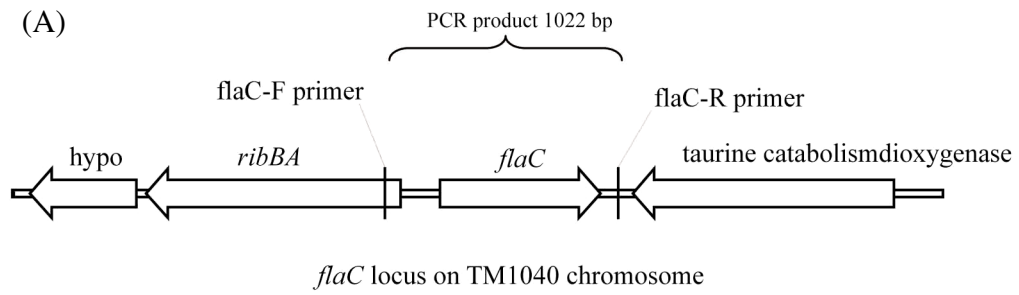


**FIG. 6** Plasmid map of pRSI505. (A) DNA fragment containing *flaC* was amplified from the chromosome using *flaC*-F and *flaC*-R primers and ligated into pCR2.1 TOPO. (B) The new plasmid was called pRSI505.

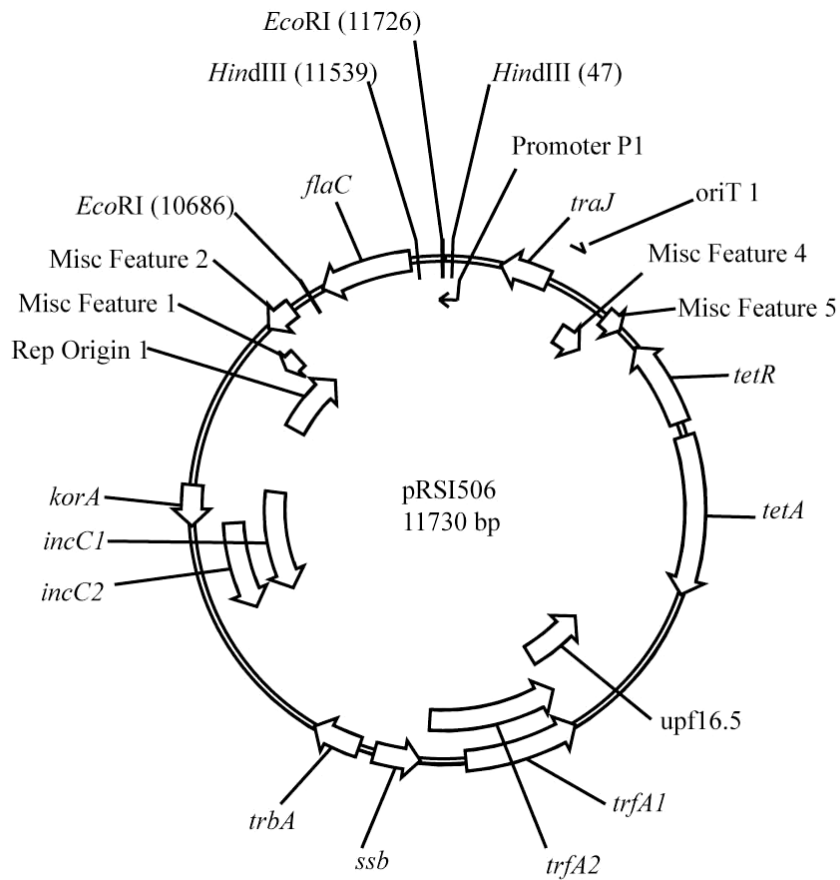


**FIG. 7** Plasmid map of pRSI506. The DNA fragment containing *flaC* was digested from pRSI505 with *EcoRI* and ligated into pRK415. The new plasmid was called pRSI506 and used for complementation and over expression of *flaC*.

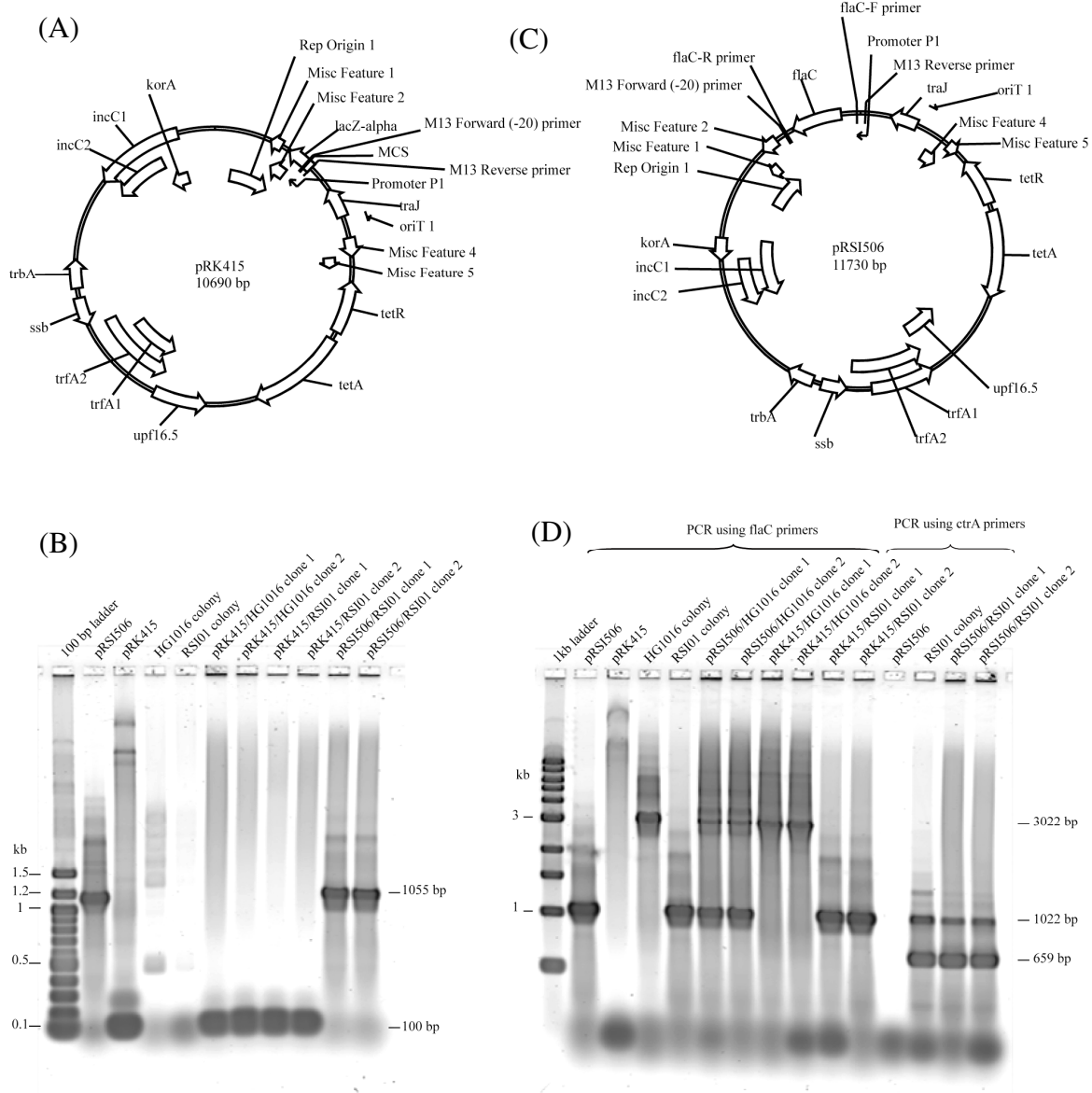


**FIG. 8** Confirming presence of pRSI506 in HG1016 and RSI01. (A) Plasmid map of pRK415 indicating the binding site of M13 Forward (-20) and M13 Reverse primers. (B) Colony PCR using M13 Forward (-20) and M13 Reverse primers. (C) Plasmid map of pRSI506 indicating the binding site of flaC-F, flaC-R, M13 Forward (-20), and M13 Reverse primers. (D) Colony PCR using flaC-F, flaC-R, inter-ctrA-F, and inter-ctrA-R primers.

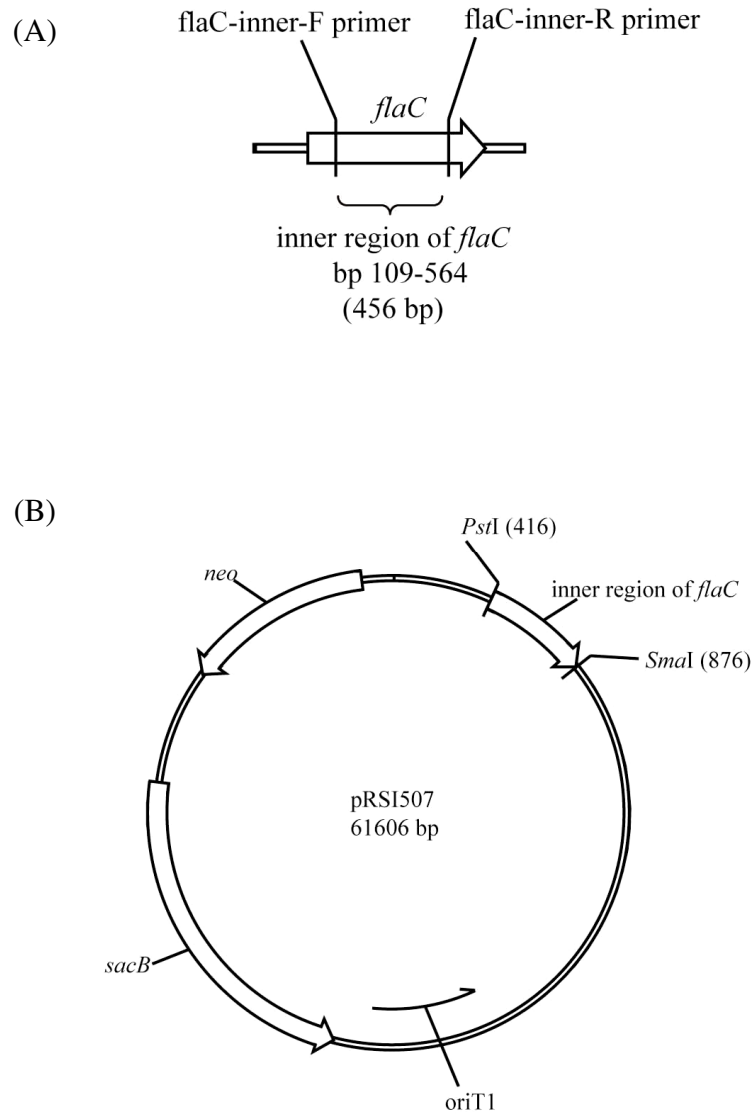


**FIG. 9** Plasmid map of pRSI507. (A) The inner region of *flaC* (456 bp), starting from bp 109-564 of *flaC*, was amplified using *flaC*-inner-F and *flaC*-inner-R primer. (B) The *flaC*-inner region of *flaC* was ligated into pK18mobsacB. The plasmid was called pRSI507.

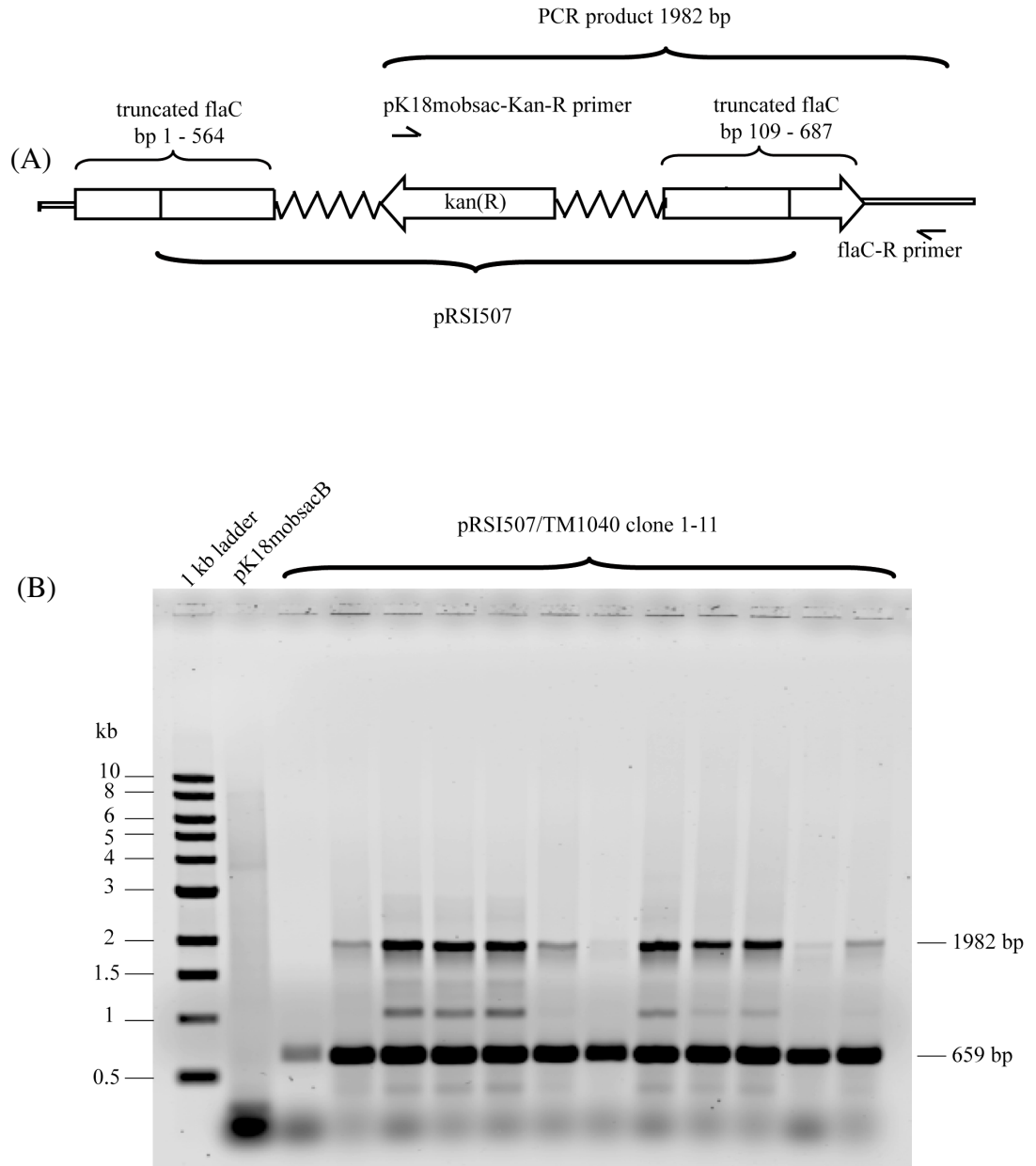


**FIG. 10** Confirming the presence of pRSI507 in TM1040. (A) Diagram of pRSI507 recombined into the chromosome. The primers that were used in the colony PCR reaction are labeled. (B) Colony PCR of pRSI507/TM1040 clone 1-11 using pK18mobsac-Kan-R primer (binds on the plasmid) and flaC-R primer (binds on the chromosome) that gives a PCR product of 1982 bp. Primers that bind in *ctrA* were used as an internal control that gives a PCR product of 659 bp.

#### 2.2.15 Measurement of cell elongation of site specific mutagenesis of *flaC* (RSI02)

Overnight cultures of RSI02, TM1040, and HG1016, grown in 2216 and marine motility medium at 30°C with shaking, were observed with phase contrast microscopy. Snap shots of at least five fields were taken and the cell length of 50 cells of each sample were measured in Volocity software, using the measure tool. The statistical analysis was done by using Newman-Keuls multiple comparison test in GraphPad software.

## 2.3. Results

### 2.3.1. Organization of the flagellar loci

In a recent study, we identified more than 40 Open Reading Frames (ORFs) in the genome of TM1040 with homology to flagellar biosynthesis genes of other bacteria (38). To continue this effort, we analyzed these flagellar ORFs on the TM1040 genome by genomic and bioinformatic approaches to provide insight into the organization and regulation of flagellar biosynthesis.

The genes responsible for the structural components of the flagellum are located in 9 loci scattered around the 3.2 mb chromosome (70), with two genes (*fliY* and *fliC1*) harbored on pSTM1 (823 kb megaplasmid) as two separate loci. No flagellar biosynthetic genes were found on pSTM2 (131 kb plasmid) (70) or pSTM3 (130 kb plasmid) (32). Among the 9 flagellar loci, the largest locus contains genes encoding TTSS, a C-ring component, motor proteins, MS-ring, P-ring, L-ring, rod components, hook, hook junction proteins, and the basal body protein (*fliL*) (Fig. 11A) (13). The novel flagellar gene *flaA*, previously described by us (65), and a homolog of *C. crescentus pflI*, a protein involved in flagella positioning (75), are also located in this locus, as are three hypothetical proteins of unknown function. The flagella biosynthetic genes in, this large flagella loci (Fig. 11A), are class II and class III genes based on *C. crescentus* hierarchy.

The first operon (*motB1-flgI*) (Fig. 11A) are class III genes encoding for motor, hook junction protein, P-ring, and hook which is organized exactly like in *R. sphaeroides* but in *S. meliloti* the *flgI* and *motB* are in different operons (Fig. 12).

The second operon (*fliF-fliP*) (Fig. 11A) contains class II genes encoding MS-ring, C-ring component, and TTSS. This operon has the same orientation as in *R. sphaeroides* except for *fliO* that is substituted with *fliH*, but still encodes for TTSS components (Fig. 12).

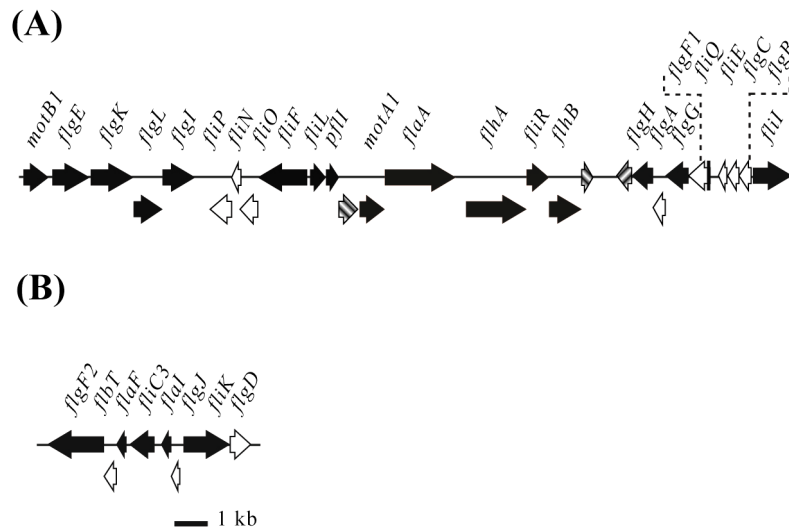
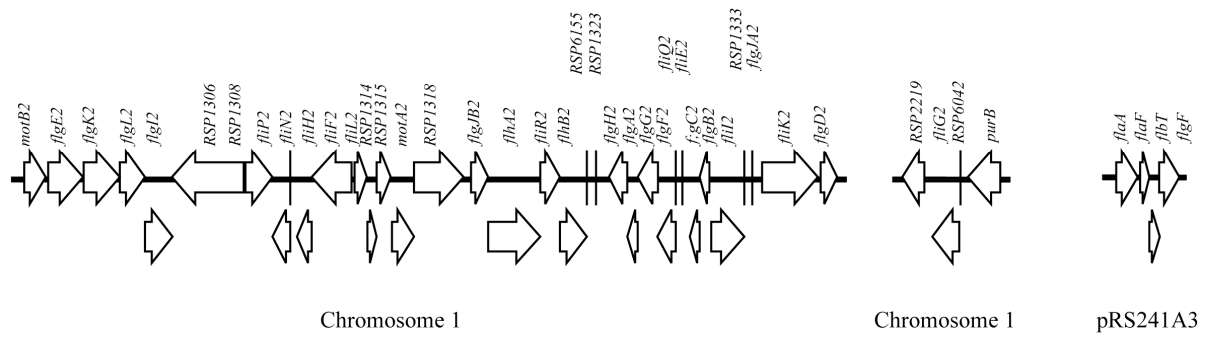


**FIG. 11** Flagellar loci on the TM1040 genome. Two large genetic loci (indicated by (A) and (B)) contain most of the flagellar structural genes and two regulatory genes. The white arrows indicate genes that were identified by genomic analysis, the black arrows are genes identified by mutagenesis, and the hashed arrows indicate hypothetical proteins that were identified by bioinformatic methods. ORFs that overlap are indicated by lowering the position of ORF.

*R. sphaeroides* fla2 flagellar loci



*S. meliloti* flagellar loci

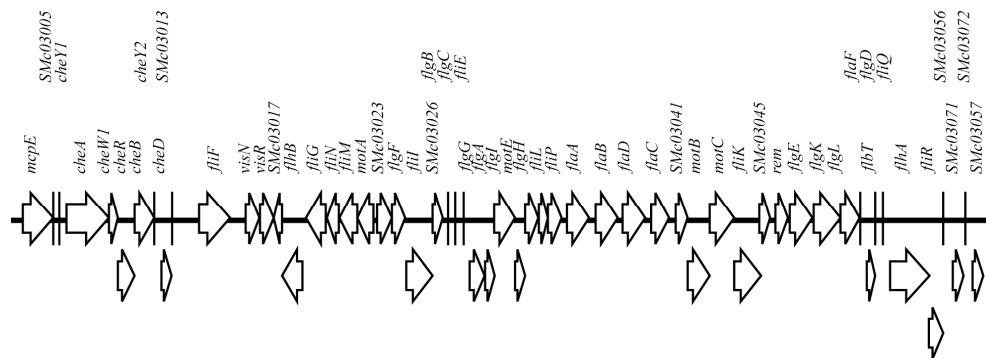


**FIG. 12** Flagellar loci of *R. sphaeroides* (fla2 flagellar loci) and *S. meliloti*. The white arrow represent the gene in the flagellar loci. Gene with small sizes are represent by vertical lines.

In *S. meliloti*, this operon is completed differently, all of the genes are in separate operons (Fig. 12).

The third operon contains *fliL* (basal body component), *pflI* (flagellar localization protein), hypothetical protein (homolog to CC\_2059, downstream of *pflI* in *C. crescentus*), *motA1* (motor), and *flaA* (novel flagellar gene) (Fig. 11A). This operon in TM1040 is similar to *R. sphaeroides* except for the *flaA* gene of TM1040 is substituted with an unknown function protein (RSP\_1318) in *R. sphaeroides* which has low homology to *flaA* in TM1040 (only 29% identity) (Fig. 12). In contrast, *S. meliloti* has the genes in different operons, the *motA* is in the same operon as *fliMNG* (C-ring) and *fliL* is in the same operon as *fliP* (TTSS) (Fig. 12).

The fourth operon (*flhA*-hypothetical protein) (Fig. 11A), are class II genes, that encode for the TTSS. This is similar to *R. sphaeroides* except that the operon starts with *flgJB2* that is a rod component (Fig. 12). This is also similar in *S. meliloti* except that *flhB* is in a separate operon with another unknown function protein (Fig. 12).

The fifth operon (*flgB*-hypothetical protein) (Fig. 11A) contains both class II and class III genes, encoding for proteins that assemble into the HBB complex (basal body rod proteins, hook basal body component, TTSS, proximal rod, L-ring). This operon is the same in *R. sphaeroides* (Fig. 12). In *S. meliloti*, *fliQ* is in a different operon but is still associated with genes encoding for the hook components, and *flgF* is upstream of *flgB*, in a different operon (Fig. 12).

The sixth operon contains only *fliI* (Fig. 11A), class II encoding for TTSS component, is the same in *R. sphaeroides* but slightly different in *S. meliloti*. In *S. meliloti*, the *fliI* is in the same operon as *flgF* that encodes for the proximal rod (Fig. 12).

The second largest locus (Fig. 11B) contains class III and IV genes, six of these genes are involved in hook and filament synthesis (*flgD*, *flgF2*, *flgJ*, *fliC3*, *fliK*). The first operon (*fliC3-flgF2*) (Fig. 11B), class III and class IV genes, encode for the proximal rod, flagellin regulators, and the flagellin. This operon is the same in *R. sphaeroides* but in *S. meliloti*, the flagellin is in a different operon than the flagellin regulators (*flbT* and *flaF*) (Fig. 12). The second operon on this flagellar locus of TM1040, contains *flgJ* (encodes for rod assembly protein) and an unknown function protein named *flaI* (Fig. 11B). *R. sphaeroides* has two *flgJ*, named *flgJA1* and *flgJA2* that are separated in different operons (Fig. 12). The *flgJA2* operon in *R. sphaeroides* is the one similar to the *flgJ* operon in TM1040. The slight difference is that *R. sphaeroides* has a gene encoding for an unknown function protein downstream of *flgJA2* (RSP1333) whereas in TM1040 is *flaI*. *S. meliloti* do not contain this operon or homologs to *flgJ* or *flaI* from TM1040. This could suggest that there are other flagellar proteins substituting for their function in *S. meliloti*. The third operon on this TM1040 flagella locus (Fig. 11B) contains *fliK* and *flgD*, encoding for hook length control and hook capping protein. This operon is the same in *R. sphaeroides* but in *S. meliloti*, these two genes are separated in two operons, *fliK* is in an operon that encodes for the motor proteins while *flgD* is in the same operon as *flbT* and *flaF* that encode the flagellin regulators (Fig. 12).

Besides the two large flagellar loci shown in Figure 11A and 11B, TM1040 has other small flagellar loci scattered around the genome (Fig. 13).

The *motA2* locus contains a gene encoding for ChaC-like protein upstream of *motA2* and *motB2* downstream in the operon (Fig. 13). This is the same in *R. sphaeroides*, where RSP2288 and RSP2289 are homologs to *motA2* and *motB2*, respectively. For *S. meliloti*

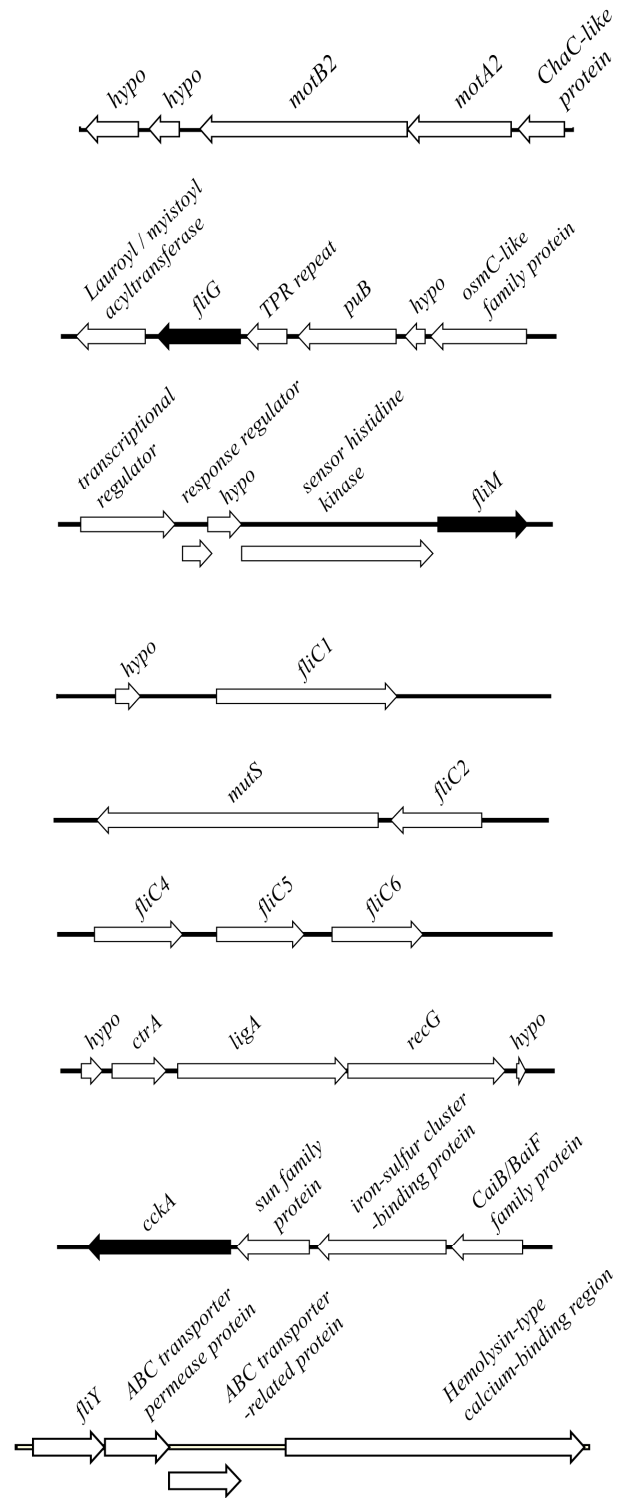


**FIG. 13** Other flagellar loci on the genome of TM1040. The white arrows indicate genes that were identified by genomic analysis, the black arrows are genes identified by mutagenesis.

flagellar loci, besides *motA* and *motB*, it has another two *mot* genes that encode for MotC that binds to *motB*, and MotE that functions as a chaperon for proper folding (Fig. 12) (29).

The *fliG* locus contains the class II gene *fliG* encoding for one of the C-ring components (Fig. 13). When compared to *R. sphaeroides* using the same criterion for genes in an operon organization as Poggio *et al.* (2007) (30 bp between stop and initiation codons of two continuing genes in the same orientation), the *fliG* in TM1040 is monocistronic and is the same as *fliG* in *R. sphaeroides* (Fig. 12). The *fliG* gene in *S. meliloti* also seems to be monocistronic based on the same criteria but is downstream of *fliM* and *fliN* that encodes for the other C-ring component whereas *fliG* in both TM1040 and *R. sphaeroides* are separated from *fliM* and *fliN*, and is also separated from the main flagellar loci (Fig. 12).

The *fliM* locus contains the *fliM* gene encoding for one of the C-ring components and has a transcription response regulator, response regulator receiver protein, hypothetical proteins, and a sensory histidine kinase protein upstream in the same operon (Fig. 13). This could suggest that these unknown regulators upstream of *fliM* could regulate *fliM* and possibly other class II genes in TM1040. Similar orientation is seen in *R. sphaeroides* which upstream of *fliM* (RSP\_6099) is a Na<sup>+</sup>/solute symporter, two hypothetical proteins, and a transcriptional regulator. In *S. meliloti*, the *fliM* is in same operon of *fliN*, that encodes for the other C-ring component, and *motA* (Fig. 12). Like *fliG*, *fliM* in *S. meliloti* is located in same locus as the other flagellar genes while in TM1040 and *R. sphaeroides*, *fliG* in both species are separated from the other flagellar loci and the other two components of the C-ring (*fliG* and *fliN*).

TM1040 has six copies of putative flagellin genes called *fliC1-6*. The *fliC3* gene is located on second largest flagellar loci (Fig. 11B) upstream of the flagellin regulators *flaF* and *flbT* while the other five flagellins are scattered though out the genome. This suggests that *fliC3* may be the essential flagellin that is required for filament biosynthesis. The flagellin loci containing *fliC1* (Fig. 13) is located on pSTM1 while the other four flagellin

genes reside on the chromosome. The *fliC4-6* are on the same locus with in the same orientation but is predicted to be monocistronic based on the bp between *fliC4-5* is 329 bp, and *fliC5-6* is 262 bp (Fig. 13). The *fliC2* gene is separated on another locus containing *fliC2* and *mutS* (encoding for a DNA mismatch repair protein) (Fig. 13). The analysis of upstream regions of these flagellin genes indicate that *fliC1*, *fliC3*, *fliC4*, and *fliC5* contain putative ribosome binding sites suggest that they could be transcribed (AGGAACT for *fliC1* and *fliC3*, AGGTGCT for *fliC 4* and *fliC5*) (the Shine-Dalgarno sequence in *E. coli* is AGGAGGT (68)). Further analysis upstream of these genes did not reveal a  $\sigma^{54}$  or  $\sigma^{28}$  binding sites based on mrNrYTGGCACG-N4-TTGCWNNw (12) and TAAA-N15-GCCGATAA (38), respectively. In *R. sphaeroides*, there is only one flagellin encoding gene in fla2 flagellar loci, called *flaA*, which on the pRS241A3 plasmid (80) and the gene neighborhood is exactly like in *fliC3* operon in TM1040 (Fig. 11B and Fig. 12). This suggests that regulation of the *fliC3* in TM1040 and *flaA* in *R. sphaeroides* should be the same. *S. meliloti* has four gene that encode flagellin, *flaA-D*, they are all in the same orientation on the flagellar locus but are transcribed separately (Fig. 12) (86). The flagellin genes are not upstream of the flagellin regulator like TM1040 or *R. sphaeroides*. Scharf *et al.* (2001) has demonstrated that *flaA* is the most essential flagellin and at least one more flagellin subunit is required for filament biosynthesis (86).

The class I genes in TM1040 (*cckA/ctrA*) are separately located in different loci on the chromosome. The *ctrA* locus contains *ctrA* with DNA ligase (*ligA*) and ATP-dependent DNA helicase (*recG*) downstream, in the gene neighborhood. On the other hand, the *cckA* locus has *cckA* with upstream genes encoding for sun family protein, iron sulfur cluster binding protein, and L-canitine dehydratase/bile acid-inducible protein (Fig. 13). To my knowledge, the class I regulator genes for the fla2 flagellar loci in *R. sphaeroides* has not be determined (80), but base on the high similarity of the organization of the flagellar gene between TM1040 and *R. sphaeroides*, it suggests that fla2 may also be regulated by *cckA* and

*ctrA* homologs in *R. sphaeroides*, RSP\_0454 and RSP\_2621, respectively. The *cckA* locus in *R. sphaeroides* contains a gene encoding for a sun family protein, upstream like in TM1040. The *ctrA* locus of *R. sphaeroides* is also exactly like in TM1040. In *S. meliloti*, the class I genes are *visN* and *visR*, and are located with other flagellar gene in one large flagellar loci (Fig. 12) (93). The location of these class I genes is not surprising, since *visN* and *visR* seem more specific to flagellar biosynthesis in *S. meliloti*, while *cckA/ctrA* in *C. crescentus* also known to regulate other phenotypes associated with cell life cycle.

The *fliY* locus contains *fliY*, a class II gene encoding for one of the TTSS components, with downstream genes encoding for ABC transporter permease protein and ABC transporter-related protein (Fig. 13). In *R. sphaeroides* *fla2* and *S. meliloti* flagellar loci do not contain *fliY*, it is possible to predict other proteins are compensating for its function.

### 2.3.2. Identification of flagellar genes by transposon mutagenesis

To provide functional significance to the flagellar ORFs that I found by genomic analyses and to identify novel genes involved in motility, I screened a mutant library containing 11,284 transposon mutants for defects in swimming motility (Mot<sup>-</sup>). 183 Mot<sup>-</sup> mutants were identified and the sequence of 77 of these genes was determined. The data revealed that the transposon had inserted in 21 out 37 flagellar structural genes and two flagellar regulatory genes (*flaF* and *cckA*) identified previously by the genomic approach, and also had inserted in six novel ORFs (*flaB*, *flaC*, *flaD*, *flaE*, *flaG*, *flaI*, Table 2). Interestingly, among the six flagellin alleles, only mutations in *fliC3* resulted in Mot<sup>-</sup> colonies; no mutations were found in any of the other *fliC* genes despite observing multiple separate mutations in several other biosynthetic genes. This suggests that the FliC3 flagellin is critical for swimming motility under laboratory conditions, while the function of the other five flagellin genes is not know.

All of the mutants were nonmotile, i.e. they did not swim under any condition, with the exception of mutations in *flaC*, *flaE*, *flaG* and *flaI*, which are partially motile (Table 2) (FIG. 14). Partial motility was observed as a motile colony that has a diameter less than TM1040 but larger than a nonmotile colony. Relative comparison in 2216 semi-solid agar, of the diameter of partial motile colonies compared to TM1040 (100%) show that partial motile colonies are only 16-70% of the diameter of TM1040 motile colony (Table 3). The interesting point of this result is that partial motility is the hallmark of mutants defective in chemotaxis genes but in this case, the mutation is in a response regulator (*flaC*), glycosyl transferase (*flaE*), Mannose 1 phosphate isomerase (*flaG*) and a hypothetical protein in the flagellar loci (*flaI*). It is possible that these genes could be indirectly related to chemotaxis or flagellar function.

### 2.3.3. Identification of three novel regulators

An analysis of the deduced amino acid sequence of the 3 out of 6 novel ORFs (*flaE*, *flaG*, and *flaI*), suggest that *flaE* functions as a glycosyl transferase, *flaG* is a Mannose 1 phosphate isomerase and *flaI* is a hypothetical protein in the flagellar loci. The mutations in these three genes have partial motility (as previously mentioned).

Most importantly, the deduced amino acid sequence analysis indicated that three ORFs (*flaB*, *flaC*, and *flaD*) encode for proteins containing regulatory domains (Table 2), based on the following data.

**Table 2.** Phenotype of Mot<sup>-</sup> mutants.

Predicted function	Transposon insertion	Flagella <sup>a</sup> (Flagella stain)	Flagella <sup>b</sup> (SDS-PAGE)	Motility in broth / semi solid agar plate
C-ring	<i>fliM</i>	-	-	-/-
	<i>fliG</i>	-	-	-/-
Export apperatus	<i>flhA</i>	-	-	-/-
	<i>flhB</i>	-	-	-/-
	<i>fliR</i>	-	-	-/-
Export ATPase	<i>fliI</i>	-	-	-/-
MS-ring	<i>fliF</i>	-	-	-/-
P-ring	<i>flgI</i>	-	-	-/-
L-ring	<i>flgH</i>	-	-	-/-
Rod	<i>flgF2</i>	-	-	-/-
	<i>flgG</i>	-	-	-/-
Hook	<i>flgE</i>	-	-	-/-
Hook-length control	<i>fliK</i>	-	-	-/-
HAP	<i>flgK</i>	-	-	-/-
	<i>flgL</i>	-	-	-/-
Flagellin	<i>fliC3</i>	-	-	-/-
Motor complex	<i>motA1</i>	+	+	-/-
	<i>motB1</i>	+	+	-/-
Motor associated	<i>fliL</i>	+	-	-/-
	<i>pflI</i>	-	-	-/-
	<i>flaA</i>	+	+	-/-
Regulators	<i>flaB</i>	-	-	-/-
	<i>flaC</i>	+	+	+ <sup>c</sup> /+ <sup>d</sup>
	<i>flaD</i>	+	+	-/-

	<i>flaF</i>	-	-	-/-
	<i>cckA</i>	-	-	-/-
Unknown function	<i>flaE</i>	+	+	+ <sup>e</sup> /+ <sup>d</sup>
	<i>flaG</i>	-	-	+ <sup>e</sup> /+ <sup>d</sup>
	<i>flaI</i>	-	-	-/+ <sup>d</sup>

---

<sup>a</sup> (+), flagella and (-), cells lack flagella

<sup>b</sup> (+), culture is motile and (-), the culture is nonmotile.

<sup>c</sup> Population of motile cells is greater than wild type.

<sup>d</sup> Diameter of the colony is smaller than wild type

<sup>e</sup> Population of motile cells is less than wild type.

**Table 3.** Comparison of the diameter of partial motile colonies to TM1040, in 2216 semi-solid motility agar plates

Strains	Diameter of motile colonies (mm)				mean	SD	Relative Percentage <sup>a</sup>
	Colony1	Colony2	Colony3	Colony4			
TM1040 (wt)	27.2	27.7	28.4	30	28.33	1.22	100
HG1101 <sup>b</sup> (nonmotile)	3.1	3.3	3.3	2.3	3	0.48	10.59
HG1016 ( <i>flaC</i> )	18.2	20.7	21.2	19.3	19.85	1.36	70.07
HG1049 ( <i>flaE</i> )	5.1	6.2	4.7	4	5	0.92	17.65
HG1100 ( <i>flaI</i> )	15	10.1	9	21.6	11.37	3.19	40.12
HG1122 ( <i>flaG</i> )	4.9	4.9	4.5	4.5	4.7	0.23	16.59

<sup>a</sup> Relative percentage of the colony diameter, compared to TM1040

<sup>b</sup> Nonmotile mutant HG1101 (*fliC3*) is included as a negative control

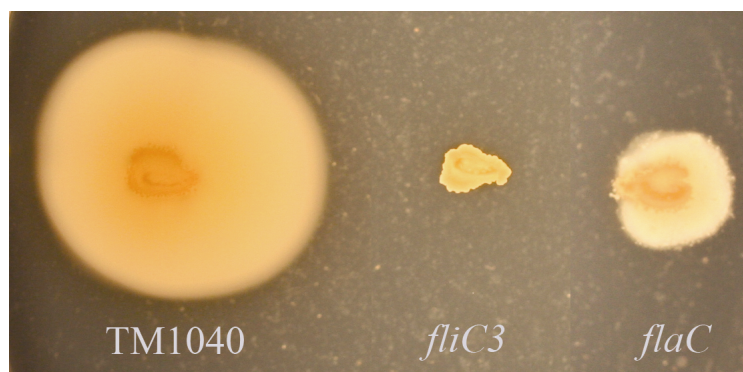


**FIG. 14** Motility in semi-solid agar. TM1040, *fliC3* mutant (representing nonmotile mutants), and *flaC* mutant (representing partial motility mutants) were grown on 2216 semi-solid agar plates (2216 motility plates). The *flaC* mutant has a smaller diameter of motile colony when compared to TM1040.

The first regulator, FlaB, has an N-terminal dimerization and phosphoacceptor domain that is frequently associated with sensory histidine kinases (15), but lacks an apparent C-terminal kinase domain typically found on these proteins (Fig. 15) (15). This suggests that FlaB may function as a phosphorelay protein. Underscoring this possibility FlaB has low homology ( $E = 5e-7$ ) to *Caulobacter virioides* ChpT (DAA06031), a protein that functions to transfer phosphoryl groups from CckA to CtrA (16). The gene neighborhood of *flaB* indicates that it is monocistronic, but did not provide additional information about its function (Fig. 16). The second regulator, FlaC, is predicted to be a DNA-binding regulatory protein, as it contains both an N-terminal CheY-phosphoacceptor domain and a C-terminal DNA binding domain (Fig. 15 and Table 2) (51, 62, 78). Proteins with similar domain architecture are often phosphorylated by a histidine kinase, as a part of a two-component system (100). To predict the histidine kinase that phosphorelates *flaC*, the deduced amino acid sequence of *flaC* was analyzed in the STRING database (Search Tool for the Retrieval of Interacting Genes/Proteins) (108). The result predicted that TM1040\_1263, histidine kinase homolog, could phosphorylate *flaC*. The BLAST analysis of FlaC indicated that it has close homology (65% identity) to CenR in *C. crescentus* which play a role in cell envelop biogenesis and structure (92). Skerker *et al.* (2005), reported that CenR is phosphorylated by CenK. The homolog of CenK was also found in TM1040, TM1040\_0316 having 34% identity to CenK. The gene neighborhood of *flaC* did not provide any further evidence of the function of *flaC* nor have a gene with homology to histidine kinase (Fig. 16). Upstream of *flaC* is a homolog to *ribBA* gene which in *S. meliloti* is required for the production of riboflavin (116), and downstream a gene predict to be a taurine catabolism dioxygenase. The third regulator, FlaD, is a MarR-type DNA-binding protein with a helix-turn-helix (HTH) domain (Fig. 15 and Table 2) (4, 51).

### FlaB



### FlaC



### FlaD



**FIG. 15** Domains of the three new regulatory proteins. SMART analysis of the deduced amino acid sequence of the three new regulatory proteins. FlaB contains a phosphoacceptor domain at the N-terminus (BLAST). The FlaC has a phosphoacceptor domain at the N-terminus (REC) and a DNA binding domain (PFAM). FlaD contains a MarR helix turn helix DNA binding domain.

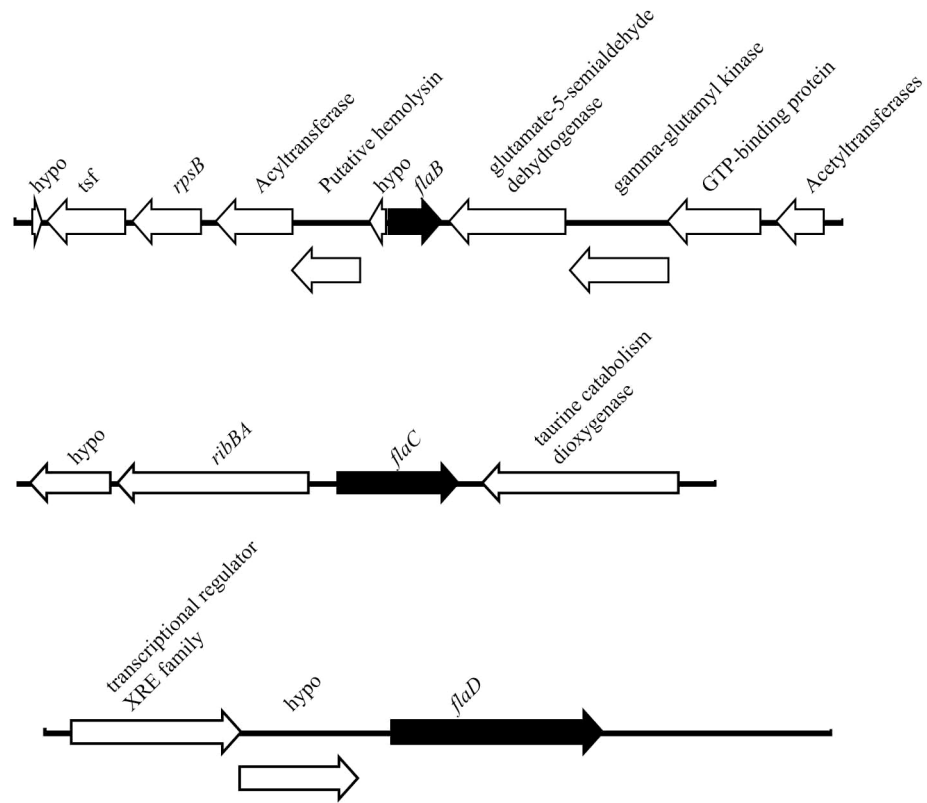


**FIG. 16** Genetic loci of *flaB*, *flaC*, and *flaD*. Arrows white arrows represent genes in the gene neighborhood and the black arrow represent *flaB*, *flaC*, and *flaD*.

The genes neighboring *flaD* suggest that *flaD* is in an operon of three genes, TM1040\_1733, TM1040\_1732 and *flaD*, with TM1040\_1733 encoding a transcriptional regulator of the XRE family (112) and TM1040\_1732 encoding a hypothetical protein (Fig. 16).

#### 2.3.4. Flagella are synthesized by some Mot<sup>-</sup> mutants

In *Salmonella* and other bacteria, defects in *motA* or *motB* result in the synthesis of nonfunctioning, paralyzed flagella (17, 18). Since *motA1* and *motB1* were mutated in our study, we hypothesized that these mutants, while nonmotile, still produced flagella. Using a combination of light and electron microscopy (Table 2) and SDS-PAGE (Fig. 17) (Materials and Methods), we found that strains with defect in *motA1*, *motB1*, *fliL*, *flaA*, *flaD*, or *flaE* have flagella, but do not swim (Table 2 and Fig. 17). Since *motA1*, *motB1*, *fliL*, *flaA*, *flaE*, and *flaD* are non-motile (Table 2) but still have flagella, this suggests that the flagella are paralyzed. Supporting these data, the EM of *motB1* mutant shows the presence of a flagellum at the cell pole of the *motB1* mutant (Fig. 18B) (kindly provided by Dr. Shin-ichi Aizawa, CREST Soft Nano-Machine Project, Innovation Plaza Hiroshima, 3-10-23 Kagamiyama, Higashi-Hiroshima 739-0046, Japan). In addition, mutation in *flaD*, *motA1* and *flaA* seem to produce less flagellin than TM1040. This shows that mutation in *flaD* has the same effect on *motA1* and *flaA* supporting the prediction that *flaD* is a regulator for the motor complex genes. Flagellin was not detected in the *flaE* mutants despite observation from a light microscope, perhaps indicating that the mutation has reduced expression of flagellin. Flagella were not detected in the remaining 22 mutants.

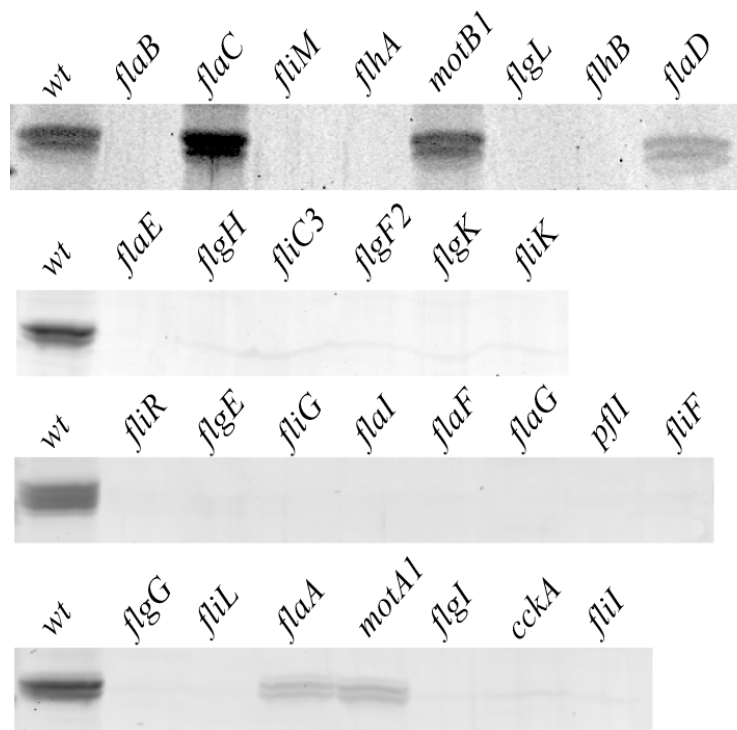


**FIG. 17** SDS-PAGE detection of flagellin. Flagella of TM1040 and mutants were precipitated with Polyethylene Glycol and loaded onto 15% SDS-PAGE gel for detection of flagellin. The upper band migrates at ca. 34 kDa band while the lower is 32 kD. The non-flagellated mutants did not show any bands but the amount of proteins were still measurable may be due to small peptides from the medium left over during the precipitation process which migrated off the SDS-PAGE.

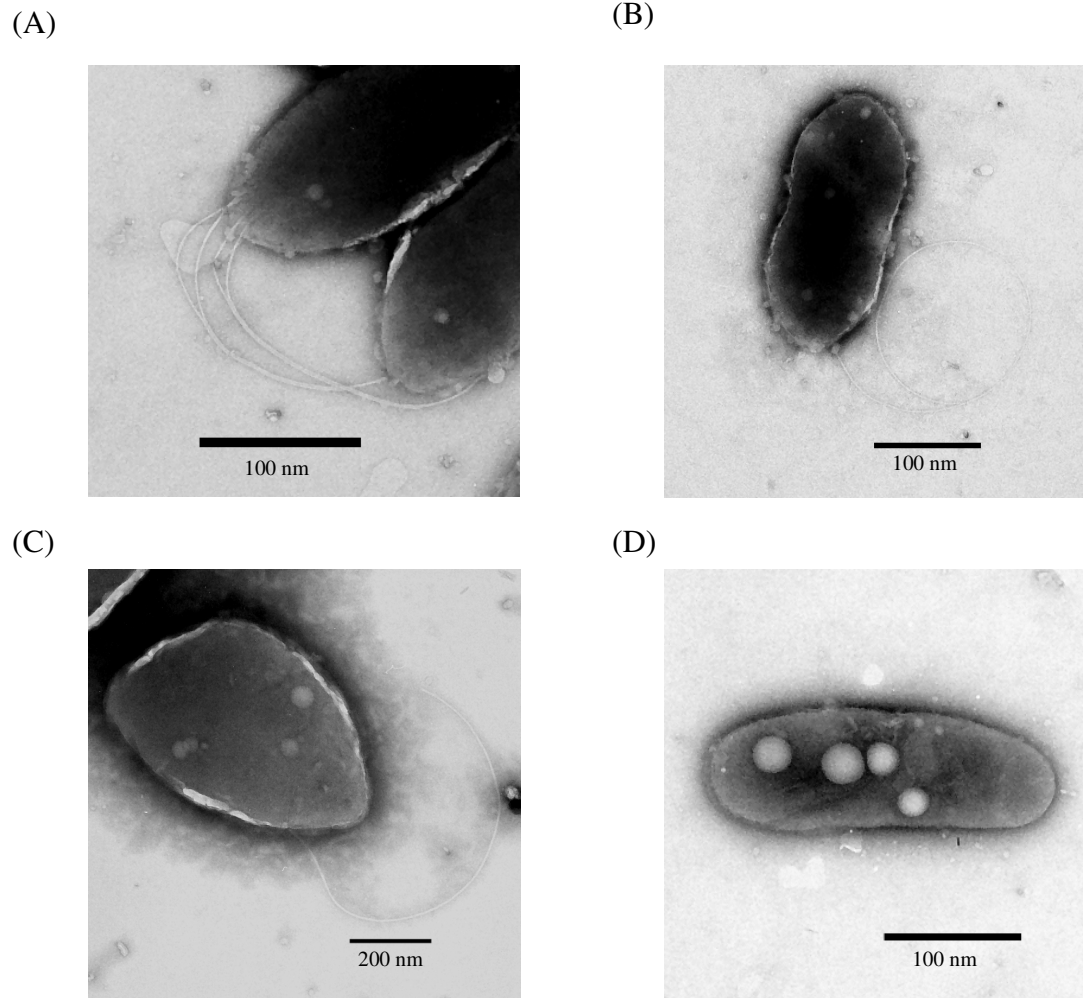


**FIG. 18** Electron microscopy of TM1040, *motB1*, *flaC*, and *fliC3* mutants. (A) TM1040 cell pole with four polar flagella, (B) *motB1* mutant with one flagellum still attached to the cell pole, (C) *flaC* mutant with a single flagellum attached to the cell pole, (D) *fliC3* with no flagella at the cell pole (image provided by Dr. Shin-ichi Aizawa, CREST Soft Nano-Machine Project, Innovation Plaza Hiroshima, 3-10-23 Kagamiyama, Higashi-Hiroshima 739-0046, Japan).

During these studies, it became evident that two flagellin bands of 32 and 34 kDa were consistently observed in SDS-PAGE of those strains that synthesized flagella (Fig. 17). This was unexpected, since the mean molecular weight of FliC is 28.925 kDa and only FliC3 (29 kDa) (Fig. 19) appears to be essential for motility. One hypothesis for the presence of two bands is that another flagellin is expressed and assembled into the filament, most likely is *fliC1* because it has the most similarity to the promoter region of *fliC3* (Fig. 20). The second hypothesis is that the lower band is a degradation product of the upper band. The hypothesis of the for an increase in size of flagellin on SDS-PAGE is that the flagellin is modified via glycosylation. Further experiments are required to support this hypothesis.

#### 2.3.5. Mutation in *flaC* bias the cell towards the motile phase

In analyzing the relative abundance of flagellin obtained from the various mutants, it became apparent that defects in *flaC* resulted in a ca. 2 fold increase, measured by band intensity, in the amount of flagellin produced compared to wild-type (Fig. 17). Even though the amount of total protein loaded is known but the real amount of each band can not be accurately estimated because the samples contain tryptone from the medium. Therefore, the intensity of the flagellin bands were measured by using the normalization function in ImageQuant software. This gives a relative value of 1 to the 34 kDa band of TM1040 and calculates in comparison to other bands. The result showed that if the 34 kDa band of TM1040 is 1, then TM1040 32 kDa is 0.5, and for *flaC* mutant the 34 and 32 kDa band is 1.6 and 1 respectively. This suggests that the amount of flagellin in *flaC* mutant has increased when compared to TM1040. There are two other phenotypes that coincided with the increase in FliC and provide hints about the function of FlaC. First, although initially scored as nonmotile, *flaC* cells are in fact poorly motile when grown in semi-solid agar media, taking much longer than TM1040 to swim outwards (Fig. 21). When calculating the expansion rate of the motile colony of from Figure 21 indicated that TM1040, *flaC*, and *fliC3* had 1.75, 1,

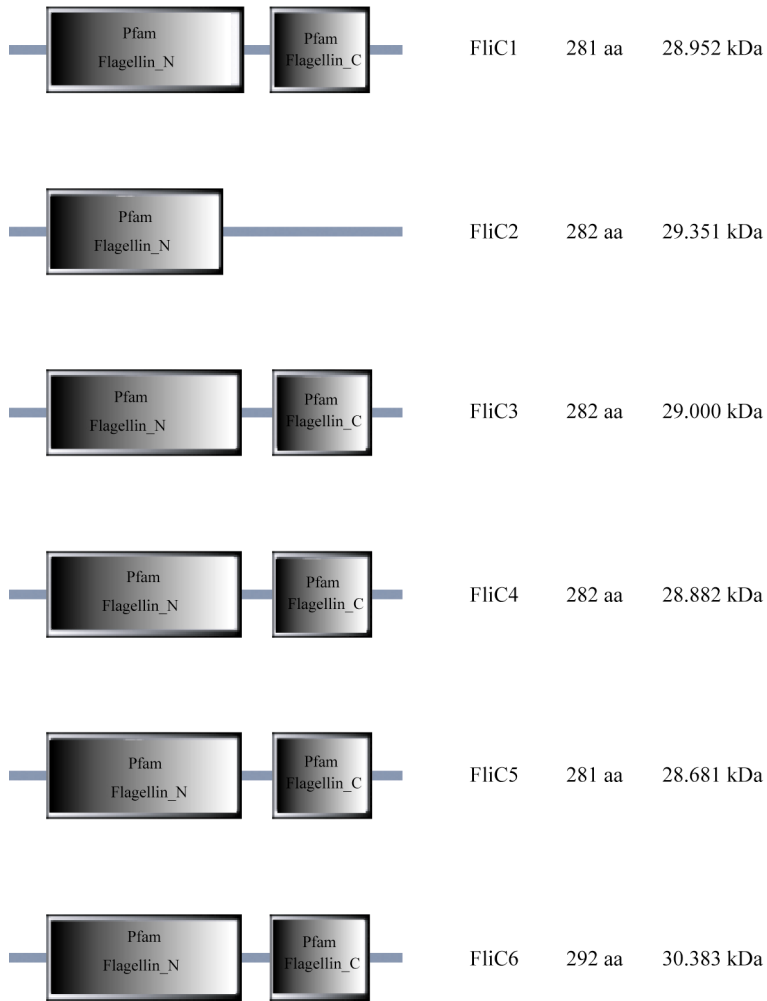


**FIG. 19** Flagellins of TM1040. The figure shows structural domains, size and molecular weight of all six flagellins (FliC1-6) of TM1040. The domains were generated by using SMART website (51) and the molecular weight was calculated by Vector nti suite software. The average molecular weight of FliC is 28.925 kDa.

```

PRO-FLIC1      TGTGGATTGACT-----CAGATTTTCGGG--AGCGAGGCTTTGCAGAATTTTGC-GCGA
PRO-FLIC3      AAAGGGTCTGGATGTCTACAATCGTTCGGGTCAGCGGACC-----AGCTTTGCCACCA
                ** * ** *      **      * * * * * * * * *      *      * * * * * * *
PRO-FLIC1      TAGATGTTGCGCGCGCGACAGGGG-GCAAGTTGCCGTTCTGCGCAATTTGACTCGCATT
PRO-FLIC3      CGGGCAGC-CTCAAAC TAGAGAAGCGCGCCTAACGGTTTTGG--AGGTCGGGACA-ATT
                *      * *      * * * * * * * * *      * * * * * * * * *
PRO-FLIC1      TAGACATATACGCCGACATT-TTAGCTCTTCATTAGCATCCT-CGCGTCAAGAGTTGGCC
PRO-FLIC3      TAAAAATGCAAATTG-CACCATTAGCACTCTCTTAGCATCTAATACGGCAAT-GTCACCT
                ** * ** *      * **      * * * * * * * * * * * * * * * * *
PRO-FLIC1      TGCATCTT-ATTGAGTTTGTGTGTGGAGGCCGAAGTGCCCCGCACGTTGAGAAAGACGAGA
PRO-FLIC3      TGCATCTCGAGCGAGGTGGC-GCGGATACCGCAAGTGAAGCACGGTCAGAATGACGACA
                * * * * * * * * * * * * * * * * * * * * * * * * * * *
PRO-FLIC1      GAGAACACCCCATAAATGGGGGAAAGGG--AATATATC-GGGGCCAAAGTGCTCCTTGCTC
PRO-FLIC3      GAGAGAGCTCCGGTATCGGAGCTGGGATTACCAAATCAGGGGCTAAAGCGCTCCA-AATC
                * * * * * * * * * * * * * * * * * * * * * * * * * *
PRO-FLIC1      AAAGGAACTCATGCT
PRO-FLIC3      AAAGGAACTCATGCT
                * * * * * * * * * * * * * * * * * * * * * * * * * *

```

**FIG. 20** Alignment of upstream region of *fliC 3* and *fliC1*. The upstream region of *fliC3* and *fliC1* (300 bp upstream from start codon) was used to do a ClusterW alignment in <http://www.ch.embnet.org/software/ClustalW.html>. Asterisks indicates identical bases.

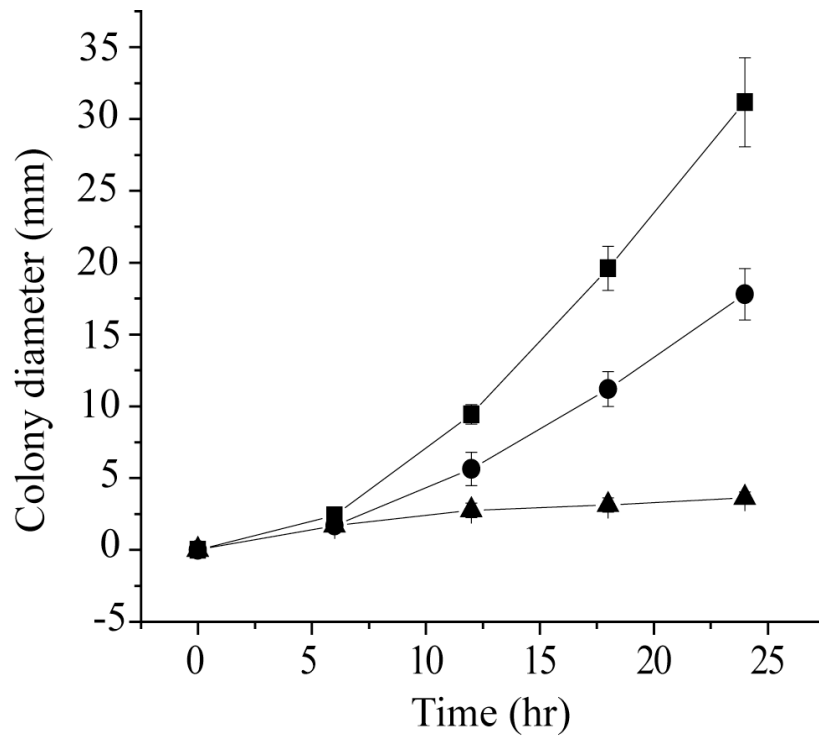


**FIG. 21** Motility of TM1040 and *flaC* mutant (HG1016) in semi-solid agar plate. Transposon insertion in *flaC* has partial motility in semi-solid agar at 30°C. Diameter of motile colonies measured from 0-24 hrs. Symbols: TM1040 (■), *flaC* mutant (●), and *fliC3* mutant (▲).

and 0.07 mm/hr suggesting an approximately 2 fold decrease in swimming rate in semi solid agar, of *flaC* when compared to TM1040. Second and quite unexpected, when grown in 2216 broth, *flaC* population had many more motile cells than wild-type (Table 4). There are ca. 3 times more motile cells in the *flaC* population than in the TM1040 population (20.85% vs. 7.24% motile cells, Table 4) and ca. 2 times less cells in rosettes (14.47% vs. 30.03%, Table 4). Other phenotypic analysis indicate that pigment (Fig. 22A), antibiotic synthesis (Fig. 22B), and biofilm formation (Fig. 23) are also defective in the FlaC<sup>-</sup> strains. Regarding the biphasic life is determined by motile stage cells are small, highly motile and chemotactic cells while in sessile stage, cell form rosettes, biofilm, pigment production and antibiotic production. The FlaC<sup>-</sup> phenotypes suggest that FlaC may be involved in the biphasic switch between motility and sessility in TM1040.

#### 2.3.6. Motility defects also alter the cell surface

We also noted that several of the Mot<sup>-</sup> mutants displayed unusual characteristics, e.g., clumping and biofilm formation, suggesting that the mutation may have resulted in a change in outer surface properties. We assessed changes to the cell surface by addition of the dye Congo Red (CR) to 2216 agar, followed by observation of the binding of the dye to the resulting colony (27). Although most of the Mot<sup>-</sup> mutants were wild-type in CR binding, there were notable exceptions (Fig. 24). FlaC defects resulted in increased CR binding (Fig. 24) and decrease in biofilm formation (Fig. 23). This result that may be anticipated by the postulated role of the protein in involved in the biphasic switch. Mutations in *flaC* are therefore pleiotropic and affect the outer surface of the bacteria in addition to motility, pigment- and antibiotic-production.

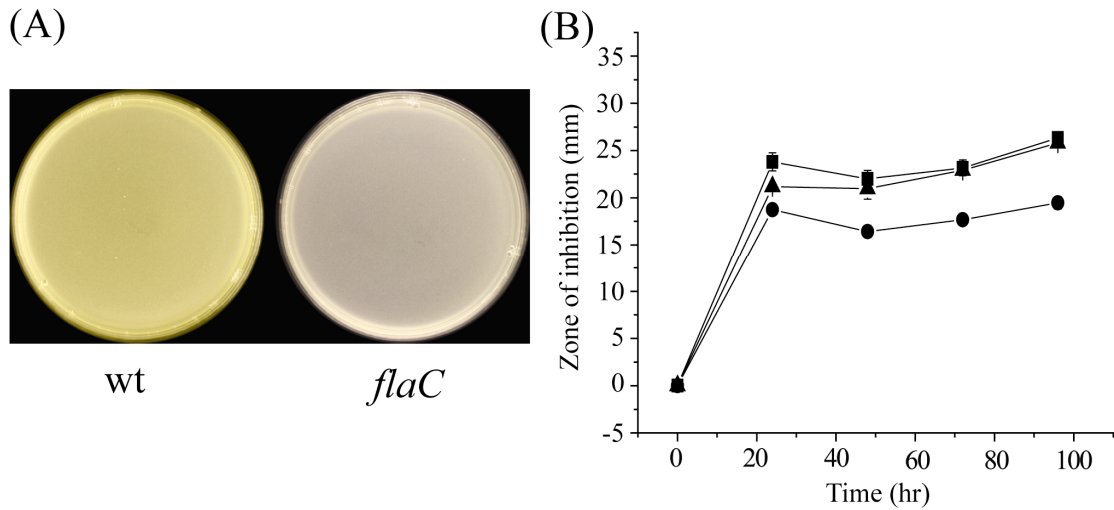
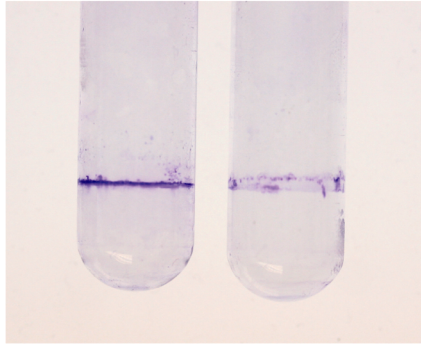


**FIG. 22** Defects in *flaC* result defect in pigment production and antibiotic production. **(A)** Pigment production. Mutation of *flaC* also results in a severe decrease in the yellow-brown extracellular pigment. **(B)** Antibiotic activity. A well-diffusion assay with *Vibrio anguillarum* as a tester strain (12) was used to detect antibiotic activity, demonstrated by a zone of clearing around the well containing the cell-free culture supernatant. Mutation of *flaC* results in a ca. 25% decrease in antibiotic during static growth compared to the controls. Symbols: TM1040 static culture (■), *fliC3* static culture (▲), *flaC* static culture (●).

**(A)**



**(B)**

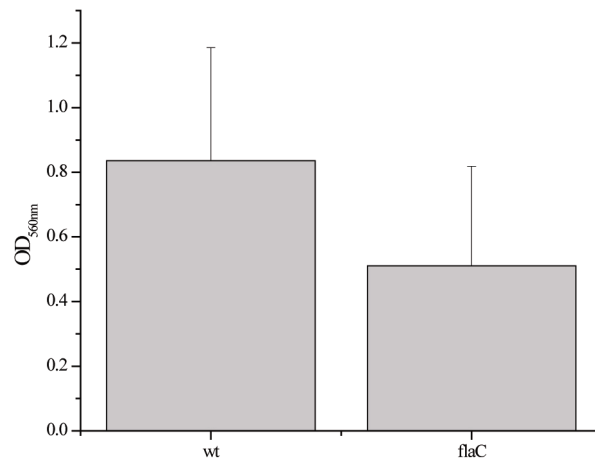


**FIG. 23** Biofilm formation. Mutation in *flaC* showed defect in biofilm production when compare to TM1040 (wt). (A) Biofilm of TM1040 (left) and *flaC* mutant (right) on the test tube. (B) Bar graph of OD<sub>560nm</sub> reading of CV eluted from the biofilm.

**Table 4.** Comparison of % motile cells and % cells forming rosettes of TM1040 and *flaC*

Strains	% Motile cells <sup>a c</sup>	% Cells forming rosettes <sup>b c</sup>	% non-motile single cells <sup>b</sup>
TM1040	7.24 ±4.66	30.03 ±12.75	62.73 ±11.73
<i>flaC</i>	20.85 ±9.01	14.47 ±13.61	64.68 ±9.27

<sup>a</sup> Mean of % motile cells ± SD

<sup>b</sup> Mean of % cells forming rosettes or % non-motile single cells, ± SD

<sup>c</sup> Means are statistically different based on unpaired t-test (95% CI, P-value < 0.05).

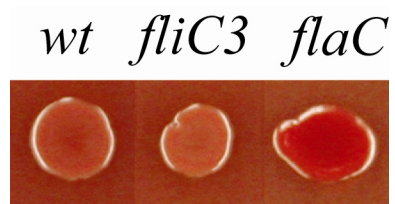


**FIG. 24** Detection of outer cell surface changes. Congo Red binding. Mutations in *flaC* shows increase binding of dye compared to wild type and *fliC3* indicating a change in outer surface properties.

### 2.3.8. Mutation in *flaC* is not defective in chemotaxis

One of the phenotypes of the *flaC* mutant mentioned previously, is that it has partial motility in semi-solid agar when compared to TM1040. This phenotype is also seen in some type of mutants with defects in chemotaxis. Therefore, the chemotaxis of the *flaC* mutant was tested in a basal medium containing 10 mM attractant, as described in Materials and Methods (Fig. 25). The result showed that the *flaC* mutant has wild-type response to all the attractants, suggesting that the mutation in *flaC* did not affect chemotaxis of the mutant.

### 2.3.9. Mutation in *flaC* has filamentous cells

Another phenotype of *flaC* is that it produces elongated cells with blebs, when grown in Marine motility medium (Fig. 26). As previously mentioned that FlaC has high homology to CenR in *C. crescentus*, the cell elongation and bleb formation phenotype seen Fig. 26 of the *flaC* mutant correlates with the mutation in *CenR* (92). In contrast, mutation in *cenR* is also lethal (92), while *flaC* is not. These data along with the bioinformatic analysis of *flaC*, previously mentioned, supports the idea that FlaC functions similar, but not the same, as CenR because of the lethality of the mutation in *cenR*.

The major difference in between 2216 broth and marine motility medium is the amount of nutrients. The 2216 broth has 0.5% peptone with 0.1% yeast extract while marine motility medium has only 0.1% peptone. Therefore, a preliminary experiment was performed to test the hypothesis that cell elongation in the *flaC* mutant is a response to decrease amount of nutrients. The preliminary experiment observed the population of cell elongation in marine motility broth supplemented with 1-0.0156% peptone in comparison to 2216 broth.

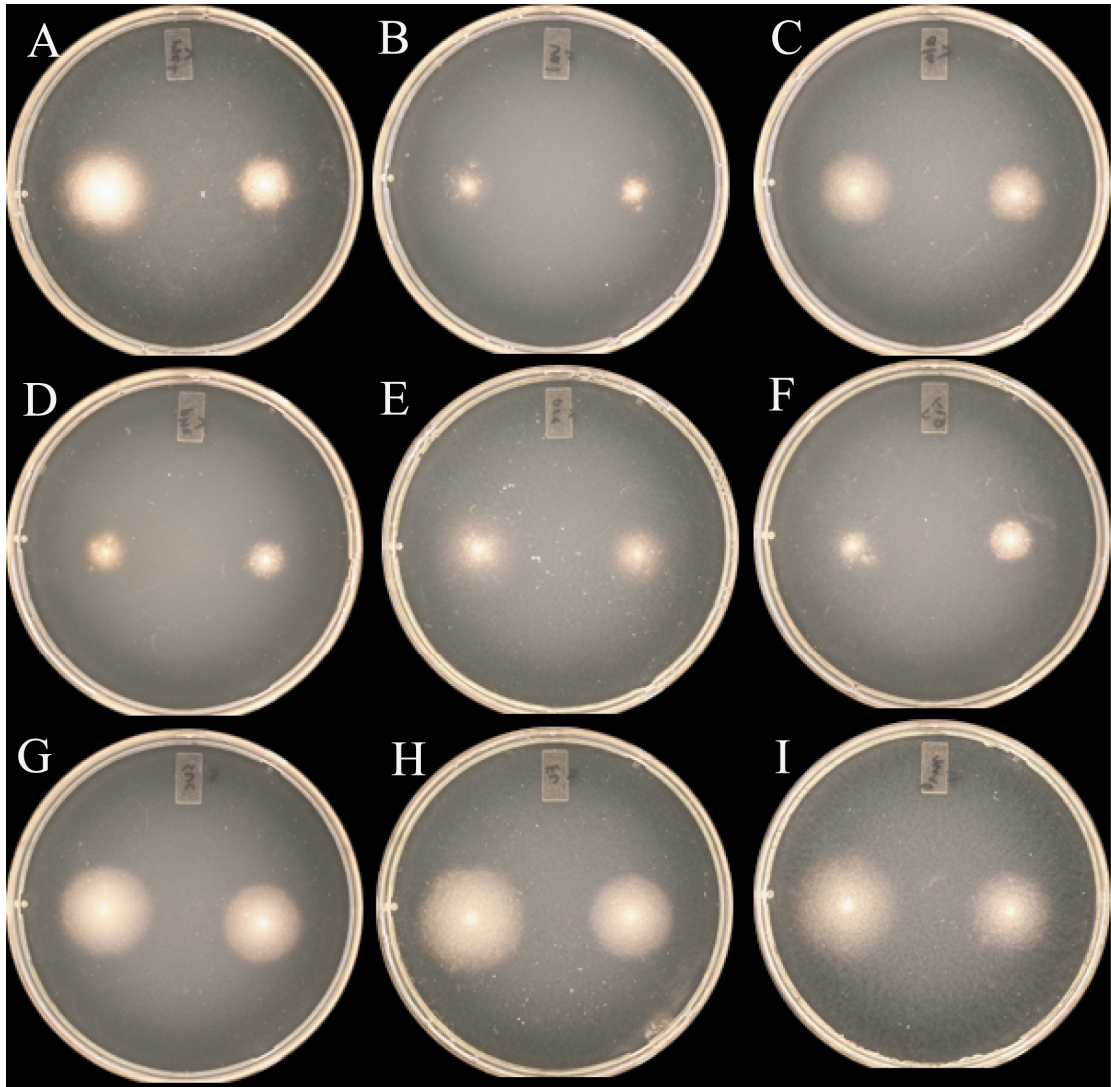


**FIG. 25** Chemotaxis plate assay. Marine motility plate containing 10 mM of attractant [(A) Methionine, (B) Valine, (C) Alanine, (D) Phenylalanine, (E) acetate, (F) Glycine, (G) Succinic acid, (H) Fumarate, (I) malic acid] were inoculated with TM1040 (left colony) and *flaC* mutant (right colony) from the periphery of a motile colony and incubated at 30°C for 2 days.

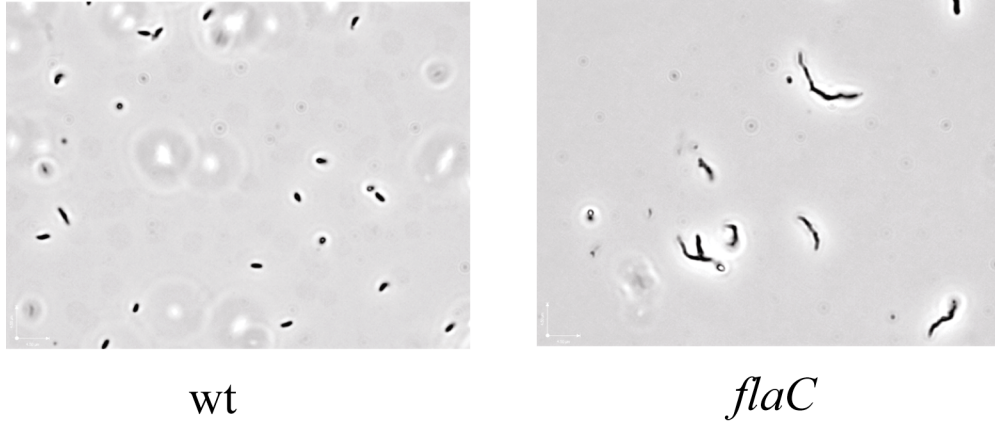


**FIG. 26** Filamentous cells of the *flaC* mutant. Phase contrast microscope images of TM1040 (wt) and the *flaC* mutant grown in Marine motility broth at 30°C with shaking overnight. The *flaC* mutant forms filament-like cells.

The result showed no difference in population of elongated cells in the various concentrations of peptone which disagrees with the hypothesis (Table 5). To investigate the affect of growth phase on the population of elongated cells, cultures of *flaC* mutant grown in marine motility medium supplemented with 0.5% peptone and 0.5% peptone+0.1%yeast extract (to mimic 2216) was observed for the population cells elongation compared to cultures grown in 2216 (as described in Material and Methods). In addition, another set of samples was observed in 25°C in comparison with 30°C to see the affect of temperature on the population of elongated cells. The result showed that 0-2 hrs the population of elongated cells were less than half of the cell population in all media in both 25C and 30C (Table 6). During this time, the reason for elongated cells of *flaC* mutant in 2216 is probably that the initial inoculum came directly from 2216 agar plate (Table 6). After 3 hrs of incubation, half of the cultures grown in 0.5% peptone and 0.5%peptone+0.1% yeast extract were elongated cells, in both temperature (Table 6). The population of elongated cells remains approximately half of the total population throughout the experiment (8 hr) (Table 6). This suggests that cell elongation correlates to cell growth. In addition, it also supports the idea that the cells could be defective in cells division because the population the elongated cells did not increase, beyond half of the population, at time points later than 3 hr (Table 6). The temperature between 25C and 30C does not seem to have any effect on the cell elongation (Table 6).

**Table 5.** Comparison of cell elongation in various concentration of peptone

Strains	2216	Percent peptone supplemented in marine motility medium					
		1%	0.5%	0.25%	0.125%	0.0625%	0.0156%
TM1040 <sup>a</sup>	-	-	-	-	-	-	-
<i>flaC</i> <sup>a</sup>	+	++++	++++	++++	++++	++++	++++

<sup>a</sup> The population of elongated cells estimated by eye, where cultures with no elongated cells are represented by (-) and cultures containing elongated cells are represented by (+). The cultures that contain distinguishable high amount of elongated cells when compared to the control in 2216 are represented by (++++).

**Table 6.** Comparison of cell elongation during growth at 25°C and 30°C

<i>flaC</i> cultures	Incubation temperature	Time of incubation							
		0 hr	2 hr	3 hr	4 hr	5 hr	6 hr	7 hr	8hr
2216	25°C	+	+	-	-	-	-	-	-
Peptone <sup>a</sup>	25°C	+	+	++	++	++	++	++	++
Peptone+ yeast <sup>b</sup>	25°C	+	+	++	++	++	++	++	++
2216	30°C	+	+	-	-	-	-	-	-
Peptone <sup>a</sup>	30°C	+	+	++	++	++	++	++	++
Peptone+yeast <sup>b</sup>	30°C	+	+	++	++	++	++	++	++

<sup>a</sup> Marine motility broth supplemented with 0.5% peptone

<sup>b</sup> Marine motility broth supplemented with 0.5% peptone + 0.1% yeast extract

### 2.3.10. Complementation of *flaC* mutant (HG1016) and over expression of FlaC

The first phenotype examined was pigment production. Spent medium of overnight cultures of pRSI506/HG1016 (complement), pRK415/HG1016 (control), pRSI506/RSI01 (FlaC over expression), pRK415/RSI01 (control) grown at 30°C with shaking, were measured at OD<sub>389 nm</sub> for pigment production. Spent medium of HG1016 and RSI01, grown in the same condition, were used to blank the spectrophotometer for HG1016 strains and RSI01 strains respectively. The result shows that pRSI506/HG1016 (complement), pRK415/HG1016 (control), pRSI506/RSI01 (FlaC over expression) did not rise above zero, indicating no pigment production above HG1016 (Table 7). The pRK415/RSI01 (control) seems to have slight increase to OD<sub>398nm</sub> to 0.0894, which is most likely background because this strain is a control (Table 7).

Antibiotic production of *flaC* complementation and over expression strain were also observed. Spent medium of static cultures of pRSI506/HG1016 (complement), pRK415/HG1016 (control), pRSI506/RSI01 (FlaC over expression), pRK415/RSI01 (control) grown at 30°C for 2 days in 2216 broth, were used in a well diffusion assay (Material and Method). TM1040, RSI01, and HG1016, grown in the condition, were also used as controls. The result of the inhibition zone showed that pRSI506/HG1016 had a slightly larger diameter of inhibition zone (21.9 mm) than pRK415/HG1016 (control) (19.9 mm) and HG1016 (18.1 mm), but is still not as large as TM1040 (33 mm) (Table 8). The slight increase of 2 mm in

**Table 7.** Pigment production of *flaC* complementation and FlaC over expression strains

Strains	OD <sub>398nm</sub>
pRK415/HG1016	-0.0080
pRSI506/HG1016	-0.0043
pRK415/RSI01	0.0894
pRSI506/RSI01	-0.0047

**Table 8.** Antibiotic production of *flaC* complementation and FlaC over expression strains

Strains	Inhibition zone (mm)
TM1040	33
HG1016	18.1
pRK415/HG1016	19.9
pRSI506/HG1016	21.9
RSI01	31.5
pRK415/RSI01	32.2
pRSI506/RSI01	32.7

inhibition could be due background. This suggests that pRSI506 did not complement the antibiotic production defect in HG1016. For the overexpression of FlaC by pRSI506/RSI01 had similar diameter of inhibition zone as pRK415/RSI01 (control), RSI01, and TM1040 (32.7, 32.2, 31.5, and 33 mm, respectively) (Table 8). This suggests that either of over expression FlaC is not effecting antibiotic production or FlaC is not expressing from the pRSI506 plasmid.

Motility of *flaC* complementation and overexpression strain was observed in 2216 semi-solid agar (Materials and Method). Cultures of pRSI506/HG1016 (complement), pRK415/HG1016 (control), HG1016, and TM1040 were inoculated in same 2216 semi-solid agar plate. Another set of cultures, pRSI506/RSI01 (FlaC over expression), pRK415/RSI01 (control), RSI01, and TM1040 were inoculated another 2216 semi-solid agar. Each set of plates had four replicates and were incubated at 30°C for 2-3 days. The diameter of motile colonies was measured which the result showed that pRSI506/HG1016 (6.78 mm) had similar diameter to HG1016 (5.45 mm) and below the pRK415/HG1016 control (12.2 mm) (Table 9). This suggests that pRSI506 is not complementing the motility defect in semi-solid agar of HG1016. The FlaC over expression strain, pRSI506/RSI01 (24.05 mm), had similar diameters to all of the controls (21.43, 25.38, and 22.18 mm for TM1040, RSI01, and pRK415/RSI01, respectively) (Table 9). The result suggests that FlaC over expression is not affecting motility in semi-solid agar or FlaC is not expressing from pRSI506.

Motility of *flaC* complementation and over expression strain were also observed in 2216 broth. The population of motile cells from overnight cultures of pRSI506/HG1016 (complement), pRK415/HG1016, pRSI506/RSI01 (FlaC overexpression), TM1040, RSI01, and HG1016 grown in 2216 broth at 30°C with shaking, was observed with phase contrast microscopy (Materials and Methods). The result shows that pRSI506/HG1016 had the same population of motile cells as HG1016 and pRK415/HG1016 (Table 10). This suggests that the pRSI506 did not complement the high population of motile cells of HG1016.

**Table 9.** Motility in 2216 semi-solid agar of *flaC* complementation and FlaC over expression strains, at 30°C

Strains	Diameter of motile colony (mm)				mean	SD
	Colony 1	Colony 2	Colony 3	Colony 4		
TM1040	23.5	15.1	20.5	12.8	17.98	4.9
HG1016	4.1	7.8	6.2	3.7	5.45	1.91
pRK415/HG1016	12.1	15	10.3	11.4	12.2	2.01
pRSI506/HG1016	8.2	5.3	8.1	5.5	6.78	1.59
TM1040	20.4	24.5	22	18.8	21.43	2.43
RSI01	29.3	28.9	22	21.3	25.38	4.31
pRK415/RSI01	17.1	24.5	23.6	23.5	22.18	3.41
pRSI506/RSI01	29.9	23.3	23.2	19.8	24.05	4.23

**Table 10.** Observation of population of motile cells in *flaC* complementation and FlaC over expression strains

Strains	Observation of motile cell population
HG1016	++++
pRK415/HG1016	++++
pRSI506/HG1016	++++
TM1040	++
RSI01	++++
pRSI506/RSI01	++

In contrast, it is also possible that the experiment was not quantitative enough to distinguish the difference between samples and control. The population of motile cells for pRSI506/RSI01 (over expression) was the same as TM1040 (Table 10). Unexpectedly, the RSI01 had about twice the amount of motile cells of TM1040 (Table 10). This could suggest that the spontaneous mutation in RSI01 may have indirectly affected the population of motile cells in broth. Even though the pRSI506 seems to reduce the amount of motile cells of RSI01 to the same level as TM1040, due to this unexpected result from RSI01, it is not clear whether over expression of FlaC had an effect on the same pathway that caused an increase of motile cells in HG1016.

Cell elongation of *flaC* complement strain in Marine motility medium was also observed. The population of elongated cells from overnight cultures of pRSI506/HG1016 (complement), pRK415/HG1016 (control), TM1040, and HG1016 grown in marine motility medium at 30°C with shaking, was observed with phase contrast microscopy (Table 11). The population of the elongated cells was estimated by eye. The result shows pRSI506/HG1016 had the same amount of elongated cells as pRK415/HG1016 and HG1016, while TM1040 did not elongate. This suggests that pRSI506 did not complement the elongation phenotype in HG1016.

**Table 11.** Cell elongation of *flaC* complementation.

Strains	Observation of cell elongation population
TM1040	-
HG1016	++
pRK415/HG1016	++
pRSI506/HG1016	++

### 2.3.11. *flaC* mutation via site specific recombination

Cell elongation was observed and the cell length of the RSI02 were compared to TM1040 and HG1016, in 2216 and marine motility broth (described in Material and Methods). The result shows that in marine motility medium, TM1040 cells (1.596  $\mu\text{m}$ ) does not elongated but HG1016 (5.813  $\mu\text{m}$ ) and RSI02 (6.208  $\mu\text{m}$ ) elongates (Fig. 27 A). Base on Newman-Keuls multiple comparison test, TM1040 is significantly different from RSI02 and HG1016, while RSI02 and HG1016 cells length are not significantly different. In 2216, TM1040 and HG1016 do not elongate while RSI02 cells are elongated (Fig. 27B). The statics analysis base on Newman-Keuls multiple comparison test, indicate that the average cell length of TM1040 (1.615  $\mu\text{m}$ ) and HG1016 (1.773  $\mu\text{m}$ ) are not significantly different in 2216 broth, but RSI02 (8.557  $\mu\text{m}$ ) is significantly different from both strains (Fig. 27B). This unexpected result leads to hypothesize that genotype of HG1016 and RSI02 are different. One possible explanation is that there is another mutation in HG1016.

Motility analysis of RSI02 in 2216 semi-solid agar was observed in comparison to HG1016 and TM1040. Cultures of RSI02, TM1040 and HG1016 were inoculated in the same 2216 semi-solid agar and incubated at 30°C for 3 days. Triplicates were made in order to find the average diameter of each motile colony. The result shows that RSI02 has a flare-like motile colony with an average of 2.7 mm while HG1016 has a partial motile colony with an average of 20.7 mm when compared to TM1040 (32.3 mm) (Fig. 28). This result further supports the idea that RSI02 is not the same as HG1016. The same explanation mention above can be used to explain this result, that is, HG1016 could have a second mutation. Since originally HG1016 was screened as a nonmotile mutant, it is also possible that the original stock of HG1016 contains two types of strains, one partially motile and the

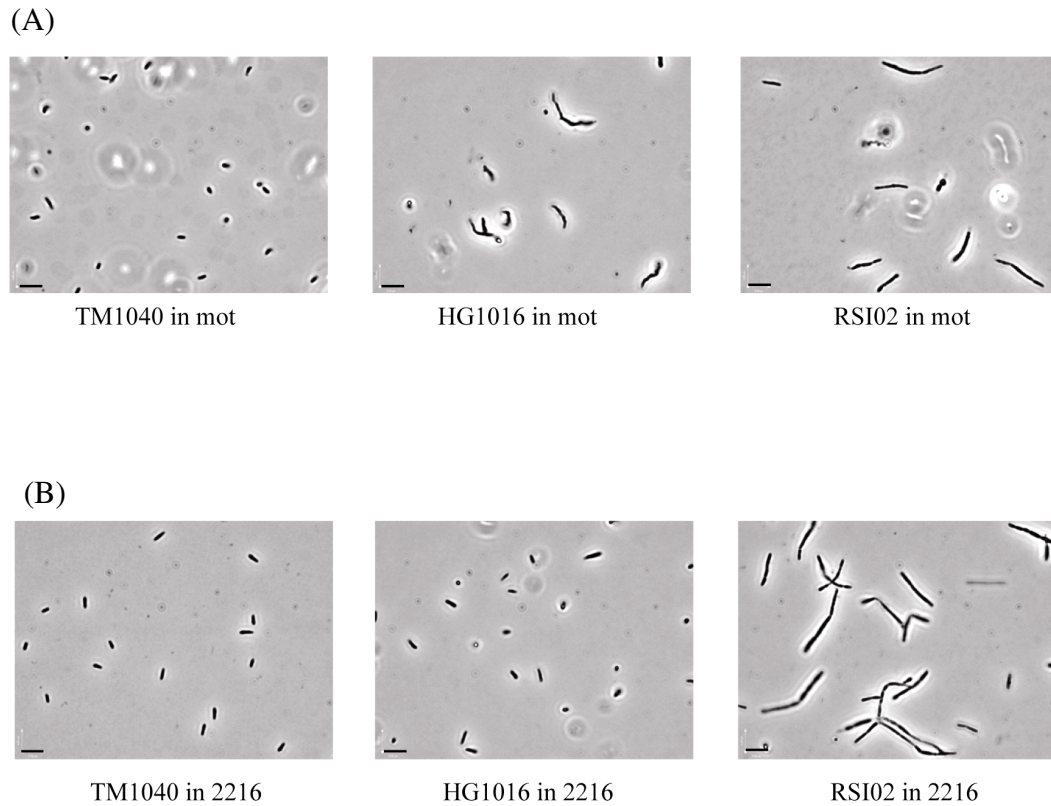


**FIG. 27** Comparison of cell elongation of RSI02 to TM1040 and HG1016. Phase contrast microscopy of RSI02 compared to TM1040 and HG1016, grown in (A) marine motility broth and (B) 2216 broth at 30°C with shaking overnight. The scale bar at the lower left corner equals to 4.5  $\mu\text{m}$ .

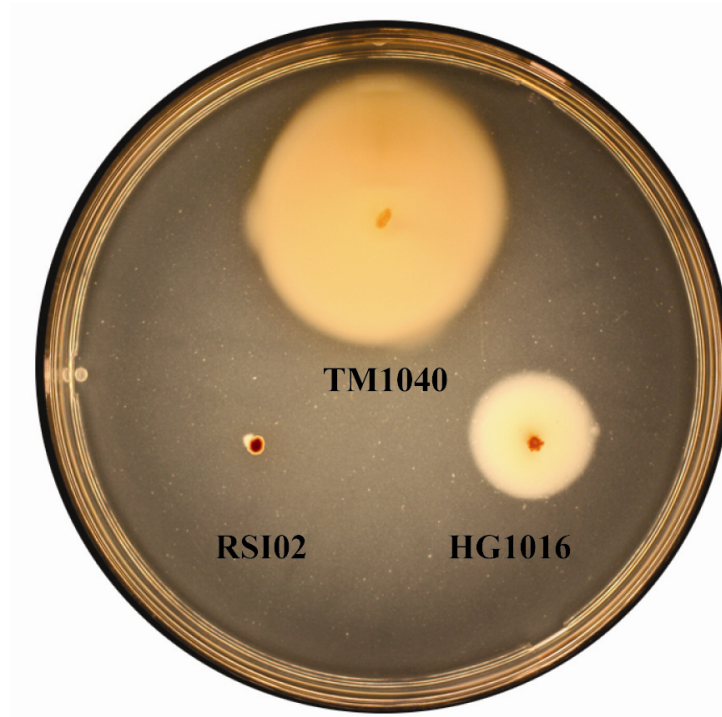


**FIG. 28** Motility of RSI02 on 2216 semi solid agar compared to TM1040 and HG1016. Cultures of TM1040, HG1016, and RSI02 were grown on 2216 semi-solid agar for 3 days at 30°C.

other is nonmotile or produces a very small flare-like motile colony during long incubation time.

#### 2.3.11. The second transposon in the *flaC* mutant

After an unsuccessful attempt to complement the *flaC* mutant and the observation of unrelated phenotypes between HG1016 and RSI02, which further supports the idea that HG1016 has a second mutation, a thorough examination was conducted to confirm the mutation in HG1016. The HG1016 was originally rescue cloned using *NcoI* to digest the chromosome followed by self-ligation and electroporation into *E.coli* DH5 $\alpha$ pir (Preston Miller, intern). The rescue cloning of the *flaC* mutant was repeated in order to confirm that only one transposon exists in its genome. A slight modification was made by substituting *NcoI* with *SmaI* to digest the chromosome. This modification should not affect the out come because both enzymes do not digest within the EZ::Tn5 transposon. After the rescue clone process, 10 rescue plasmids were analyzed by linearizing the plasmid with *SmaI* and the size were compared to the *SmaI* fragment containing *flaC* including the size of the transposon (4,788 bp). Unexpectedly, the result of the restriction analysis did not show any plasmids containing a 4,788 bp band, instead, a 9,568 bp band was observed in all 10 clones (Fig. 29A), suggesting that the transposon is not in *flaC*. In argument with this idea, the *flaC*::EZ-Tn5 transposon fragment was successfully amplified from a colony of HG1016 (*flaC*<sup>-</sup>) using primers flanking the *flaC* allele (Fig. 29B and C), meaning that the transposon was definitely inserted in *flaC*. Therefore, this leads to hypothesize that two transposons are present in

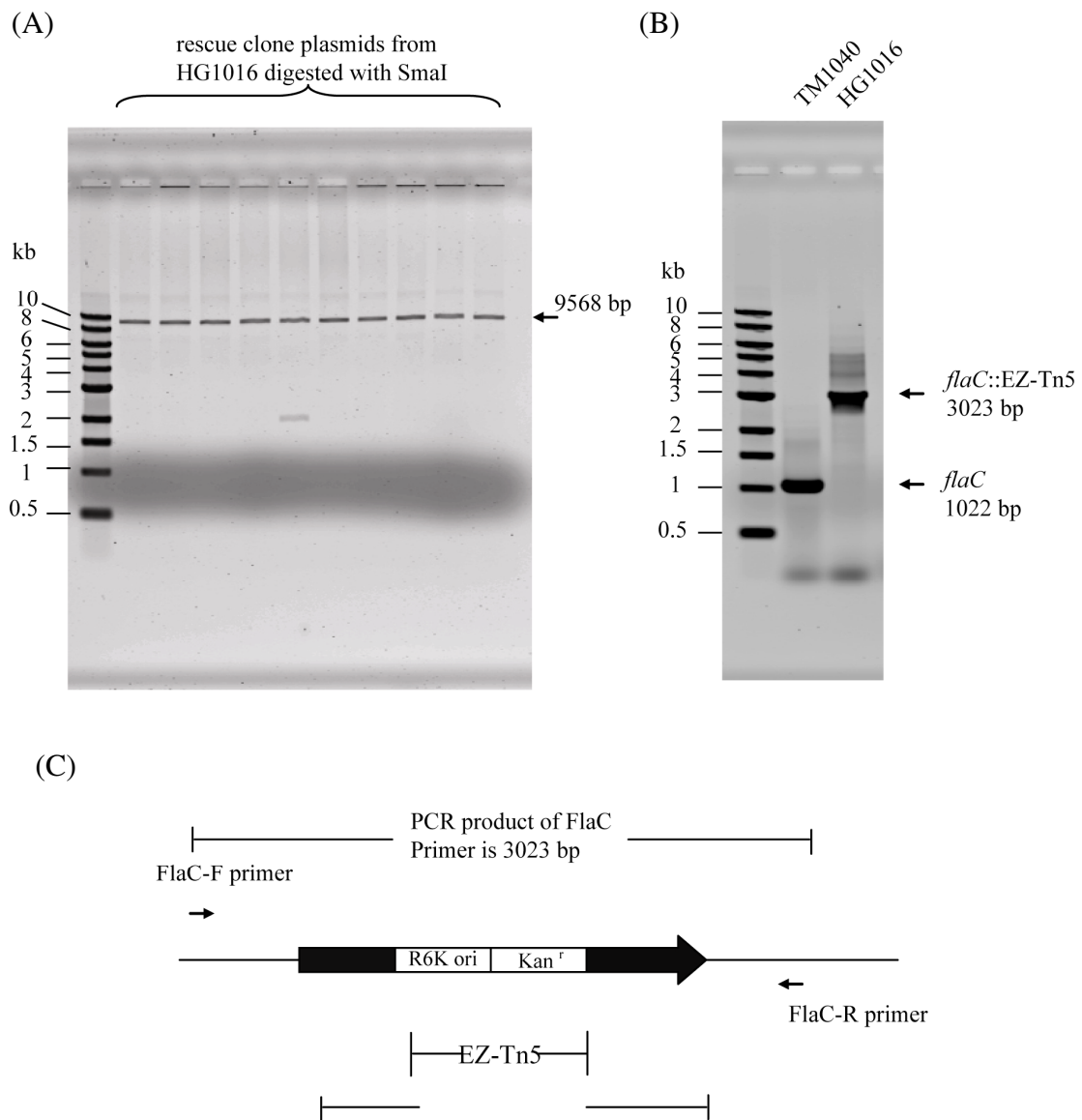


**FIG. 29** PCR of *flaC*::EZ-Tn5 fragment and restriction analysis HG1016 rescue clone plasmid. (A) Restriction analysis of 10 rescue clone plasmids (lane 2-11) from rescue cloning HG1016 (*flaC*), using *Sma*I digest. (B) Colony PCR from TM1040 (lane 2) and HG1016 (*flaC*) (lane 3) using primers flanking *flaC* gene. (C) Diagram of *flaC*::EZ-Tn5 fragment and primer binding site used to amplify *flaC*::EZ-Tn5 fragment in (B).

HG1016 (*flaC*), one in *flaC* and a second transposon in a different location on the genome. Sequence analysis of the unexpected 9568 bp band revealed that the second transposon was inserted in TM1040\_3871 encoding for  $\beta$ -glucuronidase on the pSTM2 (Fig. 30). This enzyme is classified as glycoside hydrolases that hydrolyzes glucuronides (28). It is still unclear whether the mutation in  $\beta$ -glucuronidase is contributing to the phenotypes seen in HG1016 but the gene neighborhood indicates a GntR-like regulator down stream of the  $\beta$ -glucuronidase gene (Fig. 30). It makes sense to suggest that there is a polar effect affecting transcription of the GntR-like protein, which could have direct or indirect effect towards the multiple phenotypes seen in HG1016. The finding of this second transposon supports the idea of a second mutation in HG1016 that would explain the different phenotype between RSI02 and HG1016. As for the failure to complement HG1016, it is most likely that *flaC* on the pRSI506 was not transcribed because no affect was seen in over expression of *flaC* (pRSI506/RSI01) from the phenotypes that were observed.

The hypothesis to explain the lose of the rescue clone plasmid containing the *flaC*::EZ-Tn5 fragment (4,788 bp), is that a mutation occurred on the kanamycin resistance gene on the transposon and caused the lose of the clone during selection on kanamycin. By sequencing the transposon from the PCR production containing *flaC*::EZ-Tn5 revealed a point mutation that changed the Glutamic acid at position 269 (full length is 272 aa) to Glycine (Fig. 31). The Glu269 is one of the kanamycin binding sites at the C-terminus of the aminoglycoside phosphotransferase (Kan<sup>r</sup>) (103). Mutation in this position may have caused a defect in kanamycin resistance resulting in the lost of the *flaC*::EZ-Tn5 rescue clone plasmid.

In addition, by re-streaking the original -80°C stock, further clarified the situation by the presence of two types of colonies, one type has dark pigment while the type has lighter pigment. The lighter pigment colony looks like the same type used in this work that is

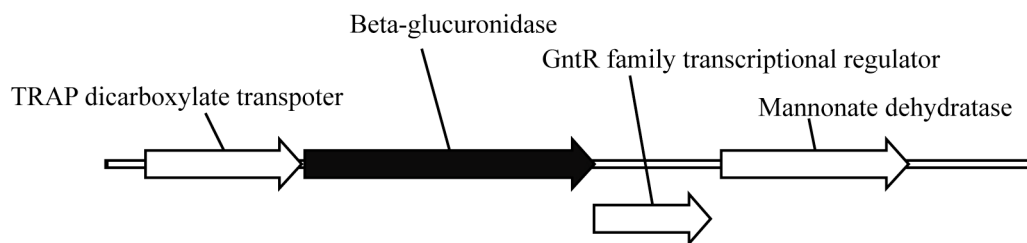


**FIG. 30**  $\beta$ -glucuronidase operon. The second transposon in HG1016 inserted in the  $\beta$ -glucuronidase gene (black arrow) on pSTM3. Besides the  $\beta$ -glucuronidase gene this operon contains a gene that encodes for TRAP dicarboxylate transporter, upstream and has genes encoding GntR family transcriptional regulator and mannose dehydratase, downstream, respectively.

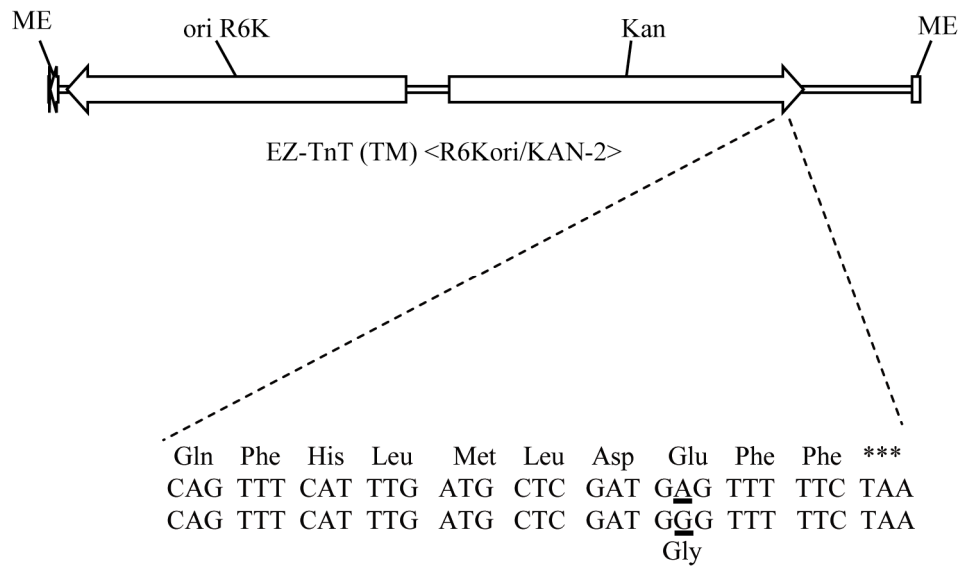


**FIG. 31** Mutation in kanamycin resistant gene in EZ-Tn5 transposon. Point mutation in the kanamycin resistant gene changed Glutamic acid at position 269 (full length is 272 aa) to Glycine.

represented as HG1016 in this thesis. This would explain why the initial rescue clone succeeded.

### 2.3.12. Distribution of the flagellar genes among the *Roseobacter* clade

The genomes of the sequenced and annotated species of *Roseobacter* currently available in the database were searched for homologs to TM1040 flagellar genes (Table 12). Overall, flagellar genes are well conserved amongst the roseobacters, emphasizing that most species are motile (21). For example, nearly 80% (11 out of the 14) of the *Roseobacter* genomes analyzed possess homologs of the C-ring, MS-ring, export apparatus, L-ring, P-ring, rod, hook, hook associate proteins, filament and regulators proteins (*flaF*, *flbT*, *flaB*, *flaC* and *flaD*) found in TM1040. Only six species (*Jannaschia* sp. CSS1, *Silicibacter pomeroyi* DSS-3, *Sagittula stellata* E-37, *Oceanicola granulosus* HTCC2516, *Roseovarius* sp. HTCC260, and *Roseovarius* sp. TM1035) have homologs to *fliL*, *pflI* and *flaA*. This is interesting because these genes are proposed to encode proteins that function to stabilize, localize, or energize the filament. FliL is proposed to function in surface sensing in *Proteus mirabilis* (13) and withstand torsional stress in *Salmonella enterica* (9).

PflI plays a role in correct localization of flagellum to the cell pole (75). The *flaA* gene is located in the same cluster as *motA1* (Fig. 11A), suggesting that it may be required for flagellar rotation. In contrast, *Roseovarius nubinhibens* ISM and *Rhodobacterales* bacterium HTCC2654 lack homologs to most of the flagellar genes found in TM1040. *Roseovarius nubinhibens* ISM is motile (33) which implies that it may use alternative proteins or mechanisms to swim.

**Table 12.** Comparison of TM1040 flagellar genes with other *Roseobacter* clade genomes<sup>a</sup>.

Predicted function	TM1040														
		<i>Jannaschia</i> sp. strain CSS1	<i>Roseovarius nubinhibens</i> ISM	<i>Silicibacter pomeroyi</i> DSS-3	<i>Sulfitobacter</i> sp EE-36	<i>Sulfitobacter</i> NAS-14.1	<i>Sagittula stellata</i> strain E-37	<i>Lokanella vestfoldensis</i> strain SKA53	<i>Oceanicola batsensis</i> strain HTCC2597	<i>Oceanicola granulosa</i> strain HTCC2516	<i>Rhodobacteriales bacterium</i> HTCC2654	<i>Roseobacter</i> sp. MED193	<i>Roseovarius</i> sp. strain 217	<i>Roseovarius</i> sp. strain HTCC2601	<i>Roseovarius</i> sp. TM1035
C-ring	<i>fliM</i>	+	+	+			+	+		+	+	+	+	+	+
	<i>fliN</i>			+	+	+	+		+				+	+	+
	<i>fliG</i>	+	+	+			+	+		+	+	+	+	+	+
	<i>fliY</i>	+	+	+	+	+	+	+	+	+	+	+	+	+	+
Export apparatus	<i>flhA</i>	+		+	+	+	+	+	+	+			+	+	+
	<i>flhB</i>	+		+	+	+	+	+	+	+			+	+	+
	<i>fliO</i>	+		+			+			+			+	+	+
	<i>fliP</i>	+		+	+	+	+	+	+	+			+	+	+
	<i>fliQ</i>	+		+	+	+	+	+	+	+			+	+	+
	<i>fliR</i>	+		+	+	+	+	+	+	+			+	+	+
	<i>fliI</i>	+	+	+	+	+	+	+	+	+	+	+	+	+	+
Export ATPase	<i>fliI</i>	+	+	+	+	+	+	+	+	+	+	+	+	+	
MS-ring	<i>fliF</i>	+		+	+	+	+	+	+	+			+	+	+
MS-ring rod junction	<i>fliE</i>	+		+	+	+	+		+	+		+	+	+	+
P-ring	<i>flgI</i>	+		+	+	+	+	+	+	+			+	+	+
Chaperon of P-ring protein	<i>flgA</i>	+		+	+	+	+	+	+	+			+	+	+
L-ring	<i>flgH</i>	+		+	+	+	+	+	+	+			+	+	+
Rod	<i>flgB</i>	+		+	+	+	+		+	+		+	+	+	+
	<i>flgC</i>	+		+	+	+	+	+	+	+		+	+	+	+
	<i>flgF1</i>	+		+	+	+	+	+	+	+			+	+	+
	<i>flgF2</i>	+		+	+	+	+		+	+		+	+	+	+
	<i>flgG</i>	+		+	+	+	+	+	+	+		+	+	+	+
	<i>flgJ</i>	+	+	+			+	+		+	+	+	+	+	+

Hook-capping protein	<i>flgD</i>	+	+	+	+	+	+	+	+	+	+	+	+	+
Hook	<i>flgE</i>	+		+	+	+	+	+	+		+	+	+	+
Hook-length control	<i>fliK</i>	+	+	+			+	+			+	+	+	+
HAP	<i>flgK</i>	+		+	+	+	+	+	+			+	+	+
	<i>flgL</i>	+		+	+	+		+	+			+	+	+
flagellin	<i>fliC1</i>	+		+	+	+	+	+	+			+	+	+
	<i>fliC2</i>	+		+	+	+	+	+	+			+	+	+
	<i>fliC3</i>	+		+	+	+	+	+	+			+	+	+
	<i>fliC4</i>	+		+	+	+	+	+	+			+	+	+
	<i>fliC5</i>	+		+	+	+	+	+	+			+	+	+
	<i>fliC6</i>	+		+	+	+	+	+	+			+	+	+
Motor complex	<i>motA1</i>	+		+	+	+		+	+				+	+
	<i>motA2</i>	+	+	+	+	+	+	+	+	+	+	+	+	+
	<i>motB1</i>	+		+	+	+		+	+			+	+	+
	<i>motB2</i>	+	+	+	+	+	+	+	+	+	+	+	+	+
Motor associated	<i>fliL</i>	+		+			+		+				+	+
	<i>pflI</i>	+		+			+		+				+	+
	<i>flaA</i>	+		+			+		+				+	+
Regulators	<i>ctrA</i>	+	+	+	+	+	+	+	+	+	+	+	+	+
	<i>cckA</i>	+	+	+	+	+	+	+	+	+	+	+	+	+
	<i>flaF</i>	+		+	+	+		+	+			+	+	+
	<i>flbT</i>	+		+	+	+		+	+			+	+	+
	<i>flaB</i>	+	+	+	+	+	+	+	+	+	+	+	+	+
	<i>flaC</i>	+	+	+	+	+	+	+	+	+	+	+	+	+
	<i>flaD</i>	+	+	+	+	+	+	+	+	+	+	+	+	+
Unknown function	<i>flaI</i>		+	+			+		+	+		+	+	+

<sup>a</sup>Amino acids sequence of TM1040 flagellar genes were used to identify flagellar genes in other Roseobacter strains based on BLASTp in [www.roseobase.org](http://www.roseobase.org) and <https://research.venterlinstitute.org/moore/>. The “+” indicate hits that have E value of 10<sup>-5</sup> or less. Blank space indicates the absence of the gene.

## 2.4 Conclusion

In conclusion, to this study, the genomic analysis identified genes involved in flagellar regulation and biosynthesis based on homologs to known genes. The analysis revealed similarity in flagellar loci orientation of TM1040 to *fla2* flagellar loci in *R. sphaeroides* with some minor difference. This includes the differences in the location of the flagellin locus in *R. sphaeroides* (*flaA* (flagellin), *flaF*, *flbT*, and *flgF*) that is on the plasmid while in TM1040, although the gene are in same orientation, is located on the chromosome. This suggests that the regulation and function of *fla2* flagellar loci in *R. sphaeroides* is similar but not exactly like TM1040. The genetic analysis using random mutagenesis confirmed the flagellar gene relation to flagella synthesis and function. Moreover, the genetic analysis indicated the essential copy of the flagellar genes with multiple alleles. Most importantly, the genetic analysis uncovered three new regulators that are involved in regulating motility in TM1040. Based on their predicted function and mutant phenotype, all three regulators can be arrange in a hierarchy which control cell phase and motility. At the upper level of the hierarchy is FlaC, a response regulator that upregulates sessile phase and down regulates the motile phase of TM1040. Further down the hierarchy or in the same level as FlaC is FlaB, a phosphorelay protein that shuttles phosphate from CckA to CtrA and/or between unknown regulators for class III genes. At the bottom of the hierarchy is FlaD, a transcriptional regulator that regulates the mot genes of the flagellar motor complex.

In further studies of the function of *flaC*, pRSI506 was used to complement the *flaC* mutant but was unsuccessful indicating that either *flaC* was not expressed from the plasmid and/or the *flaC* mutant has a second mutation. Although, a secondary mutation was found in a gene encoding for  $\beta$ -glucuronidase it still is unclear if this mutation plays a role in any of the phenotypes of the HG1016 (*flaC*) mutant. If this mutation is involved in the phenotypes of

HG1016, it is most likely that it is because polar effect on the gene encoding a GntR-like regulator downstream of the  $\beta$ -glucuronidase gene.

In the attempt to repeat the rescue clone of HG1016, I was unable to obtain the rescue and further discovered that a mutation had occurred in the kanamycin resistant gene. In addition, going back to observe the original stock of HG1016 by re-streaking the stock, I also found that there was two types of colonies, one with dark yellow pigment and the other with lighter pigment. It is possible that the original rescue clone of HG1016 was successfully obtained from the dark yellow pigment colony because HG1016 in this study has a lighter yellow pigment colony. This could also explain why the original strain of HG1016 was screened as nonmotile in semi-solid agar while the HG1016 strain in this study is partially motile.

## Chapter 3: Discussion

Previous studies from our laboratory have shown that chemotaxis and motility plays a crucial role in the symbiosis between TM1040 and *P. piscicida* (65, 66). TM1040 utilizes motility mediated chemotaxis behavior to sense, move towards, and maintain its interaction with the dinoflagellate host (65, 66). Defects adversely affecting swimming significantly reduce the ability of TM1040 to colonize and interact with *P. piscicida* (65).

In the current study, the genome analysis revealed that the majority of flagellar genes in TM1040 were organization in two large loci, that closely resemble the *fla2* cluster organization in *R. sphaeroides* (Fig. 11 and Fig. 12) (80), with minor differences. Although the *fliO* in the *fliF* operon in TM1040 is substituted with *fliH* in *R. sphaeroides*, both genes encode for a component of the TTSS. Therefore, it is most likely that the *fliF* operon in TM1040 is the same as the *fliF* operon in *R. sphaeroides*, encoding for the MS-ring and TTSS components. Another minor difference between TM1040 and *R. sphaeroides* *fla2* is that it has only one copy of *flgJ* (rod assembly protein) while *R. sphaeroides* has two copies (*flgJA2* and *flgJB2*). Both *flgJA2* and *flgJB2* have a Shine Dalgarno, suggesting that both genes could be expressed. This could also suggest that both genes are required, or at least one FlgJ is required for rod assembly in *R. sphaeroides*. The presence of *fliY* in TM1040 and the absence of this gene in *R. sphaeroides* is another difference. The *fliY* gene encodes for one of the TTSS components, the periplasmic amino acid binding protein. It is possible that *R. sphaeroides* has another protein that compensates for the function of FliY. The amount of copies of flagellin gene in TM1040 versus *R. sphaeroides* is different as well. In TM1040, there are six copies of *fliC* (*fliC1-6*), which only four copies are predicted to be expressed (*fliC1*, *fliC3*, *fliC4*, and *fliC5*) because they contain a Shine Dalgarno sequence upstream of the start codon. On the other hand, *R. sphaeroides* has only two copies of flagellin, *fliC* for

fla1 flagellar loci and *flaA* for fla2 flagellar loci (80). The electron microscopy image of TM1040 and *R. sphaeroides* flagellar indicates that both species have plain flagella (66, 80). Since the gene neighborhood of *fliC3* is the same as *flaA* in fla2 of *R. sphaeroides*, and only insertion in *fliC3* was found from the transposon mutagenesis that gave rise to a nonmotile mutant, suggests that *fliC3* is the major flagellin for the flagellar filament in TM1040. The last, but probably the most interesting, difference between the flagellar gene organization of TM1040 and fla2 of *R. sphaeroides* is in the *fliL* operon. The last gene in *fliL* operon of TM1040 contains *flaA*, an unique gene for roseobacters (65). Original studies, indicate that mutation in *flaA* of TM1040 results in a nonmotile and non-flagellated mutant (65). A more thorough study in this work indicates that *flaA* has paralyzed flagella, a phenotype related to mutation in motor genes. This suggests that *flaA* is involved in the function flagellar rotation or motor complex. In *R. sphaeroides*, RSP\_1318 has low homology (29% identity) to *flaA* in TM1040. It is also located at the same position, which is downstream of *motA*, as *flaA* in TM1040. The function of RSP1318 is still unknown but base on the location in the operon, it is possible to predict that it could be involved with the flagellar motor complex as well. The regulation of fla2 flagellar loci of *R. sphaeroides* is still unknown. These minor differences between TM1040 and fla2 flagellar loci of *R. sphaeroides* suggest that flagellar gene regulation and swimming behavior in both species, although not exactly the same but could be similar.

The genome of TM1040 contains two copies of *motA* and *motB*, that genes encoding for H<sup>+</sup> ion motor proteins (20, 119), but does not contain *motX* and *motY* that are for Na<sup>+</sup> ion motors (114). This suggests that the flagellar motor in TM1040 is energized by H<sup>+</sup> ions. Further studies from our laboratory show that motility of TM1040 is sensitive to FCCP and phenamil, proton and sodium ion channel inhibitors, respectively (63). This suggest that TM1040 has both H<sup>+</sup> and Na<sup>+</sup> motor (63). Supporting this idea is a recent study in *Bacillus calusii* that shows MotA and MotB can switch between proton and sodium ion without

another distinct set of mot protein for sodium ion (102). The presence of two set *motA* and *motB* in TM1040 could come from horizontal gene transfer because *motA2* and *motB2* are not located in the two main flagellar loci.

In contrast to other  $\alpha$ -proteobacteria, TM1040 does not possess homologs to genes that encode  $\sigma^{54}$ , FliA ( $\sigma^{28}$ ) and FlgM (an anti-sigma factor). These data suggest that TM1040 and possibly other roseobacters utilize an alternative system to regulate the expression of the flagellar genes.

As mentioned above, the genome of TM1040 contains six copies of putative flagellin-encoding genes; however, based on genetic analysis, only one allele, FliC3, appears to be essential for motility, and genomic analysis predicts four flagellins (FliC1, FliC3, FliC4 and FliC5) can be expressed. The SDS-PAGE in Figure 17 reveals two flagellin bands instead of one, which could be explained by degradation of the flagellin or flagellin expression from another copy of *fliC*. This result is in correlation with *S. meliloti* that also contains multiple copies of flagellin-encoding genes. The *S. meliloti* has four flagellin genes (*flaA-D*), FlaA is the principle flagellin and is required to form the filament with at least one other secondary flagellin for normal flagellar assembly (86). It is certainly possible that a second flagellin-encoding gene of TM1040 is required and was missed by the mutagenesis, but it is more likely that it may be due to one or more modifications affecting FliC3. The SDS-PAGE in Figure 17 also shows that both flagellin bands are larger than the predicted size from the amino acid sequence. This could be due post translation modification by glycosylation (83).

In contrast to enteric bacteria, little is known about flagellar regulatory genes of the roseobacters. Therefore, perhaps one of the most significant findings of this study is the identification of three novel and previously unknown regulatory proteins involved in controlling flagellum biosynthesis and function. Based on its domain architecture and resulting mutant phenotype, I propose that FlaB functions as a phosphorelay protein, shuttling phosphate between CckA and CtrA. This is because the domain architecture of FlaB has only

a phosphoacceptor domain but no response domain, suggesting that it can only receive phosphate. The genetic analysis indicates that mutation in *flaB* does not produce flagella which suggest that FlaB is most likely to regulate class III flagellar gene or above. In addition, FlaB has low homolog to ChpT in *C. crescentus*, which functions to shuttle phosphate from CckA to CtrA. Therefore, it is possible that FlaB has a similar function to ChpT and phosphorelays phosphate between CckA and CtrA (16). It is also equally relevant to hypothesize that FlaB phosphorelays phosphate to activate a transcription activator that regulates class III flagellar genes since down regulation of class III genes would result in lack of filament as well. Further analysis with electronmicroscopy at the cell pole of the *flaB* mutant to observe the presence of a hook would support this idea. FlaD<sup>-</sup> cells are nonmotile with paralyzed flagella. This phenotype is also seen in mutations in *motA* and *motB* of *Salmonella typhimurium* that encode for the flagellar motor (30). In addition, the bioinformatic analysis of the FlaD indicates that it is a MarR-type DNA binding protein (Fig. 15). This leads to hypothesize that FlaD may be involved in regulation of mot gene in TM1040. To my knowledge, there has not been any report on MarR-type DNA binding protein that regulates mot genes. For example, in enteric bacteria like *S. typhimurium*, uses  $\sigma^{28}$  and FlgM (antisigma factor) to regulate the mot genes (25). In *R. sphaeroides*, the mot genes are regulated by enhancer proteins FleQ/FleT (81) while in *S. meliloti* utilizes the LuxR-type proteins, VisN and VisR (93). If this hypothesis is true, then this could be a novel feature for flagellar regulation in TM1040. The last and most interesting putative regulator gene encodes FlaC. Defect in *flaC* has pleiotropic phenotypes. The population is bias towards motile cells and defective in expressing phenotypes associated with the sessile phase e.g., less rosettes, defect in biofilm formation, significant decrease in pigment production and antibiotic activity. The results suggest that FlaC is involved in upregulation of the sessile stage phenotypes. Bioinformatic analysis of FlaC predicts that FlaC is a response regulator in a two component signal transduction system. FlaC has close homology to CenR of *C. crescentus* that functions

to control cell envelope biogenesis and structure (92). CenR interacts with a histidine kinase, CenK, as part of a two-component signal circuit. Deletion of both *cenR* and *cenK* are lethal (92), but mutation in *flaC* is not deleterious, implying that FlaC and CenR may regulate different phenotypes. The pleiotropic nature of the defect in *flaC* implicates it as a regulator involved in multiple functions of the cell, perhaps acting at early stages in a regulatory hierarchy to control the biphasic swim-or-stick switch. The genome of TM1040 also encodes a protein, TM1040\_0316, with strong homology to CenK. The important aspect to explore in future studies of this sensory protein is the signal that it senses. The prediction would be that this extracellular signal from the environment or dinoflagellate would determine the cells phase of TM1040 (swim-or-stick).

Combine the information on FlaB, FlaC and FlaD together, it is hypothesize that FlaC is in the upper level of the hierarchy controlling the cell phase by upregulating the sessile phase and down regulating the motile phase through indirect regulation of CtrA level (Fig. 32). FlaB is in the same or lower position in the hierarchy shuttling phosphate between CckA and CtrA, and/or between unknown regulators for class III genes (Fig. 32). The FlaD is positioned in the same level or lower than FlaB in the hierarchy which regulates the mot genes of the flagellar motor complex (Fig. 32).

Complementation of the *flaC* mutant (HG1016) with pRSI506 plasmid did not restore the wild-type phenotype. Two possibilities can explain this situation, (i) pRSI506 is not expressing FlaC and/or (ii) HG1016 has a second mutation. The over expression of FlaC in RSI01 (TM1040 rifampicin resistance) did not show any changes in the phenotype when compared to TM1040. This implies that pRSI506 is not expressing FlaC. Observing the population of motile cells from pRSI506 in RSI01 background, the result shows that it is the same as TM1040 but unexpectedly the RSI01 without the plasmid had increase amount of the population of motile cells. The reason for this occurrence is unclear; one possibility is that the

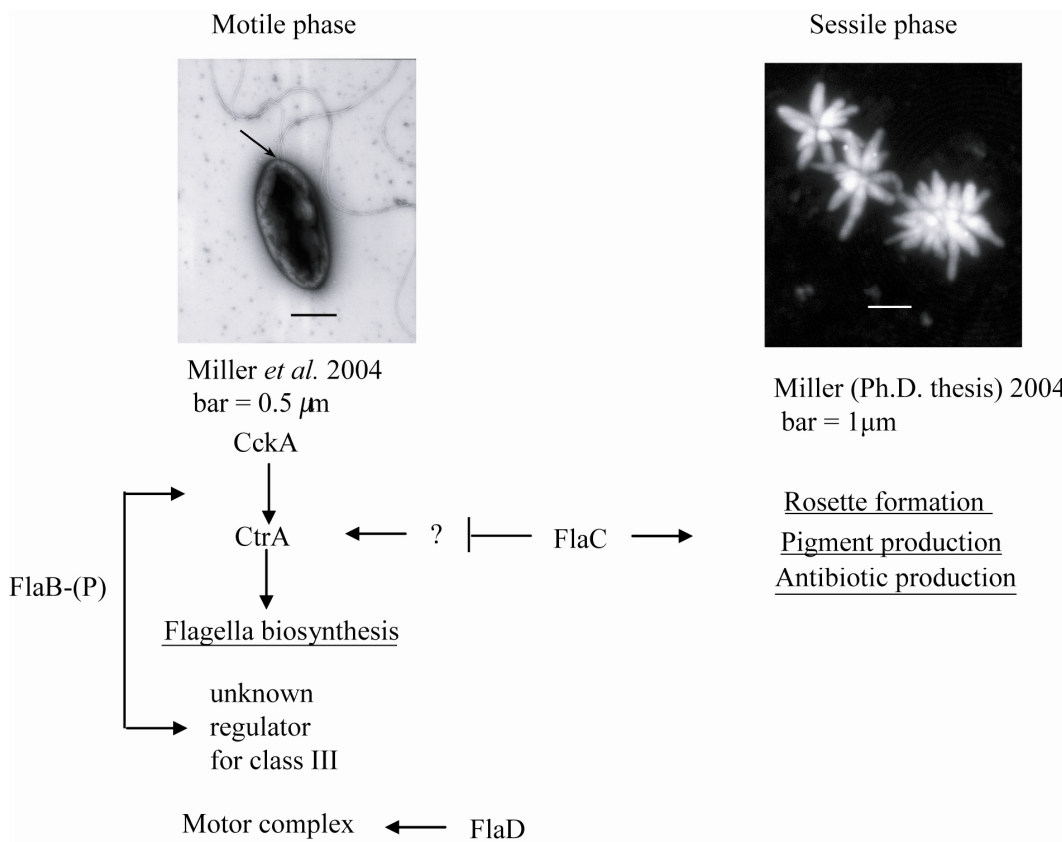


**FIG. 32** Predicted diagram of TM1040 hierarchy including FlaBCD. FlaC is predicted to control the cell phase (swim-or-stick) by upregulating the sessile phase and down regulating the motile phase through indirect regulation of CtrA level. The phosphorelated FlaB (FlaB-(P)) shuttles phosphate between CckA and CtrA, and/or between unknown regulators for class III genes. The FlaD is predicted to regulate the mot genes of the flagellar motor complex.

spontaneous mutation in RSI01 may have an indirect effect on this phenotype. However, since the control (RSI01) itself is different from TM1040, no further experiments were done to continue the investigation.

Although a second mutation in the *flaC* mutant (HG1016) was discovered, in the gene that encoded  $\beta$ -glucuronidase on pSTM2, it is still unclear if this mutation also contributes to the multiple phenotypes of the *flaC* mutant. Downstream of  $\beta$ -glucuronidase gene is a gene encoding for a GntR-like regulator, it is most likely that the pleiotropic phenotypes may come from a polar effect affecting the transcription of this gene.

For future studies, it is certainly worth constructing the null mutant of *flaC* and complementing this mutant, for a more thorough investigation of the function of FlaC. In addition, further studies of the function, molecular mechanisms, and the proteins that interact with FlaC would certainly reveal a great volume of useful information on roseobacter gene regulation of the biphasic mode of life and its role in the symbiosis between TM1040 and its phytoplankton hosts.

## Appendix A: Media and Solutions

### A.1. Media

#### A.1.1. Luria Bertani (LB) Broth

Tryptone	10	g
NaCl	5	g
Yeast Extract	5	g
H <sub>2</sub> O	1000	ml

Autoclave at 121°C for 20 min

#### A.1.2. Luria Bertani (LB) Agar

Tryptone	10	g
NaCl	5	g
Yeast Extract	5	g
Bacto Agar	15	g
H <sub>2</sub> O	1000	ml

Autoclave at 121°C for 20 min

#### A.1.3. 2216 Marine Broth

2216 Marine Broth	37.4	g
H <sub>2</sub> O	1000	ml

Autoclave at 121°C for 20 min

#### A.1.4. 2216 Marine Agar

2216 Marine Broth	37.4	g
Bacto Agar	15	g
H <sub>2</sub> O	1000	ml

Autoclave at 121°C for 20 min

#### **A.1.5. Heart Infusion Artificial Sea Water (HIASW) Broth**

Heart infusion powder	25	g
Instant Ocean sea salts	15	g
H <sub>2</sub> O	1000	ml

Autoclave at 121°C for 20 min

#### **A.1.6. Heart Infusion Artificial Sea Water (HIASW) Agar**

Heart infusion powder	25	g
Instant Ocean sea salts	15	g
Bacto Agar	15	g
H <sub>2</sub> O	1000	ml

Autoclave at 121°C for 20 min

#### **A.1.7. 2216 Marine Motility Agar**

2216 Marine Broth	37.4	g
Bacto Agar	0.3	g
H <sub>2</sub> O	1000	ml

Autoclave at 121°C for 20 min

### A.1.8. Marine Motility Agar

(Stock A) Make 2X Sea Salts (1000 ml)

400 mM NaCl	23.2	g/250 ml H <sub>2</sub> O
100 mM MgSO <sub>4</sub>	12	g/250 ml H <sub>2</sub> O
20 mM KCl	1.5	g/250 ml H <sub>2</sub> O
20 mM CaCl <sub>2</sub> ·2H <sub>2</sub> O	2.94	g/250 ml H <sub>2</sub> O

Autoclave separately, then mix together to make 2X sea salts 1000 ml

(Stock B) Make 4X BM (-NH<sub>4</sub>Cl) (525 ml)

1M Tris-HCl pH 7.5	150	ml
K <sub>2</sub> HPO <sub>4</sub>	87	mg
H <sub>2</sub> O	375	ml

Autoclave

(Stock C) Make 1% Peptone (200 ml)

Peptone	2	g
H <sub>2</sub> O	200	ml

Autoclave

(Stock D) Make 2% agar (30ml)

Bacto Agar	0.6	g
H <sub>2</sub> O	30	ml

Autoclave

After autoclaving stock A, B, C, and D separately, let stock A, B, and C cool down to room temperature. Place Stock D in 50°C water bath to bring the temperature down to 50°C. Mix Stock A 50 ml : Stock B 25 ml : Stock C 10 ml and warm to 50°C. Then add 15 ml of pre-warmed Stock D to the mixture and mix. Immediately pour into petri dishes.

### **A.1.9. Marine Motility broth**

(Stock A)      Make 2X Sea Salts (1000 ml)

400 mM NaCl	23.2	g/250 ml H <sub>2</sub> O
100 mM MgSO <sub>4</sub>	12	g/250 ml H <sub>2</sub> O
20 mM KCl	1.5	g/250 ml H <sub>2</sub> O
20 mM CaCl <sub>2</sub> .2H <sub>2</sub> O	2.94	g/250 ml H <sub>2</sub> O

Autoclave separately, then mix together to make 2X sea salts 1000 ml

(Stock B)      Make 4X BM (-NH<sub>4</sub>Cl) (525 ml)

1M Tris-HCl pH 7.5	150	ml
K <sub>2</sub> HPO <sub>4</sub>	87	mg
H <sub>2</sub> O	375	ml

Autoclave

(Stock C)      Make 1% Peptone (200 ml)

Peptone	2	g
H <sub>2</sub> O	200	ml

Autoclave

After autoclaving stock A, B, and C separately, let them cool down to room temperature. Mix  
 Stock A 50 ml : Stock B 25 ml : Stock C 10 ml : Sterile H<sub>2</sub>O 15 ml.

**A.1.10. Marine Basal Medium Formula #2 agar plates**

Formula #2 agar plates 100 ml

H <sub>2</sub> O	10	ml
FeEDTA	5	ml
2x ASW	50	ml
BM	25	ml
RPMI vitamin stock	0.1	ml
10x attractant	10	ml
Bacto Agar	0.275	g

2X ASW (1000 ml)

NaCl	23.2	g/250 ml H <sub>2</sub> O
MgSO <sub>4</sub>	12	g/250 ml H <sub>2</sub> O
KCl	1.5	g/250 ml H <sub>2</sub> O
CaCl <sub>2</sub> .2H <sub>2</sub> O	2.94	g/250 ml H <sub>2</sub> O

Autoclave separately, then mix together to make 2X ASW 1000 ml

4X BM (525 ml)

1M Tris-HCl pH 7.5	150	ml
K <sub>2</sub> HPO <sub>4</sub>	87	mg
NH <sub>4</sub> Cl	1.5	g
H <sub>2</sub> O	375	ml

Autoclave

FeEDTA

FeEDTA                    50    mg

H<sub>2</sub>O                         100   ml

**A.1.11. Heart Infusion Artificial Sea Water 10 ppt (HIASW10) broth**

Heart infusion            25    g

Seasalts (Sigma)        10    g

H<sub>2</sub>O                         1000 ml

Autoclave

**A.1.12. Heart Infusion Artificial Sea Water 10 ppt (HIASW10) agar plates**

Heart infusion            25    g

Seasalts (Sigma)        10    g

Bacto agar                15    g

H<sub>2</sub>O                         1000 ml

Autoclave

## A.2. Solutions

### A.2.1. Lysis buffer (for Quick Prep plasmid extraction)

40% Glucose (filter sterilized)	2.5	ml
0.5M EDTA pH 8.0	2	ml
1 M Tris-HCl pH 8.0	2.5	ml
H <sub>2</sub> O	93	ml

On day of use, dispense desired volume to sterile tube and add 2 mg/ml lysozyme.

### A.2.2. Alkaline SDS (for Quick Prep plasmid extraction)

NaOH	0.8	g
BioRad SDS	1	g
H <sub>2</sub> O	100	ml
Filter sterilize		

### A.2.3. Potassium Acetate (for Quick Prep plasmid extraction)

Concentrated Acetic acid	28.74	ml
H <sub>2</sub> O	60	ml

Add KOH pellets to pH 4.8

Adjust volume to 100 ml and filter sterilize

### A.2.4. Tris-EDTA (TE)

1M Tris-HCl pH 7.5	10	ml
0.5M EDTA	2	ml

Adjust volume to 1000 ml with H<sub>2</sub>O

#### **A.2.5. 50x Tris-Acetic acid-EDTA (TAE)**

Tris Base	242	g
Glacial Acetic Acid	57.1	ml
EDTA	37.2	g
Adjust volume to 1000 ml with H <sub>2</sub> O		

#### **A.2.6. 4x Polyethylene Glycol Solution (PEG)**

Polyethylene glycol 8000	80	g
NaCl	23	mg
H <sub>2</sub> O	1000	ml

#### **A.2.7. 5x Protein loading dye**

1M Tris-HCl pH 6.8	1.56	ml
Glycerol	2.5	ml
20% SDS	2.5	ml
2-β mercaptoethanol	1.25	ml
Bromphenol blue	5	mg
H <sub>2</sub> O	2.19	ml

#### **A.2.8. 15% SDS-PAGE Polyacrylamide gel**

##### 30% acrylamide/0.8% bisacrylamide

Acrylamide	30	g
N,N'-methylenebisacrylamide	0.8	g

Adjust volume to 100 ml with H<sub>2</sub>O

Filter through 0.45 μm filter

4xTris-HCl/SDS, pH 6.8

0.5 M Tris-HCl	100	ml	
SDS	0.4		g

Filter through 0.45  $\mu$ m filter

4xTris-HCl/SDS, pH 8.8

1.5 M Tris-HCl	500	ml	
SDS	2		g

Filter through 0.45  $\mu$ m filter

Separation Gel

30% acrylamide/0.8% bisacrylamide	7.5	ml
4xTris-HCl/SDS, pH 8.8	3.75	ml
H <sub>2</sub> O	3.75	ml
10% Ammonium persulfate	0.05	ml
TEMED	0.01	ml

Stacking Gel

30% acrylamide/0.8% bisacrylamide	0.65	ml
4xTris-HCl/SDS, pH 6.8	1.25	ml
H <sub>2</sub> O	3.05	ml
10% Ammonium persulfate	0.025	ml
TEMED	0.005	ml

### **A.2.9. 5x SDS-PAGE electrophoresis buffer**

Tris base	15.1	g
Glycine	72	g
SDS	5	g
Add H <sub>2</sub> O to 1000 ml		

### **A.2.10. 35 ppt ASW**

Instant Ocean sea salts	40	g
H <sub>2</sub> O	1000	ml

### **A2.11. 5x M9 salts**

Na <sub>2</sub> HPO <sub>4</sub> ·7H <sub>2</sub> O	64	g
KH <sub>2</sub> PO <sub>4</sub>	15	g
NaCl	150	g
NH <sub>4</sub> Cl	5	g
H <sub>2</sub> O	1000	ml

## Appendix B: Protocols

### **B.1. TM1040 electrocompetent cells**

1. Inoculate single colony of TM1040 into 2ml HIASW broth and incubate at 30°C overnight with shaking.
2. Transfer the culture into 250 ml HIASW broth in 1L flask and incubate at 30°C with shaking until OD<sub>600</sub> is 0.6.
3. Cool the cells in ice for 30 min.
4. Transfer the culture to pre-chilled 250 ml centrifuge bottles and centrifuge at 9000 r.p.m. for 10 min. at 4°C.
5. Discard supernatant and wash the cells four times in 200 ml ice-cold sterile water using the same centrifuge conditions as step 4.
6. Resuspend cells in 1 ml 10% glycerol (sterile).
7. Dispense 65 µl of mixture in 1.5 ml centrifuge tubes and store at -80°C until ready to use.

### **B.2. Transposon mutagenesis**

1. Add 25 ng of EZ-Tn5 transposome (Epicentre, Madison, Wisconsin) into 65 µl of TM1040 electrocompetent cells.
2. Incubate on ice for 30 min.
3. Transfer the mixture to pre-chilled 0.2 cm Electroporation cuvette and electroporate at 2.5 Kv per cm, 400 ohms and 25 µF using Bio-Rad Gene Pulser (Bio-Rad, Hercules, California).
4. Transfer the cells into 1 ml HIASW, pre-warmed at 30°C.

5. Incubate at 30°C with shaking for 2 h.
6. Spread 100 µl of culture on HIASW agar plates containing Kanamycin (120µg/ml).
7. Incubate at 30°C for 48 h.
8. Pick the Kanamycin resistant colonies onto a 7-by-7 array on 2216 agar plates containing Kanamycin 120µg/ml (Kan120) and incubate at 30°C ~2 days.
9. Screen for motility defect mutants by inoculating the transposon mutants from the 2216 agar + Kan120 plates to 2216 Marine motility plates and incubate at 30°C.

### **B.3. CTAB Chromosomal extraction**

1. Grow 50 ml of the desired strain in the appropriate medium and condition.
2. Transfer the culture into 40 ml Polypropylene centrifuge tube and centrifuge at 5000 r.p.m. for 5 min at 4°C in Beckman JA21 rotor.
3. Discard supernatant and resuspend the cells in 5.5 ml TE.
4. Add 300 µl of 10% SDS. Mix by hand until solution is homogeneous. Then add 60 µl of 10 mg/ml Proteinase K, and mix thoroughly.
5. Incubate at 37°C for 60 min so the solution appears clear.
6. Add 1 ml 5M NaCl and mix thoroughly by hand ~7 min.
7. Add 800 µl 10% CTAB, 0.7M NaCl (pre-warm to 65°C) and mix thoroughly by hand for 5 min.

8. Extract once with 6 ml CHCl<sub>3</sub>: Isoamyl Alcohol (24:1) and mix thoroughly by hand.
9. Centrifuge in Beckman JA21 rotor at 6000 r.p.m. for 10 min at 4°C.
10. Remove supernatant into a new centrifuge tube and add 6 ml of buffer phenol: CHCl<sub>3</sub>: Isoamyl Alcohol (25:24:1). Mix thoroughly by hand.
11. Centrifuge in Beckman JA21 rotor at 6000 r.p.m. for 10 min at 4°C.
12. Remove supernatant into a new tube.
13. Add 5 ml isopropanol, mix, and spool the DNA onto a Pasteur pipette (with sealed end).
14. Remove the isopropanol by dipping the spooled DNA into 70% EtOH. Invert the Pasteur pipette so that the spooled DNA faces upward and allow the excess 70% EtOH to drain.
15. Resuspend the genomic DNA by dipping the spooled DNA up and down repeatedly in 1 ml TE.

#### **B.4. Rescue-cloning TM1040 transposon mutants**

1. Extract the transposon mutant genome either by CTAB method or DNeasy Kit (Qiagen, Valencia, California).
2. Digest the genome with NcoI using the following mixture:

Genome extract	2	μg
NcoI (10 U/μl)	1	μl
NEBuffer 3	2	μl
Adjust volume to 20 μl with H <sub>2</sub> O		

Incubate at 37°C for 90 min and heat inactivate for 25°C

3. Self-ligate the digested fragments using the following mixture:

NcoI digest reaction	20	μl
10x T4 ligase buffer	4	μl
T4 ligase	1	μl
H <sub>2</sub> O	15	μl

Incubate at 16°C for 4 h.

4. Desalt the Ligation reaction:
- Mix 20 μl of ligation reaction with 20 μl of 7.5 M Ammonium Acetate and 10 μl of tRNA (10 μg/μl H<sub>2</sub>O).
  - Add 100 μl of absolute Ethanol and incubate on ice for 15 min.
  - Centrifuge at 14,000 r.p.m. for 15 min. at 4°C and discard supernatant.
  - Wash with 1 ml 70% Ethanol and centrifuge at 14,000 r.p.m. for 15 min at room temperature.
  - Discard supernatant and resuspend pellet with 20 μl sterile H<sub>2</sub>O.
5. Mix 1 μl of the desalted ligation reaction with 65 μl of DH5α λpir electrocompetent cells on ice and vortex.
6. Immediately transfer the mixture to a pre-chilled 0.2 cm electroporation cuvette and electroporate at 2.5 Kv per cm, 200 ohms and 25 μF using Bio-Rad Gene Pulser (Bio-Rad, Hercules, California).
7. Transfer the cells into 1 ml LB, pre-warmed at 37°C.
8. Incubate at 37°C static 30 min followed 37°C with shaking for 1 h.

9. Spin down 1 ml of the culture and discard supernatant.
10. Resuspend the cells with 100  $\mu$ l of LB broth and spread on LB agar plates containing Kanamycin 60  $\mu$ /ml (Kan60).
11. Incubate at 37°C overnight.
12. Extract the plasmid from the transformant and sequence the flanking DNA using the primers supplied in the EZ-Tn5 transposome kit (Epicentre catalog # TSM08KR).

#### **B.5. Quick Prep procedure for plasmid extraction**

1. Grow 2ml of overnight culture of the strain harboring the plasmid in the appropriate medium and antibiotic.
2. Spin down the cells in a desktop centrifuge at maximum speed for 10-15 seconds to pellet the cells.
3. Aspirate off the supernatant leaving behind ~50  $\mu$ l to aid in resuspension of the cells pellet.
4. Vortex the tube to resuspend the cells.
5. Add 100  $\mu$ l of Lysis solution and vortex. Incubate at room temperature for 5 min.
6. Add 200  $\mu$ l of Alkaline SDS and vortex. Incubate on ice for 5 min.
7. Add 150  $\mu$ l of sterile 5M Potassium Acetate and mix thoroughly. Incubate on ice for 5 min.
8. Centrifuge at maximum speed for 5 min.
9. Transfer 360  $\mu$ l of the clear fluid to a new microcentrifuge tube.

10. Add 720  $\mu$ l of ice cold 100% EtOH and vortex. Incubate at room temperature for 5 min.
11. Centrifuge at maximum speed for 5 min.
12. Aspirate off the fluid leaving a small pellet containing the plasmid in the tube.
13. Add 500  $\mu$ l of ice cold 70% EtOH to the tube and vortex.
14. Centrifuge at maximum speed for 5 min.
15. Dry the pellet in Savant Speed-Vac for 10 min without heat.
16. Resuspend the pellet in 50  $\mu$ l TE.

#### **B.6. Motility analysis in semi-solid agar**

1. Inoculate TM1040 or transposon mutant from a colony onto 2216 Marine Motility agar or Marine Motility agar.
2. Incubate at 30°C for 3 days.
3. Use a sterile toothpick to inoculate from the periphery of the motile colony onto a new 2216 Marine Motility agar or Marine Motility agar plate.
4. Incubate at 30°C for 1 day.

#### **B.7. Motility analysis in broth**

1. Inoculate a single colony of TM1040 or transposon mutant into 2 ml 2216 Marine broth.
2. Incubate at 30°C with shaking overnight.
3. Pipette 7  $\mu$ l onto a glass slide and cover with a cover slip.

4. Observe motility through phase contrast microscope with 20x or 40x objective lens.

**B.8. Measurement of population of motile cells, single non-motile cells, and cells in rosettes**

1. Use 14 h culture of TM1040 and HG1016 grown in 2216 Marine broth at 30°C with shaking.
2. Pipette 7 µl of culture onto a glass slide and cover with a cover slip.
3. Examine the population of the culture through a phase contrast microscope (Olympus BX60, Center Valley, Pennsylvania) and record five random fields using Qicam Fast 1394 camera. Record 1 sec (20 frame / sec) of each field for analysis using Volocity software (V4.1.0, Improvion, England).
4. Separated the population into (i) single cells, (ii) single non-motile cells, and (iii) cells in rosettes as follow.
  - a. Count the total amount of rosette in the field using these Volocity settings.
    - i. Find Object by intensity; choose area from “black” to “the base of the background peak”.
    - ii. Exclude Object by size:  $< 5-9 \mu\text{m}^2$
    - iii. Record the amount of rosettes (objects) that Volocity has selected.
  - b. Find the average amount of cells in a rosette.

- i. In Volocity, zoom-in the selected rosettes and count the amount of cells in a rosette. Repeat this count for all the rosettes in the field and calculate the average of cells per rosette.
- c. Find the amount of total single cells (non-motile and motile cells).
  - i. Use the same setting in (a.i) but set “Exclude Object size” to > 5-9  $\mu\text{m}^2$
  - ii. Add in another “exclude object size” and set to < 1  $\mu\text{m}^2$
  - iii. Record the amount of total single cells (objects) that Volocity has selected.
- d. Find the amount of motile cells
  - i. Use the same setting as (c) to select total single cells
  - ii. Add in “Track Objects” and set to
    - 1. Tracking model: Shortest path
    - 2. Ignore static objects
    - 3. Ignore new objects
    - 4. Automatically join broken tracks
    - 5. Maximum distance between objects: use this distance:  
10  $\mu\text{m}$
  - iii. Then measure all time points
  - iv. Save the measure by “Make Measure Item”
  - v. Open the “measure Item” that was just saved and pull down the filter drop bar and set to “Tracks”

- vi. Click on “Edit Filter icon” and set to “Displacement ( $\mu\text{m}$ ) is more than 1.5”
  - vii. Record the amount of tracks shown (amount of motile cells).
- e. Find percentage of cells forming rosettes.
- i. Total cells forming rosettes in the field = (average cells per rosette) x (amount of rosette)
  - ii. Total cells in the field = (amount of total single cells) + (total cells forming rosettes in the field)
  - iii. Percent cells forming rosette = [(cells forming rosettes in the field) x 100] / Total cells in the field
- f. Find percentage motile cells
- i. Percentage motile cells = [(amount of motile cells) x 100] / Total cells in the field
- g. Find percentage of nonmotile cells
- i. Percentage of nonmotile cells = [(Total single cells – amount motile cells) x 100] / Total cells in the field
5. Do this calculation for all five fields.
6. Do the experiment in quadruplicate.
7. Use Prism 4.0 static software (GraphPad) to determine the mean, standard deviation, and statistic analysis [One-way ANOVA (non parametric) and Newman-Keuls (95% CI and P-value 0.05)].

### **B.9. Flagellar staining**

1. Pipette 5  $\mu$ l of culture onto a glass slide and cover with a cover slip.
2. Add 10  $\mu$ l of RYU Flagellar stain (Remel, Lenexa, Kansas) to the side of the cover slip so that the stain carefully defuses into the culture.
3. Incubate at room temperature for 10 min. and observe through phase contrast microscope using 40x object lens.

### **B.10. Flagella precipitation and detection of flagellin**

1. Use overnight cultures of TM1040 or mutants grown in 50 ml 2216 Marine Broth in a 500 ml flask at 30°C with shaking.
2. Transfer the culture to a 40 ml centrifuge tube and centrifuge at 10,000 x g for 5 min. at 4°C.
3. Transfer the supernatant, containing the detached flagella, to a new centrifuge tube and centrifuge like step 2.
4. Carefully pipette 30 ml of the supernatant to a new centrifuge tube and add 10 ml of 4x polyethylene glycol solution (8% PEG 8000, 0.4 mM NaCl).
5. Vortex and incubate the tube on ice for 60 min.
6. Centrifuge the tube at 17,400 x g for 15 min at 4°C to precipitate the flagella bundles.
7. Discard the supernatant and resuspend the flagella bundles in 50 mM Tris-HCl pH 7.5.
8. Determine the amount of total protein in the sample with BCA kit (Pierce, Rockford, Illinois).

9. To separate the flagellin, load 3  $\mu\text{g}$  of flagella preparation on a 15% SDS-PAGE gel and run the gel until the dye run off bottom.
10. Stain the with Coomassie Fluor Orange Protein gel stain (Molecular Probes, Invitrogen, Carlsbad, California) following the manufacturer's recommendation.
11. Visualize the bands by scan the gel with the Typhoon 9410 (Amersham Biosciences, Piscataway, New Jersey) using 555 nm emission filter and a 488 nm excitation filter.

#### **B.11. Measurement of antibiotic production**

1. Use overnight cultures of TM1040, HG1016, and HG1101 to inoculate 1:100 in 2216 Marine broth.
2. Make two sets of samples.
3. Incubate one set of samples at 30°C with shaking and the other at static.
4. Pipette 1 ml of culture into a microcentrifuge tube at 0, 24, 48, 72, and 96 h.
5. Centrifuge in a desktop centrifuge at maximum speed for 1 min to pellet the cells.
6. Transfer the supernatant to a new tube and freeze at -20°C until finish collecting all time points.
7. Inoculate *Vibrio anguillarum* in 2216 Marine broth and incubate at room temperature overnight.
8. Autoclave water containing 0.5 g agar and hold it at 44°C in order to keep the agar molten.

9. Add 5  $\mu$ l of 1M CaCl<sub>2</sub>, 0.1 ml 1M MgSO<sub>4</sub>, 10 ml 5xM9 salts, 1 ml 20% glucose, 1.5 ml 10% casamino acids.
10. Make sure the agar is at 44°C and then add 50  $\mu$ l of overnight *V. anguillarum* and immediately pour into large petri dish (150x15 mm).
11. After the plate has solidified, punch wells in the agar with the end of 200  $\mu$ l pipette tip.
12. Add 60  $\mu$ l of spent medium from the bacteria culture and incubate at room temperature until a inhibition zone is seen (~24 h).

#### **B.12. Congo red binding**

1. Make congo red plates by making 2216 Marine agar and add filter sterilized Congo Red to a final concentration of 100  $\mu$ g/ml while the agar is still molten.
2. Pour mixture into a petri dish and let it solidify at room temperature overnight.
3. Inoculate single colony of TM1040 and mutants in 2ml 2216 Marine broth and incubate at 30°C with shaking overnight.
4. Spot 2  $\mu$ l of culture on the same Congo red plate
5. Incubate at 30°C overnight

#### **B.13. Biofilm staining**

1. Grow TM1040 and mutants in 2ml 2216 Marine broth at 30°C with shaking for 24 h.
2. Inoculate 3  $\mu$ l of culture into 300 $\mu$ l of fresh 2216 Marine broth in small glass test tube (1:100).

3. Incubate at 30°C with shaking overnight.
4. Aspirate out the culture.
5. Rinse with gentle streams of 35 ppt ASW
6. Stain with 1 ml Gram Crystal Violet solution (BD Bioscience, Sparks, Maryland) for 30 min at room temperature.
7. Rinse with gentle streams of 35 ppt ASW.
8. Elute with 400 µl DMSO:Ethanol (50:50).
9. Pipette into 96 well plates
10. Take OD<sub>560 nm</sub>

Note: used acid washed small test tubes (acid wash by leaving the tubes in 1% HCl overnight then wash with RBS-PF)

#### **B.14. Chemotaxis plate assay**

1. Inoculate a single colony of TM1040 and HG1016 in Marine motility agar
2. Incubate at 30°C for 3 days
3. Inoculate from the periphery of the motile colony into Marine Basal Medium Formula #2 agar plates containing 10 mM of attractant (one attractant per plate, Methionine, Valine, Glycine, Alanine, Phenylalanine, Succinic acid, Fumarate, malic acid, and acetate).
4. Inoculate both TM1040 and HG1016 on the same plate for comparison.
5. Incubate at 30°C for 3 days and measure diameter of the motile colony.
6. Make duplicates of every plate.

### B.15. Biparental mating

1. Grow overnight culture of pRSI506/S17-1 and pRK415/S17-1 in 2 ml of LB with tetracycline (15 µg/ml) at 37°C with shaking.
2. Grow overnight culture of HG1016 in 2216 with kanamycin (120 µg/ml) and RSI01 in 2216 with rifampicin (100µg/ml) at 30°C with shaking.
3. Set up the mating mixture as fellow, in a microcentrifuge tube;

Mixture	HG1016	RSI01	pRSI506/S17-1	pRK415/S17-1
pRSI506.S17-1 + HG1016	100 µl	-	100 µl	-
pRK415/S17-1 + HG1016	100 µl	-	-	100 µl
pRSI506.S17-1 + RSI01	-	100 µl	100 µl	-
pRK415/S17-1 + RSI01	-	100 µl	-	100 µl

4. Include HG1016, RSI01, pRSI506/S17-1, and pRK415/S17-1 seperately as controls.
5. Mix the culture by vortexing the tubes and centrifuge at maxium speed to pellet the cells.
6. Discard the supernatant and leave 20 µl for resuspending the pellet.
7. Spot all of the culture on HIASW10 plate
8. Incubate at 30°C for 24 hrs.

9. Take the cultures up with a sterile loop and resuspend in 200  $\mu$ l of 10ppt ASW.
10. Make 100 fold serial dilution in 10 ppt ASW (10  $\mu$ l culture into 990  $\mu$ l ASW).
11. Spread 100  $\mu$ l on HIASW10 plates with appropriate antibiotic. For selection of pRSI506/HG1016 and pRK415/HG1016 use tetracycline (15  $\mu$ g/ml) + kanamycin (120  $\mu$ g/ml). For selection of pRSI506/RSI01 and pRK415/RSI01 use tetracycline (15  $\mu$ g/ml) + rifampicin (100  $\mu$ g/ml).
12. Incubate the plates at 30°C for 2 days.

#### **B.16. Electroporation of pRSI507 into TM1040**

1. Add 100 ng to 1  $\mu$ g pRSI507 into 65  $\mu$ l of TM1040 electrocompetent cells.
2. Incubate on ice for 30 min.
3. Transfer the mixture to pre-chilled 0.2 cm Electroporation cuvette and electroporate at 2.5 Kv per cm, 400 ohms and 25  $\mu$ F using Bio-Rad Gene Pulser (Bio-Rad, Hercules, California).
4. Transfer the cells into 1 ml HIASW, pre-warmed at 30°C.
5. Incubate at 30°C with shaking for 2 h.
6. Spread 100  $\mu$ l of culture on HIASW agar plates containing Kanamycin (120 $\mu$ g/ml).

7. Centrifuge the remaining culture in the desktop centrifuge at maximum speed for 1 min to pellet the cells.
8. Discard the supernatant and leave about 100  $\mu$ l to resuspend the cells
9. After resuspending the cells, spread the culture on HIASW agar plates containing Kanamycin (120 $\mu$ g/ml).
10. Incubate at 30°C for 24 - 48 hr.

## Reference

1. **Adler, J., and B. Templeton.** 1967. The effect of environmental conditions on the motility of *Escherichia coli*. *J. Gen. Microbiol.* **46**:175-84.
2. **Alavi, M., T. Miller, K. Erlandson, R. Schneider, and R. Belas.** 2001. Bacterial community associated with *Pfiesteria*-like dinoflagellate cultures. *Environ. Microbiol.* **3**:380-396.
3. **Alavi, M. R.** 2004. Predator/prey interaction between *Pfiesteria piscicida* and *Rhodomonas* mediated by a marine alpha proteobacterium. *Microb. Ecol.* **47**:48-58.
4. **Alekshun, M. N., and S. B. Levy.** 1999. The mar regulon: multiple resistance to antibiotics and other toxic chemicals. *Trends Microbiol.* **7**:410-413.
5. **Altschul, S. F., W. Gish, W. Miller, E. W. Myers, and D. J. Lipman.** 1990. Basic local alignment search tool. *J. Mol. Biol.* **215**:403-410.
6. **Anderson, P. E., and J. W. Gober.** 2000. FlbT, the post-transcriptional regulator of flagellin synthesis in *Caulobacter crescentus*, interacts with the 5' untranslated region of flagellin mRNA. *Mol. Microbiol.* **38**:41-52.
7. **Armitage, J. P., and R. M. Macnab.** 1987. Unidirectional, intermittent rotation of the flagellum of *Rhodobacter sphaeroides*. *J. Bacteriol.* **169**:514-8.
8. **Armitage, J. P., and R. Schmitt.** 1997. Bacterial chemotaxis: *Rhodobacter sphaeroides* and *Sinorhizobium meliloti*--variations on a theme? *Microbiology* **143** (Pt 12):3671-82.
9. **Attmannspacher, U., B. E. Scharf, and R. M. Harshey.** 2008. FliL is essential for swarming: motor rotation in absence of FliL fractures the flagellar rod in swarmer cells of *Salmonella enterica*. *Mol. Microbiol.* **68**:328-41.

10. **Barnakov, A. N., L. A. Barnakova, and G. L. Hazelbauer.** 2002. Allosteric enhancement of adaptational demethylation by a carboxyl-terminal sequence on chemoreceptors. *J Biol Chem* **277**:42151-6.
11. **Barnakov, A. N., L. A. Barnakova, and G. L. Hazelbauer.** 1999. Efficient adaptational demethylation of chemoreceptors requires the same enzyme-docking site as efficient methylation. *Proc Natl Acad Sci U S A* **96**:10667-72.
12. **Barrios, H., B. Valderrama, and E. Morett.** 1999. Compilation and analysis of sigma(54)-dependent promoter sequences. *Nucleic Acids Res* **27**:4305-13.
13. **Belas, R., and R. Suvanasuthi.** 2005. The ability of *Proteus mirabilis* to sense surfaces and regulate virulence gene expression involves FliL, a flagellar basal body protein. *J. Bacteriol.* **187**:6789-803.
14. **Bibikov, S. I., R. Biran, K. E. Rudd, and J. S. Parkinson.** 1997. A signal transducer for aerotaxis in *Escherichia coli*. *J Bacteriol* **179**:4075-9.
15. **Bilwes, A. M., L. A. Alex, B. R. Crane, and M. I. Simon.** 1999. Structure of CheA, a signal-transducing histidine kinase. *Cell* **96**:131-141.
16. **Biondi, E. G., S. J. Reisinger, J. M. Skerker, M. Arif, B. S. Perchuk, K. R. Ryan, and M. T. Laub.** 2006. Regulation of the bacterial cell cycle by an integrated genetic circuit. *Nature* **444**:899-904.
17. **Blair, D. F., and H. C. Berg.** 1991. Mutations in the MotA protein of *Escherichia coli* reveal domains critical for proton conduction. *J Mol Biol* **221**:1433-1442.
18. **Blair, D. F., D. Y. Kim, and H. C. Berg.** 1991. Mutant MotB proteins in *Escherichia coli*. *J. Bacteriol.* **173**:4049-4055.
19. **Bourret, R. B., J. F. Hess, and M. I. Simon.** 1990. Conserved aspartate residues and phosphorylation in signal transduction by the chemotaxis protein CheY. *Proc Natl Acad Sci U S A* **87**:41-5.

20. **Braun, T. F., S. Poulson, J. B. Gully, J. C. Empey, S. Van Way, A. Putnam, and D. F. Blair.** 1999. Function of proline residues of MotA in torque generation by the flagellar motor of *Escherichia coli*. *J Bacteriol* **181**:3542-51.
21. **Bruhn, J. B., L. Gram, and R. Belas.** 2007. Production of antibacterial compounds and biofilm formation by *Roseobacter* species are influenced by culture conditions. *Appl. Environ. Microbiol.* **73**:442-450.
22. **Buchan, A., J. M. Gonzalez, and M. A. Moran.** 2005. Overview of the Marine *Roseobacter* Lineage. *Appl. Environ. Microbiol.* **71**:5665-77.
23. **Burkholder, J. M., and J. Glasgow, H. B.** 1995. Interactions of a toxic estuarine dinoflagellate with microbial predators and prey. *Arch. Fur. Protisten.* **145**:177 - 188.
24. **Burkholder, J. M., and J. Glasgow, H. B.** 1997. Trophic controls on stage transformations of a toxic ambush-predator dinoflagellate. *J. Euk. Microbiol.* **44**:200-205.
25. **Chilcott, G. S., and K. T. Hughes.** 2000. Coupling of flagellar gene expression to flagellar assembly in *Salmonella enterica* serovar typhimurium and *Escherichia coli*. *Microbiol Mol Biol Rev* **64**:694-708.
26. **Claret, L., and C. Hughes.** 2002. Interaction of the atypical prokaryotic transcription activator FlhD2C2 with early promoters of the flagellar gene hierarchy. *J Mol Biol* **321**:185-99.
27. **Collinson, S. K., P. C. Doig, J. L. Doran, S. Clouthier, T. J. Trust, and W. W. Kay.** 1993. Thin, aggregative fimbriae mediate binding of *Salmonella enteritidis* to fibronectin. *J. Bacteriol.* **175**:12-18.
28. **Doyle, M. L., P. A. Katzman, and E. A. Doisy.** 1955. Production and properties of bacterial beta-glucuronidase. *J Biol Chem* **217**:921-30.

29. **Eggenhofer, E., M. Haslbeck, and B. Scharf.** 2004. MotE serves as a new chaperone specific for the periplasmic motility protein, MotC, in *Sinorhizobium meliloti*. *Mol Microbiol* **52**:701-12.
30. **Enomoto, M.** 1966. Genetic studies of paralyzed mutant in Salmonella. I. Genetic fine structure of the mot loci in *Salmonella typhimurium*. *Genetics* **54**:715-26.
31. **Gallagher, S. R.** 1999. One-Dimensional SDS-PAGE Gel Electrophoresis of Proteins, p. 10.2A.1-10.2A.9. *In* F. M. Ausubel, R. Brent, R. E. Kingston, D. D. Moore, J. G. Seidman, J. A. Smith, and K. Struhl (ed.), *Current protocols in molecular biology*, vol. 2. John Wiley & Sons, Inc.
32. **Geng, H., J. B. Bruhn, K. F. Nielsen, L. Gram, and R. Belas.** 2008. Genetic dissection of tropodithietic acid biosynthesis by marine roseobacters. *Appl. Environ. Microbiol.* **74**:1535-45.
33. **Gonzalez, J. M., J. S. Covert, W. B. Whitman, J. R. Henriksen, F. Mayer, B. Scharf, R. Schmitt, A. Buchan, J. A. Fuhrman, R. P. Kiene, and M. A. Moran.** 2003. *Silicibacter pomeroyi* sp. nov. and *Roseovarius nubinhibens* sp. nov., dimethylsulfoniopropionate-demethylating bacteria from marine environments. *Int. J. Syst. Evol. Microbiol.* **53**:1261-1269.
34. **Gonzalez, J. M., R. P. Kiene, and M. A. Moran.** 1999. Transformation of sulfur compounds by an abundant lineage of marine bacteria in the alpha-subclass of the class Proteobacteria. *Appl. Environ. Microbiol.* **65**:3810-3819.
35. **Gonzalez, J. M., and M. A. Moran.** 1997. Numerical dominance of a group of marine bacteria in the alpha-subclass of the class Proteobacteria in coastal seawater. *Appl. Environ. Microbiol.* **63**:4237-4242.
36. **Harrison, D. M., H. L. Packer, and J. P. Armitage.** 1994. Swimming speed and chemokinetic response of *Rhodobacter sphaeroides* investigated by natural manipulation of the membrane potential. *FEBS Lett* **348**:37-40.

37. **Harrison, D. M., J. Skidmore, J. P. Armitage, and J. R. Maddock.** 1999. Localization and environmental regulation of MCP-like proteins in *Rhodobacter sphaeroides*. *Mol Microbiol* **31**:885-92.
38. **Helmann, J. D.** 1991. Alternative sigma factors and the regulation of flagellar gene expression. *Mol Microbiol* **5**:2875-82.
39. **Jacobs, C., I. J. Domian, J. R. Maddock, and L. Shapiro.** 1999. Cell cycle-dependent polar localization of an essential bacterial histidine kinase that controls DNA replication and cell division. *Cell* **97**:111-120.
40. **Jansen, M., and T. A. Hansen.** 2001. Non-growth-associated demethylation of dimethylsulfoniopropionate by (homo)acetogenic bacteria. *Appl Environ Microbiol* **67**:300-6.
41. **Kaiser, J.** 2002. Microbiology. The science of *Pfiesteria*: elusive, subtle, and toxic. *Science* **298**:346-9.
42. **Kanbe, M., J. Yagasaki, S. Zehner, M. Gottfert, and S. Aizawa.** 2007. Characterization of two sets of subpolar flagella in *Bradyrhizobium japonicum*. *J. Bacteriol.* **189**:1083-1089.
43. **Keller, M. D., and W. Korjeff-Bellows.** 1996. Physiological aspects of the production of dimethylsulfoniopropionate (DMSP) by marine phytoplankton, p. 131-153. *In* R. P. Kiene, P. T. Visscher, M. D. Keller, and G. O. Kirst (ed.), *Biological and Environmental Chemistry of DMSP and Related Sulfonium Compounds*. Plenum Press, New York.
44. **Kiene, R. P., L. J. Linn, and J. A. Bruton.** 2000. New and important roles for DMSP in marine microbial communities. *J. Sea Res.* **43**:209-224.
45. **Kolter, R., M. Inuzuka, and D. R. Helinski.** 1978. Trans-complementation-dependent replication of a low molecular weight origin fragment from plasmid R6K. *Cell* **15**:1199-208.

46. **Kondoh, H., C. B. Ball, and J. Adler.** 1979. Identification of a methyl-accepting chemotaxis protein for the ribose and galactose chemoreceptors of *Escherichia coli*. *Proc Natl Acad Sci U S A* **76**:260-4.
47. **Kuo, S. C., and D. E. Koshland, Jr.** 1987. Roles of cheY and cheZ gene products in controlling flagellar rotation in bacterial chemotaxis of *Escherichia coli*. *J Bacteriol* **169**:1307-14.
48. **Lafay, B., R. Ruimy, C. R. de Traubenberg, V. Breittmayer, M. J. Gauthier, and R. Christen.** 1995. *Roseobacter algicola* sp. nov., a new marine bacterium isolated from the phycosphere of the toxin-producing dinoflagellate *Prorocentrum lima*. *Int. J. Syst. Bacteriol.* **45**:290-296.
49. **Laub, M. T., S. L. Chen, L. Shapiro, and H. H. McAdams.** 2002. Genes directly controlled by CtrA, a master regulator of the *Caulobacter* cell cycle. *Proceedings of the National Academy of Science of the United States of America* **99**:4632-7.
50. **Ledyard, K., and J. Dacey.** 1994. Dimethylsulfide production from dimethylsulfoniopropionate by a marine bacterium. *Mar. Ecol. Prog. Ser.* **110**:95-103.
51. **Letunic, I., R. R. Copley, B. Pils, S. Pinkert, J. Schultz, and P. Bork.** 2006. SMART 5: domains in the context of genomes and networks. *Nucleic Acids Res.* **34**:D257-260.
52. **Levit, M. N., and J. B. Stock.** 2002. Receptor methylation controls the magnitude of stimulus-response coupling in bacterial chemotaxis. *J Biol Chem* **277**:36760-5.
53. **Lewitus, A. J.** 1999. Mixotrophy and nitrogen uptake by *pfisteria piscicida* (dinophyceae). *J. Phycol.* **35**:1430-1437.
54. **Lewitus, A. J., J. Glasgow, H. B., and J. M. Burkholder.** 1999. Kleptoplastidy in the toxic dinoflagellate *Pfiesteria piscicida* (Dinophyceae). *J. Phycol.* **35**:303-312.

55. **Litaker, R. W., M. W. Vandersea, S. R. Kibler, V. J. Madden, E. J. Noga, and P. A. Tester.** 2002. Lifecycle of the heterotrophic dinoflagellate *Pfiesteria piscicida* (Dinophyceae). *J. Phycol.* **38**:442-463.
56. **Liu, Y., M. Levit, R. Lurz, M. G. Surette, and J. B. Stock.** 1997. Receptor-mediated protein kinase activation and the mechanism of transmembrane signaling in bacterial chemotaxis. *EMBO J* **16**:7231-40.
57. **Llewellyn, M., R. J. Dutton, J. Easter, D. O'Donnol, and J. W. Gober.** 2005. The conserved *flaF* gene has a critical role in coupling flagellin translation and assembly in *Caulobacter crescentus*. *Mol. Microbiol.* **57**:1127-1142.
58. **Lupas, A., and J. Stock.** 1989. Phosphorylation of an N-terminal regulatory domain activates the CheB methyltransferase in bacterial chemotaxis. *J Biol Chem* **264**:17337-42.
59. **Macnab, R. M.** 2003. How bacteria assemble flagella. *Annu Rev Microbiol* **57**:77-100.
60. **Macnab, R. M.** 2004. Type III flagellar protein export and flagellar assembly. *Biochimica et Biophysica Acta* **1694**:207-217.
61. **Manson, M. D., V. Blank, G. Brade, and C. F. Higgins.** 1986. Peptide chemotaxis in *E. coli* involves the Tap signal transducer and the dipeptide permease. *Nature* **321**:253-6.
62. **Martinez-Hackert, E., and A. M. Stock.** 1997. The DNA-binding domain of OmpR: crystal structures of a winged helix transcription factor. *Structure* **5**:109-124.
63. **Miller, T. R.** 2004. SWIMMING FOR SULFUR: ANALYSIS OF THE ROSEOBACTER-DINOFLAGELLATE INTERACTION. Ph.D. thesis. University of Maryland, College Park.
64. **Miller, T. R., and R. Belas.** 2004. Dimethylsulfoniopropionate metabolism by *Pfiesteria*-associated *Roseobacter* spp. *Appl. Environ. Microbiol.* **70**:3383-91.

65. **Miller, T. R., and R. Belas.** 2006. Motility is involved in *Silicibacter* sp. TM1040 interaction with dinoflagellates. *Environ. Microbiol.* **8**:1648-1659.
66. **Miller, T. R., K. Hnilicka, A. Dziejcz, P. Desplats, and R. Belas.** 2004. Chemotaxis of *Silicibacter* sp. strain TM1040 toward dinoflagellate products. *Appl. Environ. Microbiol.* **70**:4692-701.
67. **Mitchell, J. G., L. Pearson, A. Bonazinga, S. Dillon, H. Khouri, and R. Paxinos.** 1995. Long Lag Times and High Velocities in the Motility of Natural Assemblages of Marine Bacteria. *Appl Environ Microbiol* **61**:877-882.
68. **Moat, A., J. Foster, and M. Spector.** 2002. *Microbial Physiology*, Fourth Edition ed. Wiley-Liss, Inc., New York.
69. **Moat, A., J. Foster, and M. Spector.** 2002. *Microbial Physiology*, Fourth Edition ed. Wiley-Liss, Inc., New York.
70. **Moran, M. A., R. Belas, M. A. Schell, J. M. Gonzalez, F. Sun, S. Sun, B. J. Binder, J. Edmonds, W. Ye, B. Orcutt, E. C. Howard, C. Meile, W. Palefsky, A. Goesmann, Q. Ren, I. Paulsen, L. E. Ulrich, L. S. Thompson, E. Saunders, and A. Buchan.** 2007. Ecological Genomics of Marine Roseobacters. *Appl. Environ. Microbiol.* **73**:4559-4569.
71. **Moran, M. A., J. M. Gonzalez, and R. P. Kiene.** 2003. Linking a bacterial taxon to sulfur cycling in the sea: Studies of the marine Roseobacter group. *Geomicrobiol. J.* **20**:375-388.
72. **Morrison, T. B., and J. S. Parkinson.** 1994. Liberation of an interaction domain from the phosphotransfer region of CheA, a signaling kinase of *Escherichia coli*. *Proc Natl Acad Sci U S A* **91**:5485-9.
73. **Muir, R. E., T. M. O'Brien, and J. W. Gober.** 2001. The *Caulobacter crescentus* flagellar gene, *fliX*, encodes a novel trans-acting factor that couples flagellar assembly to transcription. *Mol Microbiol* **39**:1623-37.

74. **O'Toole, G. A., and R. Kolter.** 1998. Initiation of biofilm formation in *Pseudomonas fluorescens* WCS365 proceeds via multiple, convergent signalling pathways: a genetic analysis. *Mol Microbiol* **28**:449-461.
75. **Obuchowski, P. L., and C. Jacobs-Wagner.** 2008. PflI, a protein involved in flagellar positioning in *Caulobacter crescentus*. *J. Bacteriol.* **190**:1718-29.
76. **Okumura, H., S. Nishiyama, A. Sasaki, M. Homma, and I. Kawagishi.** 1998. Chemotactic adaptation is altered by changes in the carboxy-terminal sequence conserved among the major methyl-accepting chemoreceptors. *J Bacteriol* **180**:1862-8.
77. **Packer, H. L., H. Lawther, and J. P. Armitage.** 1997. The *Rhodobacter sphaeroides* flagellar motor is a variable-speed rotor. *FEBS Lett* **409**:37-40.
78. **Pao, G. M., and M. H. Saier, Jr.** 1995. Response regulators of bacterial signal transduction systems: selective domain shuffling during evolution. *J. Mol. Evol.* **40**:136-154.
79. **Platzer, J., W. Sterr, M. Hausmann, and R. Schmitt.** 1997. Three genes of a motility operon and their role in flagellar rotary speed variation in *Rhizobium meliloti*. *J Bacteriol* **179**:6391-9.
80. **Poggio, S., C. Abreu-Goodger, S. Fabela, A. Osorio, G. Dreyfus, P. Vinuesa, and L. Camarena.** 2007. A Complete Set of Flagellar Genes Acquired by Horizontal Transfer Coexists with the Endogenous Flagellar System in *Rhodobacter sphaeroides*. *J. Bacteriol.* **189**:3208-16.
81. **Poggio, S., A. Osorio, G. Dreyfus, and L. Camarena.** 2005. The flagellar hierarchy of *Rhodobacter sphaeroides* is controlled by the concerted action of two enhancer-binding proteins. *Mol Microbiol* **58**:969-83.
82. **Poole, P. S., M. J. Smith, and J. P. Armitage.** 1993. Chemotactic signalling in *Rhodobacter sphaeroides* requires metabolism of attractants. *J Bacteriol* **175**:291-4.

83. **Power, P. M., and M. P. Jennings.** 2003. The genetics of glycosylation in Gram-negative bacteria. *FEMS Microbiol Lett* **218**:211-22.
84. **Pukall, R., D. Buntfuss, A. Fruhling, M. Rohde, R. M. Kroppenstedt, J. Burghardt, P. Lebaron, L. Bernard, and E. Stackebrand.** 1999. *Sulfitobacter mediterraneus* sp. nov., a new sulfite-oxidizing member of the  $\alpha$ -Proteobacteria. *International Journal of Systematic Bacteriology* **49**:513-519.
85. **Quon, K. C., G. T. Marczynski, and L. Shapiro.** 1996. Cell cycle control by an essential bacterial two-component signal transduction protein. *Cell* **84**:83-93.
86. **Scharf, B., H. Schuster-Wolff-Buhring, R. Rachel, and R. Schmitt.** 2001. Mutational analysis of the *Rhizobium lupini* H13-3 and *Sinorhizobium meliloti* flagellin genes: importance of flagellin A for flagellar filament structure and transcriptional regulation. *J. Bacteriol.* **183**:5334-5342.
87. **Shiba, T.** 1991. *Roseobacter litoralis* gen. nov., sp. nov., and *Roseobacter denitrificans* sp. nov., aerobic pink-pigmented bacteria which contain bacteriochlorophyll a. *Syst. Appl. Microbiol.* **14**:140-145.
88. **Shin, S., and C. Park.** 1995. Modulation of flagellar expression in *Escherichia coli* by acetyl phosphate and the osmoregulator OmpR. *J Bacteriol* **177**:4696-702.
89. **Silva, E. S.** 1985. The association dinoflagellate-bacteria: Their ultrastructural relationship in two species of dinoflagellates. *Protistologica* **21**:429-446.
90. **Silva, E. S. E.** 1978. Endonuclear bacteria in two species of dinoflagellates. *Protistologica* **14**:113-119.
91. **Silverman, M., and M. Simon.** 1974. Characterization of *Escherichia coli* flagellar mutants that are insensitive to catabolite repression. *J Bacteriol* **120**:1196-203.
92. **Skerker, J. M., M. S. Prasol, B. S. Perchuk, E. G. Biondi, and M. T. Laub.** 2005. Two-component signal transduction pathways regulating growth and cell cycle progression in a bacterium: a system-level analysis. *PLoS Biol.* **3**:e334.

93. **Sourjik, V., P. Muschler, B. Scharf, and R. Schmitt.** 2000. VisN and VisR are global regulators of chemotaxis, flagellar, and motility genes in *Sinorhizobium* (*Rhizobium*) *meliloti*. *J. Bacteriol.* **182**:782-788.
94. **Soutourina, O., A. Kolb, E. Krin, C. Laurent-Winter, S. Rimsky, A. Danchin, and P. Bertin.** 1999. Multiple control of flagellum biosynthesis in *Escherichia coli*: role of H-NS protein and the cyclic AMP-catabolite activator protein complex in transcription of the *flhDC* master operon. *J Bacteriol* **181**:7500-8.
95. **Soutourina, O. A., E. Krin, C. Laurent-Winter, F. Hommais, A. Danchin, and P. N. Bertin.** 2002. Regulation of bacterial motility in response to low pH in *Escherichia coli*: the role of H-NS protein. *Microbiology* **148**:1543-51.
96. **Sperandio, V., A. G. Torres, and J. B. Kaper.** 2002. Quorum sensing *Escherichia coli* regulators B and C (QseBC): a novel two-component regulatory system involved in the regulation of flagella and motility by quorum sensing in *E. coli*. *Mol Microbiol* **43**:809-21.
97. **Springer, M. S., M. F. Goy, and J. Adler.** 1977. Sensory transduction in *Escherichia coli*: two complementary pathways of information processing that involve methylated proteins. *Proc Natl Acad Sci U S A* **74**:3312-6.
98. **Springer, M. S., and B. Zanolari.** 1984. Sensory transduction in *Escherichia coli*: regulation of the demethylation rate by the CheA protein. *Proc Natl Acad Sci U S A* **81**:5061-5.
99. **Springer, W. R., and D. E. Koshland, Jr.** 1977. Identification of a protein methyltransferase as the *cheR* gene product in the bacterial sensing system. *Proc Natl Acad Sci U S A* **74**:533-7.
100. **Stock, A. M., V. L. Robinson, and P. N. Goudreau.** 2000. Two-component signal transduction. *Annu. Rev. Biochem.* **69**:183-215.

101. **Tawa, P., and R. C. Stewart.** 1994. Kinetics of CheA autophosphorylation and dephosphorylation reactions. *Biochemistry* **33**:7917-24.
102. **Terahara, N., T. A. Krulwich, and M. Ito.** 2008. Mutations alter the sodium versus proton use of a *Bacillus clausii* flagellar motor and confer dual ion use on *Bacillus subtilis* motors. *Proc Natl Acad Sci U S A* **105**:14359-64.
103. **Thompson, P. R., J. Schwartzenhauer, D. W. Hughes, A. M. Berghuis, and G. D. Wright.** 1999. The COOH terminus of aminoglycoside phosphotransferase (3')-IIIa is critical for antibiotic recognition and resistance. *J Biol Chem* **274**:30697-706.
104. **Toews, M. L., M. F. Goy, M. S. Springer, and J. Adler.** 1979. Attractants and repellents control demethylation of methylated chemotaxis proteins in *Escherichia coli*. *Proc Natl Acad Sci U S A* **76**:5544-8.
105. **Toker, A. S., and R. M. Macnab.** 1997. Distinct regions of bacterial flagellar switch protein FliM interact with FliG, FliN and CheY. *J Mol Biol* **273**:623-34.
106. **Visscher, P. T., B. F. Taylor, and R. P. Kiene.** 1995. Microbial consumption of dimethyl sulfide and methanethiol in marine coastal sediments. *FEMS Microbiol. Ecol.* **18**:145-154.
107. **Vogelbein, W. K., V. J. Lovko, J. D. Shields, K. S. Reece, P. L. Mason, L. W. Haas, and C. C. Walker.** 2002. *Pfiesteria shumwayae* kills fish by micropredation not exotoxin secretion. *Nature* **418**:967-70.
108. **von Mering, C., L. J. Jensen, M. Kuhn, S. Chaffron, T. Doerks, B. Kruger, B. Snel, and P. Bork.** 2007. STRING 7--recent developments in the integration and prediction of protein interactions. *Nucleic Acids Res.* **35**:D358-362.
109. **Wadhams, G. H., and J. P. Armitage.** 2004. Making sense of it all: bacterial chemotaxis. *Nat Rev Mol Cell Biol* **5**:1024-37.

110. **Ward, M. J., D. M. Harrison, M. J. Ebner, and J. P. Armitage.** 1995. Identification of a methyl-accepting chemotaxis protein in *Rhodobacter sphaeroides*. *Mol Microbiol* **18**:115-21.
111. **Welch, M., K. Oosawa, S. Aizawa, and M. Eisenbach.** 1993. Phosphorylation-dependent binding of a signal molecule to the flagellar switch of bacteria. *Proc Natl Acad Sci U S A* **90**:8787-91.
112. **Wood, H. E., K. M. Devine, and D. J. McConnell.** 1990. Characterisation of a repressor gene (*xre*) and a temperature-sensitive allele from the *Bacillus subtilis* prophage, PBSX. *Gene* **96**:83-8.
113. **Wu, J., A. K. Benson, and A. Newton.** 1995. Global regulation of a sigma 54-dependent flagellar gene family in *Caulobacter crescentus* by the transcriptional activator FlbD. *J Bacteriol* **177**:3241-50.
114. **Yagasaki, J., M. Okabe, R. Kurebayashi, T. Yakushi, and M. Homma.** 2006. Roles of the intramolecular disulfide bridge in MotX and MotY, the specific proteins for sodium-driven motors in *Vibrio spp.* *J Bacteriol* **188**:5308-14.
115. **Yamamoto, K., and Y. Imae.** 1993. Cloning and characterization of the *Salmonella typhimurium*-specific chemoreceptor Tcp for taxis to citrate and from phenol. *Proc Natl Acad Sci U S A* **90**:217-21.
116. **Yang, G., T. V. Bhuvanewari, C. M. Joseph, M. D. King, and D. A. Phillips.** 2002. Roles for riboflavin in the *Sinorhizobium-alfalfa* association. *Mol Plant Microbe Interact* **15**:456-62.
117. **Yoch, D. C.** 2002. Dimethylsulfoniopropionate: its sources, role in the marine food web, and biological degradation to dimethylsulfide. *Appl. Environ. Microbiol.* **68**:5804-5815.

118. **Yoch, D. C., J. H. Ansedé, and K. S. Rabinowitz.** 1997. Evidence for Intracellular and Extracellular Dimethylsulfoniopropionate (DMSP) Lyases and DMSP Uptake Sites in Two Species of Marine Bacteria. *Appl Environ Microbiol* **63**:3182-3188.
119. **Zhou, J., L. L. Sharp, H. L. Tang, S. A. Lloyd, S. Billings, T. F. Braun, and D. F. Blair.** 1998. Function of protonatable residues in the flagellar motor of *Escherichia coli*: a critical role for Asp 32 of MotB. *J Bacteriol* **180**:2729-35.
120. **Zhulin, I. B., A. F. Lois, and B. L. Taylor.** 1995. Behavior of *Rhizobium meliloti* in oxygen gradients. *FEBS Lett* **367**:180-2.
121. **Zubkov, M. V., B. M. Fuchs, S. D. Archer, R. P. Kiene, R. Amann, and P. H. Burkil.** 2001. Linking the composition of bacterioplankton to rapid turnover of dissolved dimethylsulphoniopropionate in an algal bloom in the North Sea. *Environ. Microbiol.* **3**:304-311.
122. **Zubkov, M. V., B. M. Fuchs, S. D. Archer, R. P. Kiene, R. Amann, and P. H. Burkil.** 2001. Linking the composition of bacterioplankton to rapid turnover of dissolved dimethylsulphoniopropionate in an algal bloom in the North Sea. *Environ Microbiol* **3**:304-11.